The Dielectric Properties of Water and Their Role in Enzyme-Substrate Interactions

by

P. O. Vogelhut

ELECTRONICS RESEARCH LABORATORY

UNIVERSITY OF CALIFORNIA
BERKELEY, CALIFORNIA

Electronics Research Laboratory
University of California
Berkeley, California

THE DIELECTRIC PROPERTIES OF WATER AND THEIR ROLE IN ENZYME-SUBSTRATE INTERACTIONS

by

P. O. Vogelhut

August 24, 1962

ACKNOWLEDGMENT

SUMMARY

The structures of water, aqueous solutions, and ice are briefly reviewed, primarily with regard to their electrical characteristics. A new model of water is proposed, based on the concept of double-bond and vacant-bond orientational defects, and is used for the computation of the frequency and temperature dependence of pure and contaminated water (solutions).

A new cavity-perturbation measurement technique is used to obtain the dielectric constant of water and of aqueous solutions at microwave frequencies. The results agree well with our model of water and its solutions, and are accurate enough to permit continuous measurements of changes of the dielectric constant of enzyme-substrate mixtures as a function of time after mixing. The data are interpreted on the basis of our new model of water (the concepts of defect and excess protons as charge carriers) and the analogy with catalytic properties of surfaces of electronic semiconductors; water bound to the surface of the enzyme molecule (itself constituting a surface) strongly suggests a protonic semiconductor. The energy levels of the water surface are modified by the presence of residues on the enzyme molecule and may be conveniently expressed by circuit diagrams similar to those used in integrated solid-state circuits. The postulated circuit is a tunnel-diode oscillator, tuned to the characteristic frequency of the substrate molecule, which it attracts and whose bond it breaks by positive feedback.

How general the postulated scheme of reaction is remains to be resolved by further experiments. The present contribution links together previously separate areas of study and has therefore many unexploited concepts of both fields as a possible resource.

TABLE OF CONTENTS

LIST OF FIGURES

LIST OF TABLES

I. OBJECTIVES OF THE INVESTIGATION

A. GENERAL

The intent of the present investigation was to examine the
dielectric constant of solutions of protein molecules in an inert
state (enzymatically inactive) and then to follow any changes of the
dielectric constant as the protein (in our case the enzyme pepsin)
interacts with its substrate. In order to permit the measurement
of such rapid changes of both parts of the dielectric constant
simultaneously, a new technique was developed for the measurement
of changes in the resonant frequency and Q of a microwave cavity.
From these changes the respective dielectric constants could be
easily computed. We observed a pronounced change in the dielectric
parameters as the enzyme assumed its activated state.

The interpretation of our data posed several problems. We
had to determine what structural changes give rise to the observed
changes in the electrical parameters. For this purpose we developed
a new model of the dielectric constant of water and applied this theory
to the case where impurities (solute molecules) were present in
the water medium. In this manner we were able to see that the
changes in the values of the dielectric constant during enzymatic
activity are caused by changes in the number of defects of the
water that is adsorbed at the surface of the protein molecules.

A theory of the static dielectric constant of water advanced
by Haggis et al.[1] can be used to give an estimate of the number of
water molecules that are irrotationally bound to the surface of the
protein molecule. If this theory were applied to our data we would
interpret our observations to mean that the number of adsorbed
water molecules does not change during the active period of the
catalysis, since the dielectric constant extrapolated to its static
value, which Haggis et al. relate to the number of bound water
molecules, stays constant with time.

The model developed here seems to be a more inclusive
one since it not only gives the correct values of the static dielectric
constant, but also the relaxation time of water in its pure state and

for aqueous solutions, all as a function of temperature. We therefore prefer to interpret our data in accordance with the new model. If information about the water of hydration (a concept that is not too well defined) of protein molecules is desired, then the Haggis et al. theory should be used.

Our data are quite similar to those of Takashima and Lumry[2] if taken in conjunction with the experiments of Gibson and Roughton.[3] They also observe a peak in the dynamic dielectric constant with time for the process of oxygenation of the hemoglobin molecule. This reaction has often been thought of as a catalytic action similar to the first step of the enzymatic reaction that we observed.

Our analysis of the data in terms of changes in the defect concentration on the surface of the enzyme molecule warrants a discussion of the views about the nature of the charge-transfer process on the protein molecule. Our data indicate that the charge carriers on the wet protein surface are protons. This view is also held by many other investigators, notably King and Medley,[4] Cardew and Eley,[5] Fuoss,[6] Riehl,[7] and Taylor.[8] These investigators reached their conclusions by studies of dc conductivity measurements. Rosenberg[9] has performed experiments on crystalline bovine hemoglobin that led him to the opposite conclusion, namely that the charge carriers are electrons. His experiment, however, does not seem to present conclusive evidence for his hypothesis. He states that if an isolated sample of wet protein is placed between electrodes known to block the passage of protons (his glass electrode is probably a new type of conductive glass which, unlike all others, does not pass protons), but known to pass electrons freely, one of two things may occur:

(1) If the conduction process is electronic, the current should be constant in time.

(2) If the conduction is ionic, water must be electrolysed; and the water content must decrease in time. Therefore the current should decrease in time.

To justify the assumption made in point (2)--that water is electrolysed and should be lost from the protein surface--that process should be experimentally verified. Since he operated at a hydration level of 7.5%, whereas the experiment conducted by King and Medley[4] at hydration levels below 15% did not show any electrolysis of the water, one should be careful in the interpretation of Rosenberg's data

As has been shown by Eyring, Glasstone, and Laidler[10] in their theory of overvoltage, the protons that are transferred from the solution to the electrode do not come from the hydrogen ions in solution, but from water molecules. For the evolvement of hydrogen at the electrode surface, the authors state that the cathode has to be covered with a layer of adsorbed water which in turn is surrounded by water molecules in solution. There may just be sufficient water at the electrodes in King and Medley's experiment, whereas in Rosenberg's there may not be enough water molecules for this process; in any case some experimental proof of the assumption that electrolysis occurs should have been attempted in view of the fact that all his other observations and theoretical interpretations hinge on the correctness of this assumption. In a later paper Rosenberg[11] heated his hemoglobin samples to $70^{\circ}C$ and observed an actual decrease of the current with time. This technique surely must have removed some water; and his observation therefore substantiates his alternative view, namely that the conduction process is ionic. This fact again places the electrolysis assumption into question.

Views of the nature of the ionic conduction mechanism vary, although the law of conduction is the same for quite different substances, such as hemoglobin, nylon, cellophane, metal films, insulators, and cytochrome C, whose one common feature is their ability to adsorb water. There is an agreement in the various theories of ionic conduction, since all postulate the protons to be the charge carriers. In view of the recent theory of the conduction process in ice advanced by Gränicher et al. (cf. Section IV-A-1),

which states that a dc conductivity requires not only protons but also the simultaneous participation of ionized states and orientational defects, we undertook in our experiment to show that a current actually flows on the surface of a protein resulting in part from a change in the number of orientational defects. We were able to arrive at this conclusion only after a reinvestigation of the theory of the dielectric constant of water, as well as the formulation of a new theory based on previous ones and on the experimental support provided by the observation of the dielectric constant of an enzyme while it was acting on its substrate molecule. This conclusion sheds new light on the phenomenon of conduction of protein molecules in the wet and dry state. We tentatively suggest that the conduction of electricity in the dry protein molecule may proceed by a cooperative effort of defects in the hydrogen bonds of the protein and ionized states of the elements of those bonds, whereas in the wet state the conduction is enhanced by the participation of the water molecules, which can perform the same rotational and translational motions with a smaller amount of activating energy.

Our experiment was only designed to show the existence of a current resulting from defects on the surface of a protein when it is immersed in a water medium. Different experimental evidence is needed for the demonstration of the existence of defects in the dry protein. There is some indication of the existence of a high-frequency dispersion region in nylon[8] owing to the amorphous regions of the polymer. This relaxation process may well be due to defects, which can be responsible for the amorphous structure of the polymer. (The designation "amorphous" only means that the structure is like that of a supercooled liquid.) Since such a structural arrangement is not very different from that of water with respect to the possibility of a creation of structural defects, the analogy may not be too far off. It also appears from the work of Taylor[8] that cytochrome has such a dispersion region and a similar polymer crystallite structure. The activation energy for the creation of defects in dry proteins

should be rather high, since the whole planar amide unit has to rotate. This supposition is borne out by the rather low-frequency (and high-temperature) dispersion region observed by Taylor.

In conclusion we may say that the new way of looking at ionic conduction discussed in Section IV-A leads one to speculate about the conduction phenomenon in wet and dry proteins; one may, first, construct an adequate model of the dielectric constant of water, and second, design an experiment that could demonstrate the existence of predicted defects on the surface of an enzyme. That these defects--or rather currents resulting from these defects-- are only observed under the special condition of the active state of the enzyme is a drawback from the generality of the theory; but a different experiment, in which a direct current is passed through proteins while the microwave dielectric constant is observed, may well confirm the generality of the hypothesis of defects in wet and dry proteins. The static electric field would align the defects on the protein and thereby concentrate those defects so that the dipole moment of the proteins is correspondingly altered, resulting in a different value of the dielectric constant.

B. PRESENT EXPERIMENT

Two methods were used in our experimental investigation: a cavity perturbation method for the measurement of the real and imaginary parts of the dielectric constant, and the ninhydrin reaction method for the determination of the extent of the hydrolysis that occurred in the enzymatic reaction. The two methods are discussed in Sections II-A and II-D, respectively.

The experimental results fall into three categories: time-independent measurements of the dielectric constant, observation of the dielectric constant as a function of time during the enzymatic reaction process, and determination of the extent of the hydrolysis by a spectrophotometric technique. In the first category we measured the dielectric constant as a function of temperature of

(1) pure water, (2) ionic solutions, and (3) solutions of hydrogen bond-forming substances (one of the latter being a solution of pepsin). The data are given in terms of the observed frequency shift of the resonant frequency of the cavity and the changes in the Q of the cavity. From those values the changes in the dielectric constant are computed; a predetermined calibration factor is used that was obtained from measurements of the cavity dimensions and checked by use of an accurately known dielectric constant (that of benzene). We also give an estimate of the experimental error in each measurement.

The discussion of our experimental observations proceeds as follows:

The present state of knowledge about the structure of water and solutions as well as the structure of ice are reviewed. A recent theory of the structure of ice both in its pure state and contaminated with foreign molecules suggested to us the possibility of applying those concepts of defects in the arrangement of the water molecules to the construction of a new model of water and aqueous solutions. This new model does not depart radically from the generally accepted structural concepts of water but supplements them in such a way as to make it easier to understand and compute the electrical behavior of water and its solutions. Instead of considering the hydrogen bonds between the molecules responsible for its electrical characteristics we assume, by extrapolation of the recent theory of ice, that the defects in the structure play the dominant role. This new model may be used in gaining a better understanding of many physical properties of water, but we are primarily interested in its electrical behavior. We use the model to construct an adequate description of the dielectric constant of water as a function of temperature and compare the theoretical results with our experimental data. Then we apply the concepts of our model in computing the dielectric constant of aqueous solutions, and finally interpret our observations about the time-dependent

-6-

behavior of the dielectric constant of enzyme-substrate solutions on the basis of our new model. Since this method yields new information about the behavior of enzymes we review the mechanisms of enzyme action that rest on the electrical characteristics of the proteins, and we find that many investigators have speculated about the importance of water, in particular its special physical characteristics, in the mechanisms that can be constructed to explain the catalytic activity of proteins. We use our newly gained information to advance a model of enzymatic action whose actual physical operation depends to a great extent on our model of the structure of water. We postulate that the excess energy which distinguishes a catalytic reaction from a normal chemical reaction is supplied by an oscillator on the surface of the enzyme molecule. This oscillator can only exist and operate under the special conditions that prevail at the surface of the protein molecule. Our data at present support our hypothesis of enzyme action somewhat incompletely; furthermore, they cannot be reconciled with similar theories of enzyme action that rest on the electrical properties of the enzyme-substrate solution, mostly because such theories are too general.

The contribution of the present investigation to the present state of knowledge consists of a new method of measurement of the dielectric constant of aqueous solutions at microwave frequencies, a new model of the structure of water and aqueous solutions, and an application of this model to an enzymatic reaction with a resulting proposal of a new mechanism of the catalytic action of the enzyme.

In more general terms, however, this report points to new avenues of investigation of biophysical processes by convenient electronic methods and opens up the possibility of looking at dynamic information transfer inside the living cell.

II. METHODS

A. MEASUREMENT OF THE DIELECTRIC CONSTANT OF WATER AND AQUEOUS SOLUTIONS AT MICROWAVE FREQUENCIES

Our method is an adaptation of the two-cavity method proposed by Birnbaum and Franeau.[12] A perturbation theory developed by Slater[13] gives the change in the resonant frequency and Q of a cavity produced by the introduction of a dielectric material into the cavity. Two cavities, designated by subscripts 1 and 2, differ slightly owing to the presence of some material in cavity 2. If the material has a complex dielectric constant (relative to vacuum) given by $\epsilon^* = \epsilon' - j\epsilon''$ and a permeability of unity in the absolute practical unit system, then the shift in frequency is given by

$$\frac{f_1 - f_2}{f_1} = \Delta\epsilon' \frac{\int_v \vec{E}_1 \cdot \vec{E}_2 \, dv}{2 \int_V E_1^2 \, dV} \tag{1}$$

where v and V are the volumes of the dielectric and the cavity, respectively, $\vec{E}$ is the electric field intensity, and $\Delta\epsilon'$ is the difference between the real parts of the dielectric constants. This equation is useful if $\vec{E}_2$ can be obtained easily from a known unperturbed field $\vec{E}_1$; e.g., when the surface of the dielectric is everywhere parallel to the electric field, as in the case of a dielectric rod or tube that is aligned with the field lines. With the further restrictions that both the dielectric and field lines end on the walls of the cavity, $\vec{E}_2$ is set equal to $\vec{E}_1$.

The change in the Q of the cavity that results from the introduction of the dielectric is given by

$$\frac{1}{Q_2} - \frac{1}{Q_1} = \Delta \epsilon '' \frac{\int_V \vec{E}_1 \cdot \vec{E}_2 \, dv}{\int_V E_1^2 \, dV} \tag{2}$$

Since we are concerned entirely with liquid samples, we analyze further the special case of a rectangular cavity with a glass tube parallel to the electric field lines (Figure 1). The cavity operates in the TE_{104} mode. Let the subscript (s) denote properties pertaining to a solution and (w) to pure water; then the above expressions for the two parts of the dielectric constant may be rewritten

$$\Delta \epsilon ' = \epsilon_w ' - \epsilon_s ' = \frac{2C}{f_0} (f_s - f_w) \tag{3}$$

$$\Delta \epsilon '' = \epsilon_w '' - \epsilon_s '' = C \left(\frac{1}{Q_s} - \frac{1}{Q_w} \right) \tag{4}$$

where $(f_s - f_w)$ is the shift in the resonant frequency of the cavity due to the replacement of water by an equal volume of solution, f_0 is the resonant frequency of the empty cavity, and C is a constant derived from the cavity dimensions, given by

$$C = \frac{V_0}{4 A V_T} \tag{5}$$

where V_0 is the volume of the empty cavity, V_T is the volume of total dielectric material, and A is a correction factor for the position of the tube relative to E_{max}.

In practice the constant C cannot be calculated sufficiently accurately from the parameters defining it since the coupling irises in the cavity cause some uncertainty in the value of A. We therefore calibrated our instrument by introducing a material with a well-known dielectric constant (benzene) into the glass tube, replacing the air in the tube, and thus producing a frequency shift corresponding to the difference between the dielectric constant of benzene $(\epsilon ' = 2.2835[14])$ and of air.
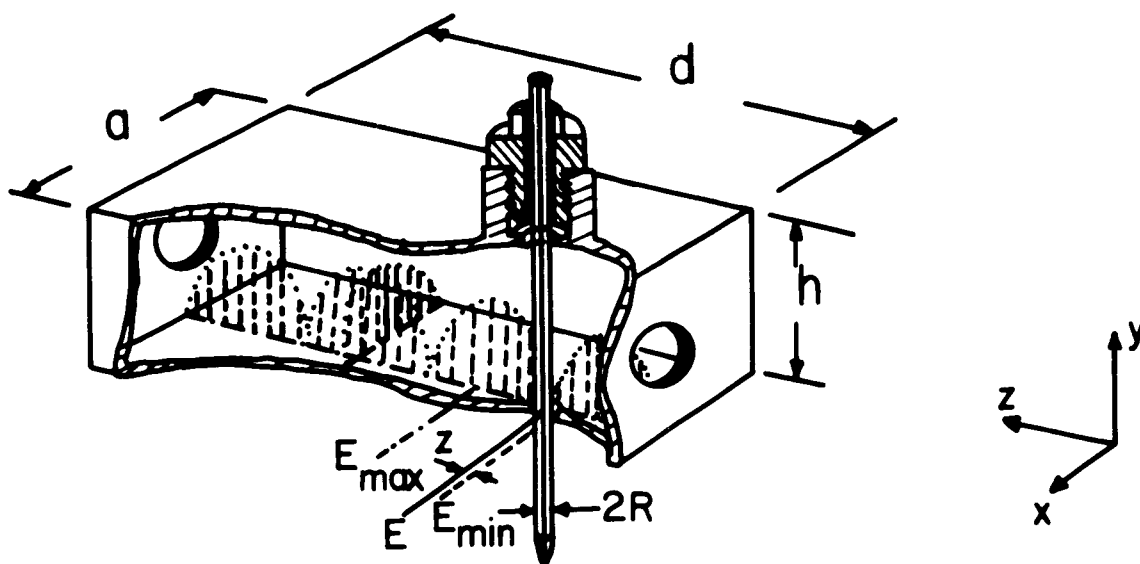
FIGURE 1. --Drawing of sample cavity.

B. ELECTRONIC INSTRUMENTATION

The electronic equipment that makes the measurement of change in resonant frequency and cavity Q possible is shown in Figure 2. The backward-wave oscillator produces a frequency-modulated signal that is proportional to a sawtooth wave, which is also used to synchronize the oscilloscope. Part of the signal is mixed with a local oscillator to produce two intermediate-frequency (IF) signals, which are detected by a tunable receiver. One signal is the sum of the local-oscillator and signal-generator frequencies, the other is the difference. The receiver can be calibrated with a heterodyne frequency meter. The IF signals are amplified, detected, and used for z-axis (intensity) modulation of the oscilloscope trace to produce intensity markers of accurately known frequency separation in units of frequency. Then the oscilloscope trace is photographed and the response curve of the cavity is superimposed on the same picture.

A rectangular cavity operating in the TE_{104} mode is used. It was found that changes in Q and in resonant frequency could be measured with much greater sensitivity when the sample was placed in a position off the maximum electric field--in fact, quite near the node. It is found that changes in the electric field vector show best there; if the sample tube were at the maximum electric field the resulting attenuation would be too great to yield any signal at all. In order to reduce the attenuation either the volume of the sample or the position of the sample has to be changed. Since the volume cannot be reduced below a practical limit, the position is adjusted instead.

The reason why the TE_{104} mode is used is similarly a practical one: it is to optimize the ratio of cavity volume to sample-tube volume in order to obtain an easily detectable signal. This ratio influences the Q of the system. The better the Q the greater the signal-to-noise ratio. An increase in cavity volume increases Q, increase in sample volume lowers Q; values of
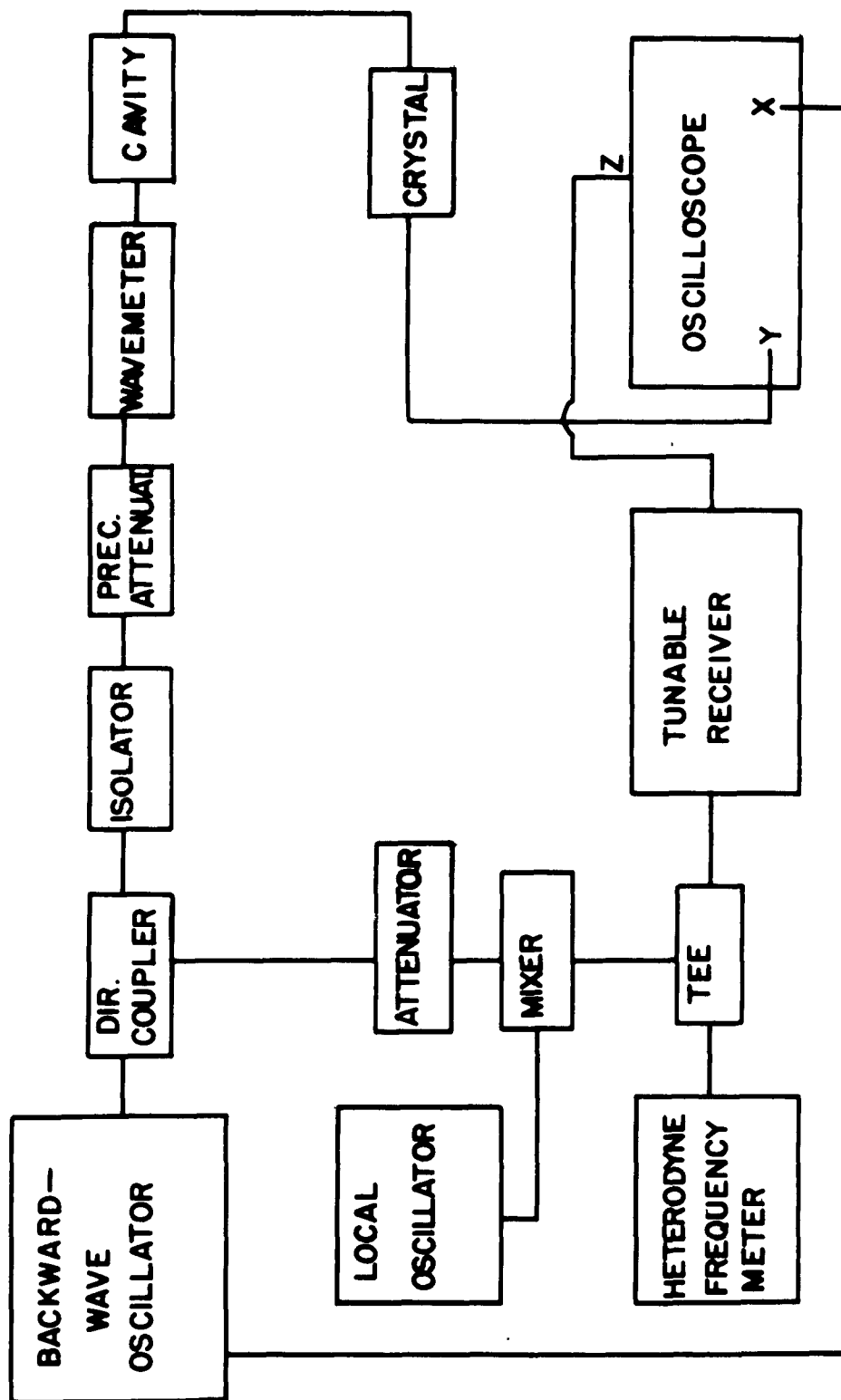
FIGURE 2. --Schematic block diagram for perturbation analysis.

these parameters were chosen that optimize the conditions to yield the best signal-to-noise ratio. The noise itself is predominantly residual line-frequency modulation (in amplitude and frequency) of the microwave generator and local oscillator. Crystal noise and vibrations of the equipment also contribute.

Similar considerations apply in determining the size of the coupling holes. All of these parameters prove to be quite critical.

C. ACCESSORY EQUIPMENT

The only accessory equipment used in the experimental determination of the dielectric constant of aqueous solutions was a waterbath with a well-regulated temperature and syringes to pump the liquid samples into the sample tube.

D. THE ENZYMATIC REACTION

Pepsin attacks the peptide bond in the substrate so that the products of the reaction are leucine and tyrosine. Amounts of the intact substrate and its amino acids are present in the solution and are functions of time after mixing.

The enzyme pepsin is mixed with a synthetic substrate (L-leucyl-L-tyrosine) and the dielectric constant of the reaction is followed as a function of time. The substrate, owing to its low concentration $(10^{-2} M)$, does not affect the value of the dielectric constant of the pure pepsin and water solution. The changes observed must be therefore caused by changes in the characteristics of the enzyme water relation only. Since the concentration of the pepsin had to be rather high (3.64% or $10^{-3} M$) to affect the value of the dielectric constant of pure water sufficiently, the reaction proceeded quite rapidly. To correlate the data of the electrical behavior of the reaction with the actual chemical changes the appearance of the product of the enzymatic reaction had to be observed.

The enzyme is stopped from further action after the dielectric constant has been measured by addition of ethylene glycol

monomethyl ether. Ninhydrin is then added to the solution, and the solution is heated to let the ninhydrin react with the free amino groups present in the solution. As the enzyme concentration stays constant with time, the color that is produced by the ninhydrin varies in accordance with the appearance of the products. By comparing the light absorption of a standard solution consisting of the enzyme and the products of the reaction (10^{-3}M pepsin, 10^{-2}M leucine, 10^{-2}M tyrosine) with the light absorption of the solution at time t, the relative amount of substrate and products can be found. L-leucyl-L-tyrosine has only one free amino group, whereas leucine and tyrosine not linked by the peptide bond have two free amino groups. At the end of the reaction the amount of light absorbed should therefore be just twice the value of light absorbed at t = 0, the start of the reaction.

The above method of monitoring the enzymatic reaction is an adaptation of a method used by Baker[15] and originally developed by Moore and Stein.[16]

III. EXPERIMENTAL RESULTS

A. CALIBRATION

1. CAVITY DIMENSIONS. As we have seen in Section II, the determination in the change in the real part of the dielectric constant depends on the knowledge of several factors: the resonant frequency of the empty cavity, the shift in frequency owing to the change in the dielectric constant of the material filling the glass tube, and a calibration factor C. The calibration factor C in turn depends on the ratio of the volume of the empty cavity to the volume occupied by all dielectric material (glass tube and filling material) and on a factor that measures the position of the glass tube relative to the location of the maximum electric field strength in the cavity.

The volume of the empty cavity can easily be determined from a measurement of the inside dimensions of the cavity. The

other dimensions similarly can be determined by such measurements, and A is found from the ratio of the square of the electric field at its maximum to that at the position of the sample tube. This ratio can be simplified to

$$A = (E/E_m)^2 = \sin^2 (4\pi z/d) \tag{6}$$

The factor 4 appears in the argument of the sine because the cavity operates in the TE_{104} mode and therefore has four maxima along the z axis.

The dimensions (in inches) as shown in Figure 1 are as follows: $a = 0.900$, $d = 3.482$, $R = 0.0408$, and $z = 0.0305$. The relations between those parameters are expressed as follows:

$$V_0 = ahd \tag{7}$$

$$V_{TD} = \pi R^2 h \tag{8}$$

$$V_0/V_{TD} = ad/\pi R^2 \tag{9}$$

so that

$$A = \sin^2 (4\pi z/d) = 1.191 \tag{10}$$

$$C = V_0/4V_{TD}A \tag{11}$$

$$C = (1.26 \pm 0.009) \times 10^4 \tag{12}$$

The accuracy of the measurements could have been improved to four significant figures, but such a procedure was deemed unnecessary because frequency shift and Q could be measured by the present method only to three significant figures.

2. CALIBRATION WITH BENZENE. Since the dielectric constant of benzene was accurately determined in the microwave range by a different method[14] we used this substance to determine C in an alternate way. As the air with a dielectric constant $\epsilon' = 1.0006$ is displaced by benzene with a constant $\epsilon' = 2.2835$ the $\Delta\epsilon' = 1.284$. The measured change in resonant frequency was $(4.81 \pm 0.02) \times 10^5$ cps.

The resulting value of C is $(1.260 \pm 0.006) \times 10^4$, in very good agreement with the value obtained above.

3. **RESONANT FREQUENCY OF CAVITY** The resonant frequency of the empty cavity is determined by superimposing the "pip" of an absorption type of wavemeter on the test-cavity response curve. This positioning can be made quite accurately by adjusting the resonant frequency of the wavemeter so that the resulting waveform has two peaks instead of one and the peaks are of equal height; then the wavemeter absorption curve is positioned at the center of the response curve of the sample cavity. By this procedure the resonant frequency of the empty cavity was found to be 9.49×10^9 cps. Here again the value of the resonant frequency could have been determined much more accurately, but a value with only three significant figures was deemed to be sufficient.

4. **DETERMINATION OF THE FREQUENCY SHIFT.** To determine the frequency shift of the resonant frequency of the sample cavity the following procedure was applied. The response curve of the cavity with one known dielectric in the glass tube and the unknown constant were photographically recorded from the oscilloscope trace on Polaroid Land Type 46 projection film and then enlarged. The separation of the maxima of the curves was converted by means of a calibration curve to values in terms of frequency separation. The oscilloscope trace was calibrated by the output of the tunable receiver, which gave an amplitude-modulated signal whose two peaks were separated on the time axis of the trace by twice the value of the frequency to which the receiver was tuned. The accuracy of the receiver could be checked with a heterodyne frequency meter. The picture of the output of the receiver was also enlarged and provided the sought conversion factor. The errors inherent in this procedure could not be reduced to less than 1 per cent because of the finite width of the trace and slight inaccuracies in fixing the location of the maximum of the response curve. Much more sensitive techniques could be devised for more accurate measurements, but would involve more electronic equipment and lead to a considerable additional cost.

5. CHANGE IN Q OF THE SAMPLE CAVITY. The oscillographs were also used to determine the change in the Q of the resonant cavity with the standard and the unknown dielectric constant. After calibration of the amplitude of the oscilloscope deflection with the precision attenuator in terms of decibels) the values of the Q's were computed using the standard formula for the Q of a cavity response curve. Here again the error could not be reduced below 1 per cent owing to the same uncertainties as were mentioned above, namely width of oscilloscope trace and noise in the trace. By an electronic system specifically designed to measure the Q of the cavity response curves these errors could very well be reduced by at least a factor of 10.

B. EXPERIMENTAL DATA

1. TIME-INDEPENDENT MEASUREMENTS OF DIELECTRIC CONSTANTS. (a) Dielectric Constant of Water as a Function of Temperature. Pure distilled water was heated or cooled to the appropriate temperature in the water bath and then injected into the sample tube of the sample cavity. Almost simultaneously the oscilloscope trace was photographed and superimposed on a picture of a response curve taken with water at a temperature of $25^{\circ}C$. Another standard for comparison of the response curves was dried air in the sample tube. Table 1 shows the shifts of the resonant frequencies when air was replaced by water at different temperatures and also the resulting changes in the reciprocal values of the Q's as illustrated by Figure 3a, in which response curves of pure water and two salt solutions are shown. The corresponding changes in the real and imaginary parts of the dielectric constant are computed and also tabulated, together with the values of the extrapolated static dielectric constant. The static dielectric constant was computed from the real and imaginary parts of the measured dielectric-constant values ϵ' and ϵ'' by use of Debye's relation for these constants.[17*] Graphs of the static dielectric constant are shown with our values and those

---

[*] $\epsilon_s = \epsilon' + [\epsilon''^2/(\epsilon' - \epsilon_\infty)]$, where ϵ_s is the static dielectric constant and ϵ_∞ the dielectric constant at optical frequencies, to be taken as 5. 5.
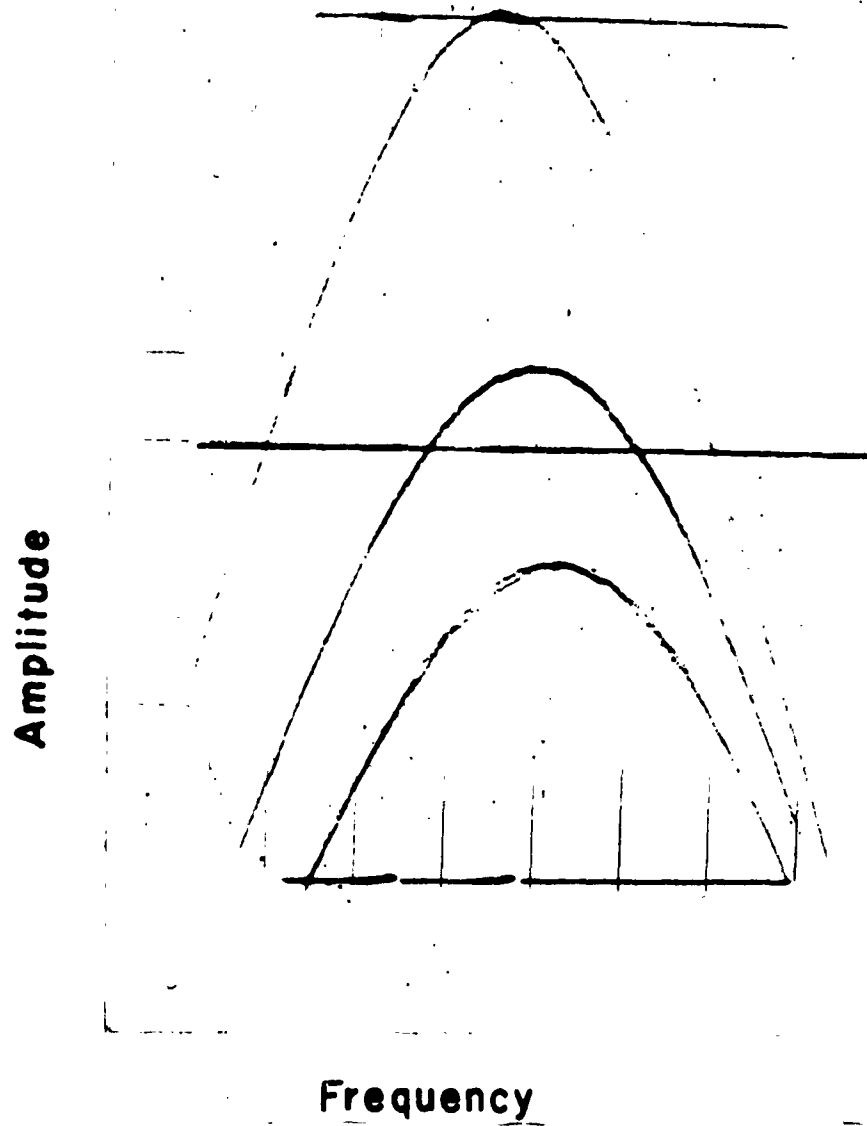
FIGURE 3a. --Oscillograph of cavity response curves.

-18-

TABLE 1. Dielectric-constant measurement of pure distilled water as function of temperature.

$T (^\circ C)$	Δf_R (Mc)	$\Delta (1/Q) \times 10^{-4}$	$\Delta \epsilon'$	$\Delta \epsilon''$	ϵ_w'	ϵ_w'	ϵ_s
10	19.6	30.5	52.0	38.5	53.0	38 5	84.1
15	21.2	28 5	56.3	35 9	57.3	35 9	82.2
20	22.5	26.1	59.8	32 9	60.8	32.9	80.4
25	23.4	23.3	62 3	29.4	63.3	29.4	78.3
30	24.0	21.2	63 8	26.7	64.8	26 7	76.7
35	24.2	19.3	64.2	24.3	65.2	24.3	75.0
40	24.2	17 5	64.2	22.1	65.2	22.1	73 4
45	24.0	16.1	63.8	20.3	64.8	20.3	71.7

of Hasted and El Sabeh[18] over the same temperature range and are seen to agree very well (Figure 3b). The real and imaginary parts of the dielectric constant are also compared with data taken at frequencies close to the one which we used, and are shown in Figures 4 and 5, respectively.

(b) Dielectric Constants of Solutions of Ions and Hydrogen-Bond-Forming Materials as a Function of Concentration. Sodium chloride, sodium iodide, and propionic acid solutions of different molarities were compared with water at 25° C. The solutions were at the same temperature. The procedure followed in obtaining these values was the same as described above. The results were tabulated in Table 2. The solution of pepsin was compared with water at 37° C. This solution was held at a constant pH of 4.00 by use of a buffer of that pH value as supplied by Braun, Knecht, and Heimann (BKH)
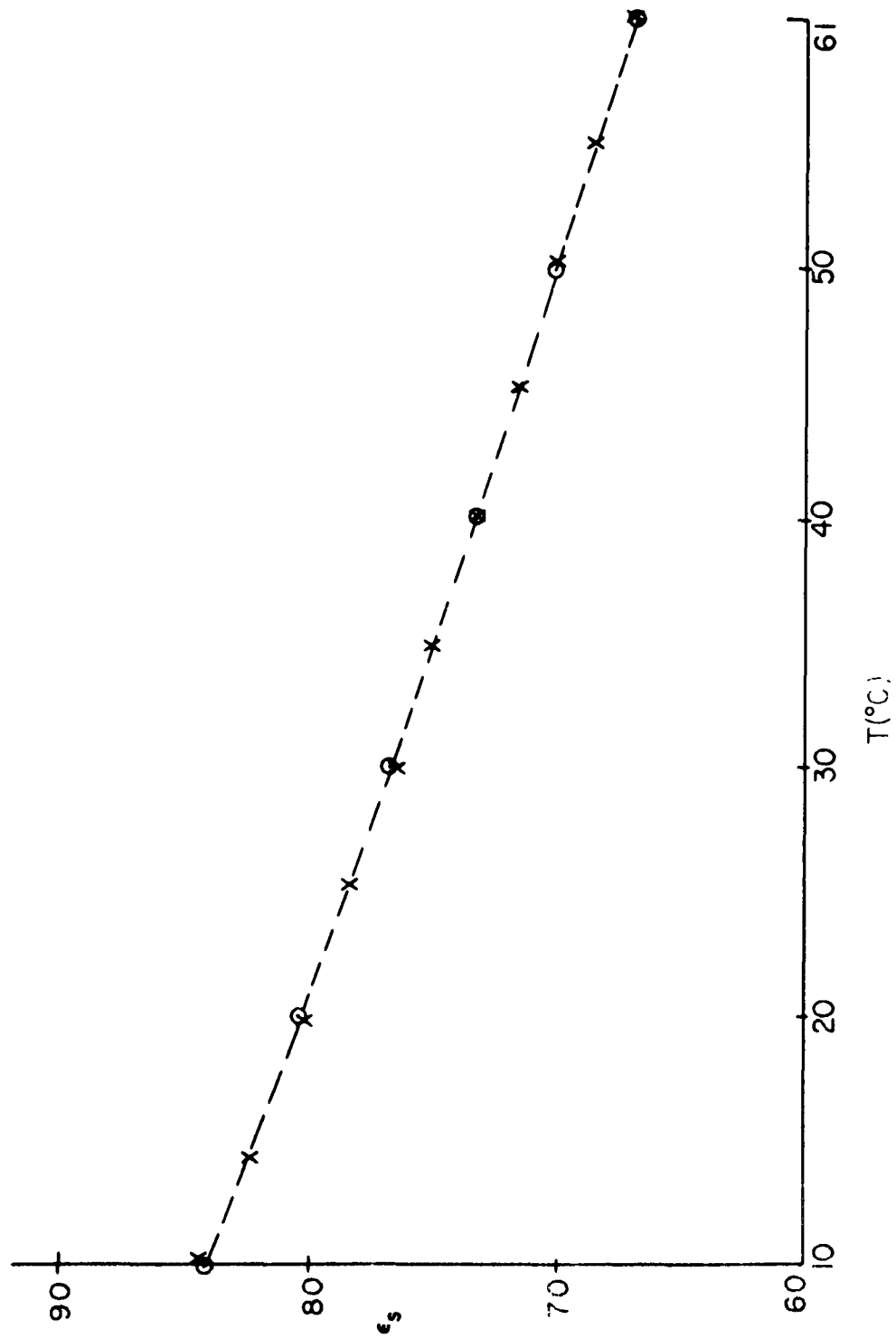
Figure 3b.--Static dielectric constant as function of temperature.
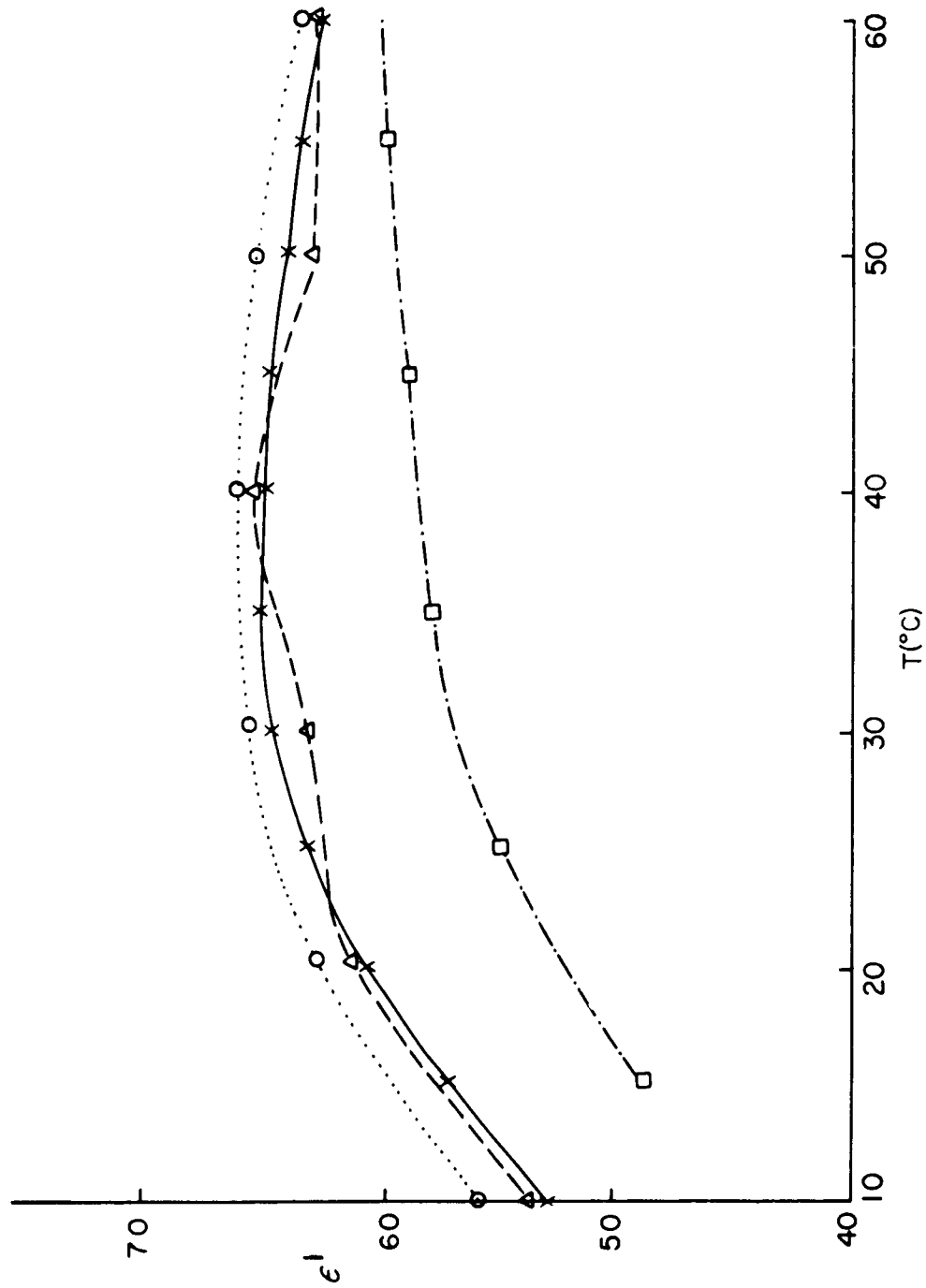
FIGURE 4. -- Real part of dielectric constant of water as function of temperature at several frequencies. □ 3.00 cm, x 3.175 cm, △ 3.21 cm, O 3.28 cm.
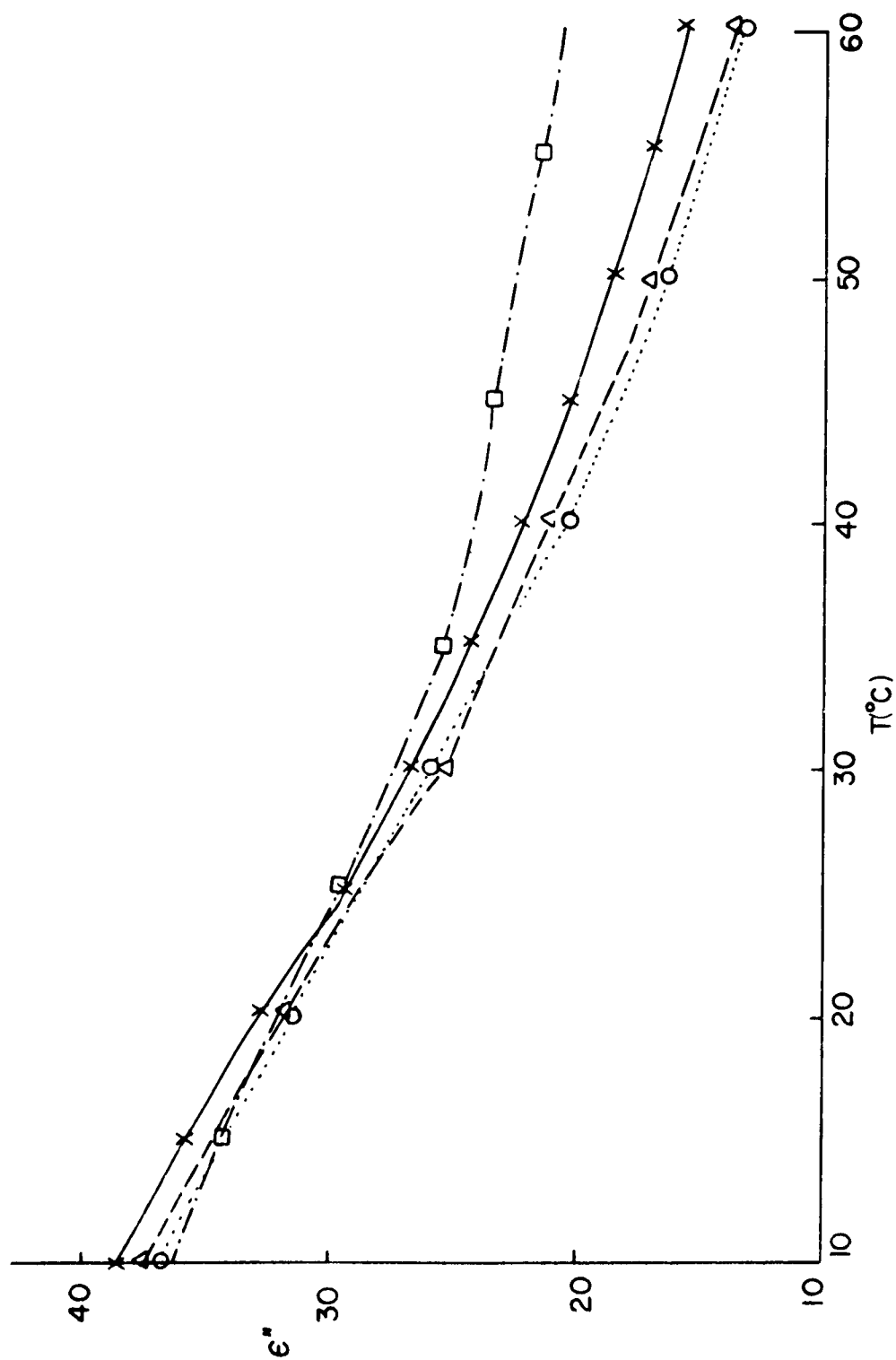
FIGURE 5.--Imaginary part of dielectric constant of water as function of temperature at several frequencies. □ 3.00cm, x 3.175 cm, △3.21 cm, O 3.28 cm.

TABLE 2. Dielectric-constant measurement of aqueous solutions as function of concentration.

1. Sodium chloride at 25° C

Molarity	Δf_R (Mc)	$\Delta(1/Q) \times 10^{-4}$	$\Delta\epsilon'$	$\Delta\epsilon''$	ϵ'	ϵ''
0.33	1.43	2.78	3.8	3.5	59.5	25.9
0.66	2.37	4.45	6.3	5.6	57.0	23.8
1.00	3.35	6.04	8.9	7.6	54.4	21.8

2. Sodium iodide at 25° C

Molarity	Δf_R (Mc)	$\Delta(1/Q) \times 10^{-4}$	$\Delta\epsilon'$	$\Delta\epsilon''$	ϵ'	ϵ''
0.33	1.02	2.46	2.7	3.1	60.6	25.5
0.66	2.26	5.37	6.0	6.7	57.3	22.7
1.00	3.12	6.91	8.3	8.7	55.0	20.7

3. Propionic acid at 25° C

Molarity	Δf_R (Mc)	$\Delta(1/Q) \times 10^{-4}$	$\Delta\epsilon'$	$\Delta\epsilon''$	ϵ'	ϵ''
0.5	1.58	0.78	4.2	1.0	59.1	28.4
1.0	3.01	0.72	8.0	0.9	55.3	28.5
1.5	4.51	0.55	12.0	0.7	51.3	28.7

4. Pepsin solution at 37°C and pH 4.00

Concentr. (%)	Δf_R (Mc)	$\Delta(1/Q) \times 10^{-4}$	$\Delta\epsilon'$	$\Delta\epsilon''$	ϵ'	ϵ''
0.00	-	-	-	-	65.2	24.2
3.64	2.29	-1.04	6.1	1.3	59.1	25.5
5.46	3.72	-2.22	9.9	2.8	55.3	27.0

2. DIELECTRIC CONSTANT OF AN ENZYME SUBSTRATE
MIXTURE AS A FUNCTION OF TIME AFTER MIXING. In this
experiment the standard for comparison of the cavity parameters
was water at a temperature of 37°C. Pictures were taken after
the solution was injected into the sample tube within 1 - 2 sec.
The solution was collected at these time intervals in a vessel
partially filled with ethylene glycol monomethyl ether to stop the
process of reaction and to analyze for the extent of the hydrolysis
of the substrate molecules. Since this experiment extended over a
relatively long time interval a small correction for the drift of the
frequency of the sweep oscillator had to be applied. The values of
the frequency and Q change are shown in Table 3 as functions of
time after mixing of the enzyme and the substrate molecules,
together with their respective values of changes in dielectric
constants.

3. MEASUREMENT OF THE APPEARANCE OF THE
PRODUCTS OF THE ENZYMATIC REACTION BY SPECTROPHOTO-
METRIC TECHNIQUE. The enzyme-substrate mixture flows
through the glass tube in the sample cavity, where its dielectric
constant is determined, and from there into a beaker where the
solution is mixed with ethylene glycol monomethyl ether. This
substance stops the process of the enzymatic reaction, so that the
products of the reaction may be analyzed at the times when their
dielectric constants are determined. The mixture of the enzyme-
substrate product solution and the added inhibitor are then diluted
by a factor of 100 and boiled for 15 minutes with the ninhydrin
reagents, care being taken to insure that loss of solution during
this process by evaporation is minimized. A standard solution
consisting of the same enzyme concentration as used in the
experiment (10^{-3}M) and products of the reaction (10^{-2}M leucine
and 10^{-2}M tyrosine) is subjected to the same treatment as the
reacting enzyme-substrate mixture solution. The standard and
the reacting mixtures are then compared in a Klett-Summerson
photoelectric colorimeter. The variation in the reading of that

TABLE 3. Dielectric-constant measurement of pepsin and
L-leucyl-L-tyrosine as function of time after mixing.

t(min)	Δf_R	$\Delta(1/Q) \times 10^{-4}$	$\Delta \epsilon'$	$\Delta \epsilon''$	ϵ'	ϵ''	x
0	2.29	-1.04	6.1	-1.3	59.1	25.5	0.476
3.6	2.29	0.08	6.1	0.1	59.1	24.1	0.450
4.6	2.33	0.24	6.2	0.3	59.0	23.9	0.439
6.0	2.41	-0.24	6.4	-0.3	58.8	24.5	0.460
7.1	2.41	-0.40	6.4	-0.5	58.8	24.7	0.463
10.0	2.49	-0.48	6.6	-0.6	58.6	24.8	0.467
15.0	2.37	-0.40	6.3	-0.5	58.9	24.7	0.463
20.0	2.41	-0.32	6.4	-0.4	58.8	24.6	0.462
25.0	2.49	-0.09	6.6	-0.1	58.6	24.3	0.458
30.0	2.37	-0.55	6.3	-0.7	58.9	24.9	0.467
35.0	2.30	-0.72	6.1	-0.9	59.1	25.1	0.468
40.0	2.61	-0.88	6.9	-1.1	58.3	25.3	0.479
45.0	2.37	-0.96	6.3	-1.2	58.9	25.4	0.476
60.0	2.49	-0.96	6.6	-1.2	58.6	25.4	0.469

mixture with time is shown in Figure 6. By comparison of these
readings with those of the standard the concentration of free
aminogroups relative to those of the standard can be determined,
and from that concentration the extent of the hydrolysis can be
computed to vary with time (Figure 7). The error in this determi-
nation is about 2.5 per cent (which is rather high) and is mostly
due to errors in dilution, possible evaporation, and reading of the
instrument scale.
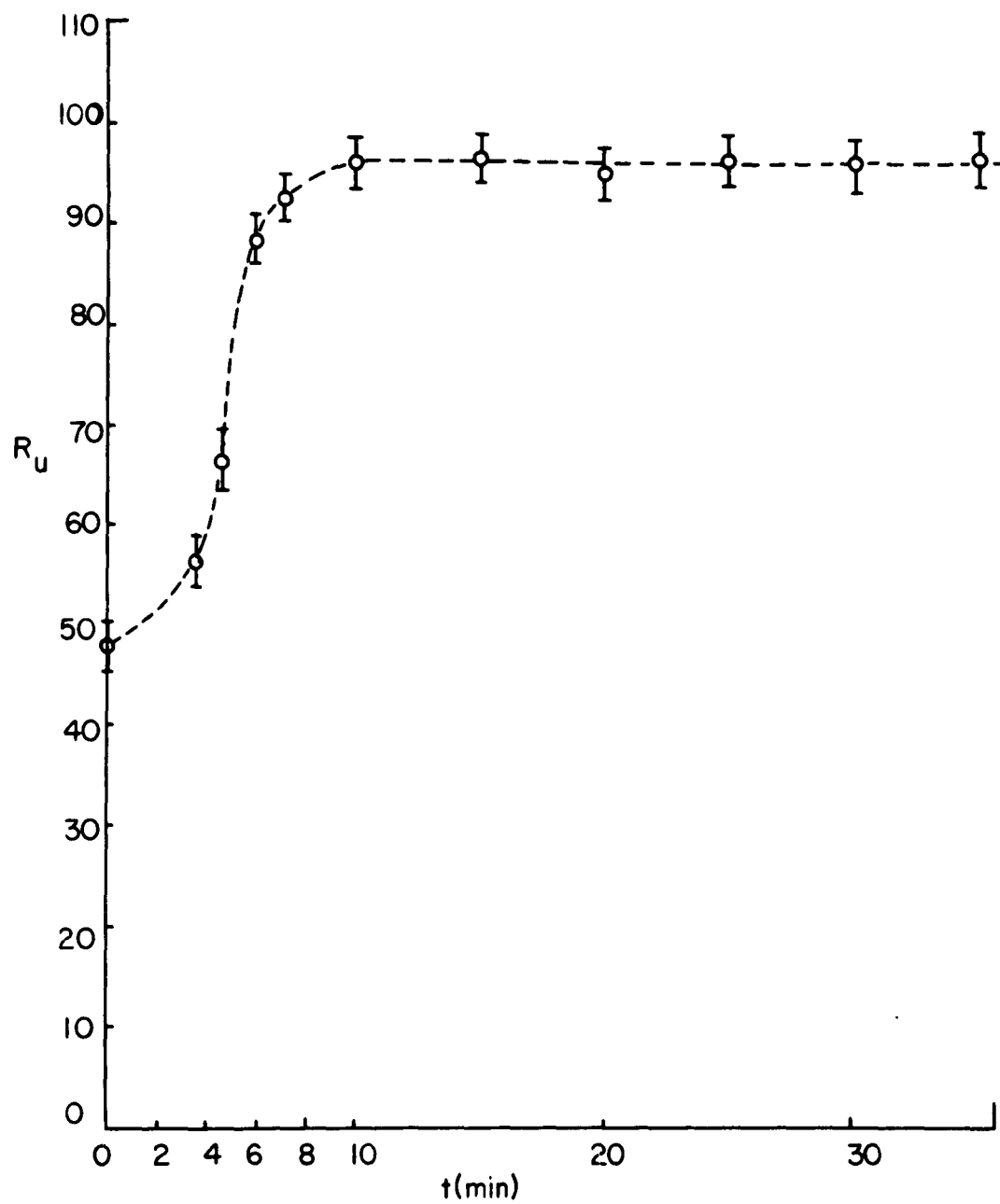
FIGURE 6. --Absorptivity R_u of enzyme-substrate mixture as function of time after mixing.
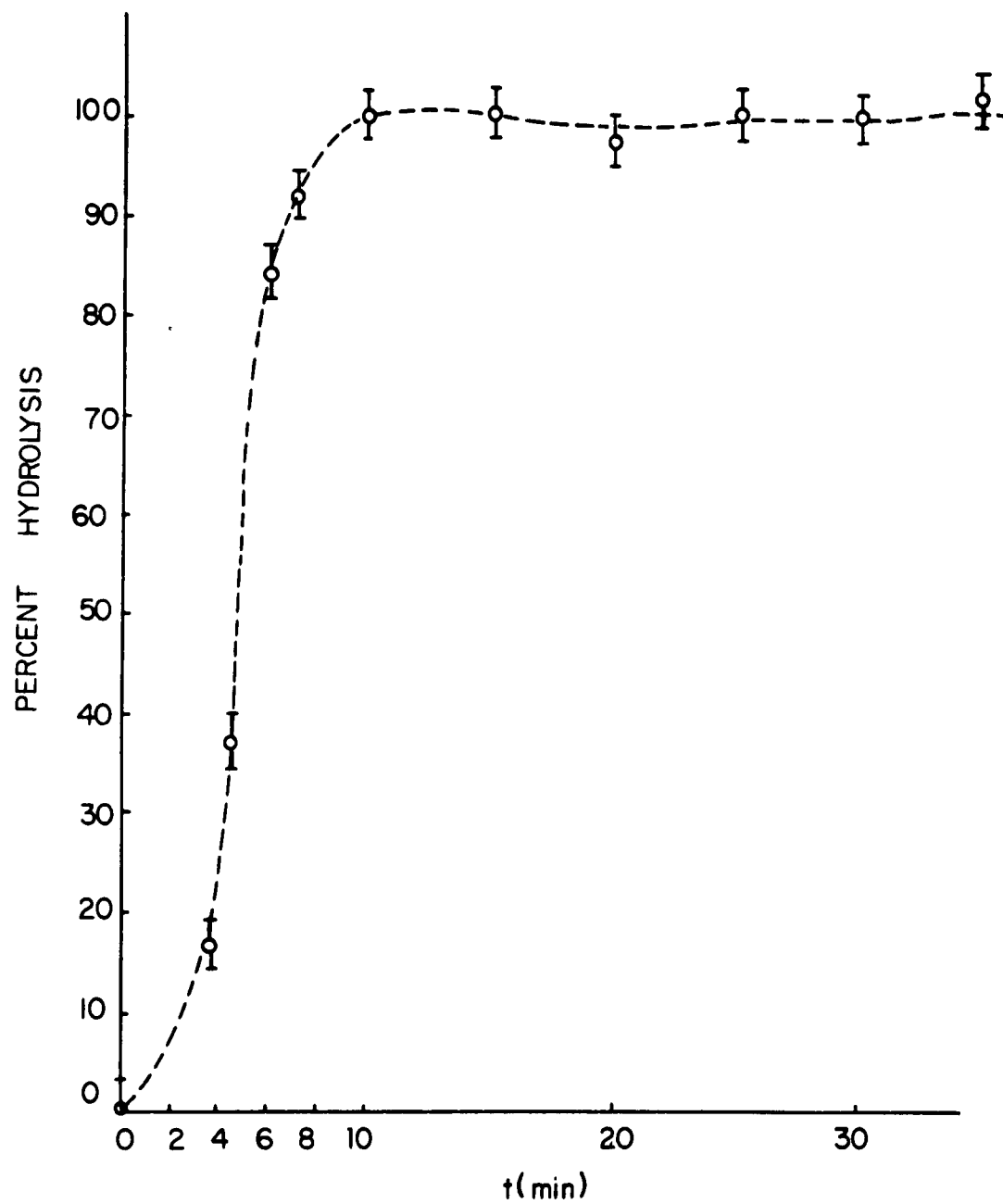
FIGURE 7. --Degree of hydrolysis as function of time after
mixing.

IV. DISCUSSION

A. REVIEW OF THE STRUCTURE OF ICE AND WATER

Water has often been described by the term "broken-down ice structure." We shall first review this "ideal" arrangement of the water molecules and then the structure of water proper, in order to show how some concepts about the structural arrangement in ice are modified by thermal and steric perturbations. This procedure will enable us to gain more insight into the intricacies of the structure of the liquid state of water.

1. THE STRUCTURE OF ICE. Under ordinary conditions water crystallizes in a hexagonal structure of space group $D_{6h}^4 - P6_3/mnc$.[21] Each oxygen atom is surrounded by four oxygen atoms at a distance of 2.76 Å. The tetrahydra thus formed are practically ideal. This is a very open structure which causes ice to have a low density. This structure is the one expected in case O - H . . O hydrogen bonds are formed, with each bond making greater or less use of one of the four valence electron pairs of each of the two bonded oxygen atoms. A given hydrogen atom is closer to one oxygen atom than to the other and each O atom has two H atoms bonded to it by strong bonds. In the gas molecule the O-H distance is 0.96 Å; a rather small difference is found in the frequencies of the vibrational motions of the molecule involving the stretching of the O-H bonds observed for ice and water vapor; this difference has been interpreted[22] as corresponding to the value 0.99 Å for the O-H bond distance in ice.

Bernal and Fowler[23] suggested the following rules for the hydrogen positions:

(1) The H atoms lie on the lines connecting the neighboring O atoms;

(2) there is only one H atom on each such linkage; and

(3) each O atom has two H atoms at a short distance and hence water molecules are preserved.

Pauling[24] calculated the number of possible configurations that are compatible with these three rules to be $(3/2)^N$, where N is the number of oxygen nuclei per mole of ice. It can change from one configuration into another by rotation of some of the molecules (observable at lower frequencies) or by vibrational motion of some of the hydrogen nuclei (at higher frequencies), each oscillating along the line connecting two neighboring oxygen atoms. Both these processes probably occur. The fact that at temperatures above about $200^\circ K$ the dielectric constant of ice is of the order of magnitude of that of water shows that the molecules can orient themselves with considerable freedom, the crystal changing in the stabilizing presence of the electric field from unpolarized to polarized configurations satisfying the above conditions.

Many experimental facts, predominantly the zero-point entropy, the neutron diffraction data,[25] the results of investigations of nuclear magnetic resonance,[26,27] and the electrical properties as interpreted by Gränicher et al.[21] are consistent with a concept of the structure of ice that can be summarized in the following statements:

(1) The half-hydrogen model advanced by Pauling gives an essentially correct description of the long-range or average structure of ice. Polarized regions of opposite orientation or regions that are partially disordered can be joined together without violating the Bernal and Fowler rules governing the positions of the hydrogen atoms. Spontaneous polarization arising from an ordering of protons along a certain axis may be possible up to 20%.

(2) A statistically disordered hydrogen arrangement exists in an ice crystal that strictly obeys the Bernal-Fowler rules,[23] so that changes among the $(3/2)^N$ possible configurations do not occur. A high activation energy would be necessary for such reconstructive transitions, since a considerable number of bonds would have to be broken.

(3) The electrical properties of ice are explained by the following types of imperfections in the lattice of the crystal:

(a) orientational defects

(b) ionized states

These imperfections can diffuse in the crystal and can cause changes in the configurations of the ideal crystal. Since the number of lattice imperfections is quite small, however, these changes are local; furthermore, the concentration of the defects decreases exponentially with temperature so that at very low temperatures no configurational changes can occur at all.

As was mentioned above, the electrical properties of ice can be explained by the existence of lattice imperfections. Bjerrum[28] pointed out that one has to assume the existence of two types of defects:

(a) Orientational defects, generated by the rotation of a water molecule around one of its four bonds, preferentially around one of the bonds with a close-lying proton.

Two normal bonds (B) .... -OH. .O-
give one doubly occupied bond (D) .... -OH. HO-
and one vacant bond (L)   .... -O. . . O-

The reaction equation of this process may be written

$$2B \rightleftharpoons D + L \tag{14}$$
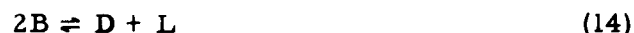
The mass-action law yields for equal numbers of D- and L-defects,

$$n_D \cdot n_L = a^2 \exp(-E_0/kT) = w_0^2 \tag{15}$$

$$n_D = N_D/N_B; \quad n_L = N_L/N_B \tag{16}$$

Here the number of normal bonds N_B is twice the number N of O atoms per unit volume. The constant a takes into account the lattice disturbance created in the proximity of a lattice defect; $n_D = n_L$ is the probability of finding a double or vacant bond on any linkage. If the molecule adjacent to a defect rotates, the defect can move to a neighboring linkage and is thereby enabled to move through the crystal.

(b) Ionized states. Hydroxyl OH^- and H_3O^+ hydronium ions are formed when an H atom actually leaves the O atom to which it was bound and attaches itself to a neighboring water molecule. If such translational motions of protons follow each other, both ionized states can propagate through the structure.

This dissociation mechanism is described by the reversible reaction for liquid water,

$$2H_2 O \rightleftharpoons H_3 O^+ + OH^- \tag{17}$$
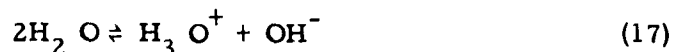
and again the mass-action law gives, for thermal equilibrium,

$$n_+ n_- = b^2 \exp(-E_I/kT) = W_I^2, \quad n_+ = N^+/N; \; n_- = N^-/N \tag{18}$$

where E_I is the activation energy for pair formation and b is a constant similar to the a used in describing the orientational defects. However, this dissociation process has much higher acti-- vation energies than the rotational and vibrational shifts described under "orientational" defects. These ions only take small part in the electrical conduction process at room temperature, since their relaxation times are relatively long (of the order of minutes at $260^{\circ}K$). Actually in pure ice the ratio of hydronium ions to orientational-defect bond vacancies is of the order of 10^{-6}.

2. THE STRUCTURE OF WATER. On the basis of the kinetic theory of matter it is to be expected that collisions between dipole molecules result in at least some cases in the colliding molecules remaining for a time close together and mutually oriented in a preferred manner, as a result of the attraction between the dipoles. While so bonded they act as a single unit. These associated molecules may consist of two or more simple (vapor) molecules and may be themselves bonded more or less strongly with other molecules, associated or simple, if all the molecules are crowded rather closely together as in the case of a liquid. This bonding together of associated molecules may result

in the formation throughout the liquid of numerous mutually independent groups of many molecules, all in any one group having at any instant a similar orientation but each group undergoing a relatively slow but continuous change in its personnel, size, and orientation. Thus the entire volume of the liquid may at any instant be semicrystalline, the direction of the crystal axis varying from point to point even over minute distances, and the entire picture changing from instant to instant.

The x-ray pattern for both ice and water indicates that on the average each oxygen atom has four or very nearly four others as near neighbors. Taking account of this observation in connection with the tetrahedral molecule, Bernal and Fowler[23] developed their theory of the quasicrystalline structure of water. Katzoff[29] thinks that in water there is little if any periodicity in arrangement, and that what little there may be is entirely incidental. In his view the important thing is the relative position of adjacent molecules. They are probably held together in nearly the same manner as in the crystal, but except for that, the arrangement of the molecules is a random one. He found no evidence for the definite "quartz-like" arrangement or for the extensive degree of close packing as postulated by Bernal and Fowler; his observations were in fact incompatible with the assumption of a quartz-like arrangement. His proposed picture is that of a broken-down ice structure.

Warren[30] admits of neither as close nor permanent a binding as is postulated by Bernal and Fowler. He regards the crystal form merely as a kind of ideal that is more or less closely approached in water at any instant, but that is seldom, if ever, fully realized.

Lennard-Jones and Pople[31] recently have put forward the viewpoint that there is very little breaking but considerable bending of the bonds. They obtain very good agreement between the theoretical and experimental temperature variation of the dielectric constant in the range of $0-80^{\circ}$ C but their absolute values are 20% low. Although there must be some bending of bonds which our treatment

neglects, it seems likely that Lennard-Jones and Pople exaggerate its extent in attributing the broadening of the peak in the x-ray radial distribution curve and the temperature variation of the dielectric constant entirely to this effect. The experimental curve rather suggests more molecules at intermediate distances and less bending of bonds.

Pauling[24] alternatively has estimated that the number of broken bonds in water at $0°C$ is approximately 15%.

If one tries to discuss the dielectric properties of solutions and in particular the effect of solutes on the relaxation time of water, it becomes important to arrive at a good estimate of the number of bonds that are broken by the introduction of the solute molecules. A qualitative description of this change in the relaxation time has been given by Collie, Hasted, and Ritson.[19] They picture liquid water as consisting of microcrystalline domains whose boundaries are in continuous movement. When an electric field is applied the boundaries move, with the net result of an orientation of the water molecules in the direction of the applied field. An increase of the temperature or the addition of inorganic ions to the solution is thought to break up the structure to some extent, to increase the boundary area, and to shorten the relaxation time. An increase in structural temperature is shown also by the x-ray and spectroscopic data for ionic solutions. Haggis, Hasted, and Buchanan,[1] however, present conflicting evidence. They show that solutions of organic ions with polar groups have longer relaxation times than pure water. It is difficult to see how these molecules can decrease the boundary area. Stimulated by this incongruity, they attempt to develop a statistical approach to supersede the structural concept. In their approximation they neglect the bending of the bonds and also introduce some uncertainty in the use of the term "breaking of hydrogen bonds," but neverthe- less are able to give good estimates of the static dielectric constant of water as a function of temperature and of the numbers of water

molecules irrotationally bound to different types of solute molecules.

(a) Orientational Defects. The basic similarity of the structures of water and ice and of the concurrent electrical properties leads us to assume that imperfections exist in both that determine their behavior. One approach to that problem is to note that a vacant bond (L) is nothing else but a missing bond in an array of molecules.

Haggis, Hasted, and Buchanan[1] have computed from currently available data the relative numbers of four-, three-, two-, one-, and zero-bonded molecules that exist in water at a certain temperature. Figure 8 shows these values as a function of temperature. The total number of missing bonds or vacancy defects is then easily computed from the relation

$$n_L = \sum_i [(4-i)/4] \, n_i \qquad i = 0, 1, 2, 3, 4 \qquad (19)$$

where n_L is the probability of finding a vacancy on any linkage and n_i is given in the calculation of Haggis, Hasted, and Buchanan.[1] The function n_i is also plotted vs temperature on Figure 8. In their analysis they have assumed that a bond can either be broken or normal, whereas in our interpretation three possibilities can characterize the linkage of two molecules: vacant, normal, and double bonds. Our interest is focused here on the vacant and double bonds that are present in addition to the normal single bonds.

(b) Ionized States. The concentration of OH^- and H_3O^+ ions in water is obtained from the direct measurements of the ion product of the substance. Values for the probability of occurence of the ionized states are plotted vs temperature on Figure 9.

We have shown that one can obtain values for the probabilities of occurrence of lattice imperfections in water. The concentration of these defects is homogeneous in the bulk of the material since they are able to diffuse through the crystal. Whenever a lattice
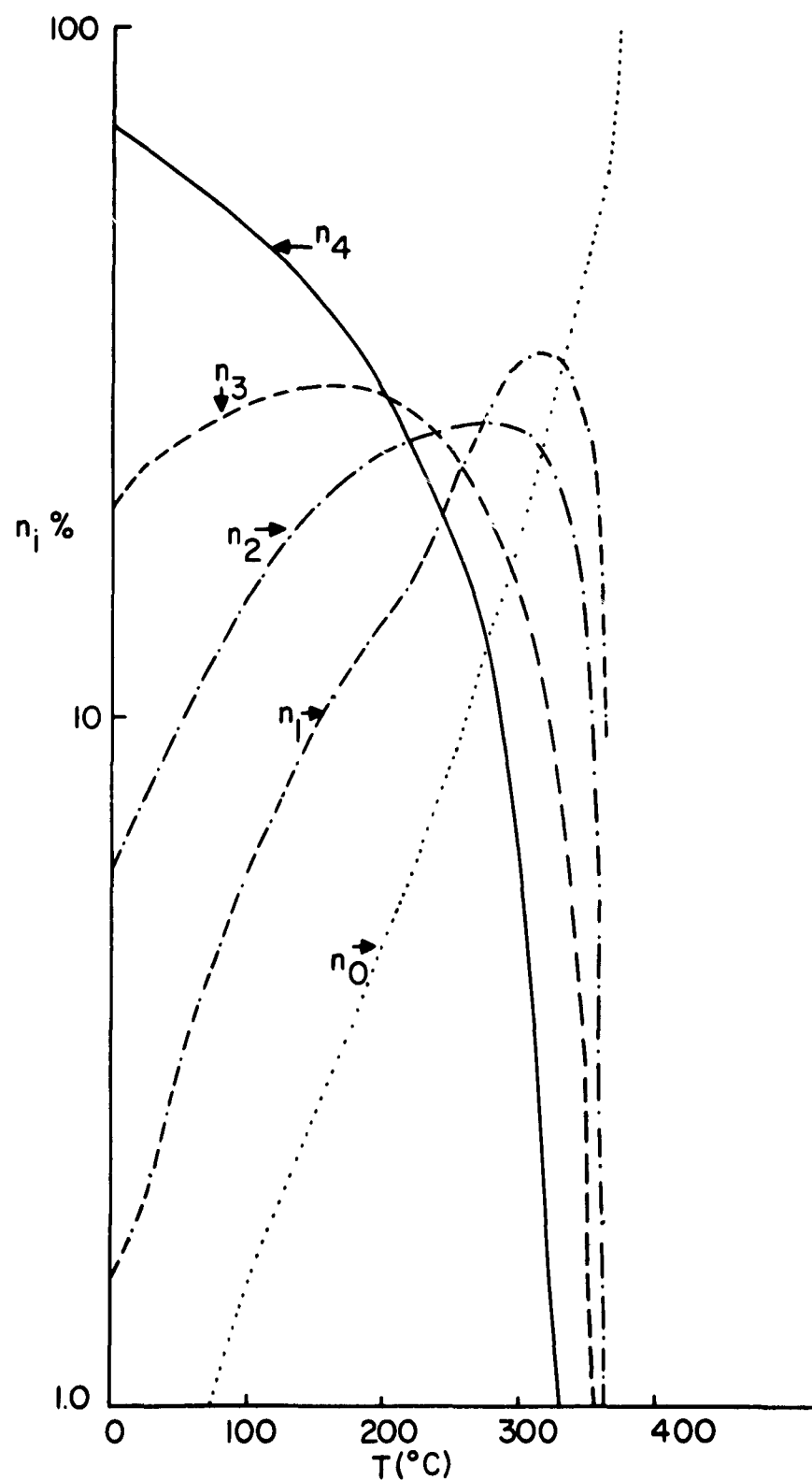
FIGURE 8. --Relative number of water molecules bound to neighboring molecules as function of temperature.
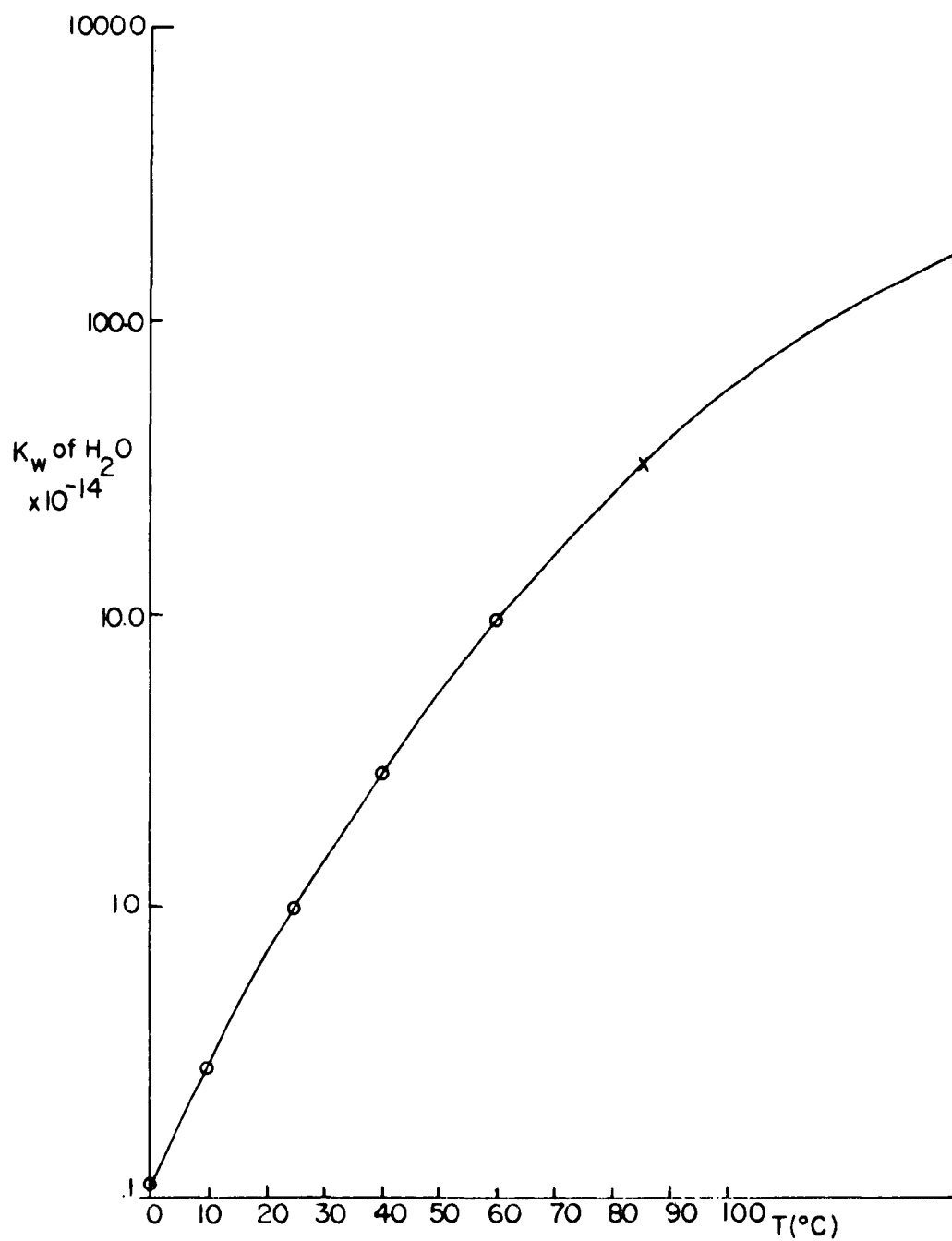
Figure 9. --Ion product of water as function of temperature.

defect has moved past a certain molecule--owing to either ordinary diffusion or a field-induced motion--the molecule is left behind in an orientation depending on the path and nature of the defect. Hence a change in polarization has occurred. Since in all such processes only one proton per molecule is actually shifted, one can either consider the polarization change brought about by the individual shifts or that resulting from the change in the orientation of the dipole moments of all the molecules. In our theory of the dielectric behavior of water we should be able to compute the polarization of the substance in two different ways, one by considering only the individual shifts of protons, the other by computing the dipole moments of all the molecules.

B. NEW MODEL OF WATER USED FOR THE COMPUTATION OF THE DIELECTRIC CONSTANT

As was pointed out by Eigen and de Maeyer,[32] the rate-determining step for proton transport in water is the reorientation of the molecules, so that the dispersion of the dielectric constant in water may be identified as being caused by this reorientation process. This rotation of the molecules occurs normally in water without the influence of external agencies and is due to the thermal energy of the substance. Haggis et al.[1] have computed the relative number of bonds of a water molecule at different temperatures, and we take the missing bonds to be vacancy defects as illustrated in Figure 10. Whereas there is a one-to-one correspondence between the missing bonds and the vacancy defects, the relation of the numbers of double-bond defects to the number of normal bonds is more complicated since rotation of a normally doubly bound or singly bound water molecule does not produce a double-bond defect. One would therefore expect the number of double defects to follow mainly the number of normally four-bound water molecules, and perhaps a little increased by the presence of the three-bound molecules.
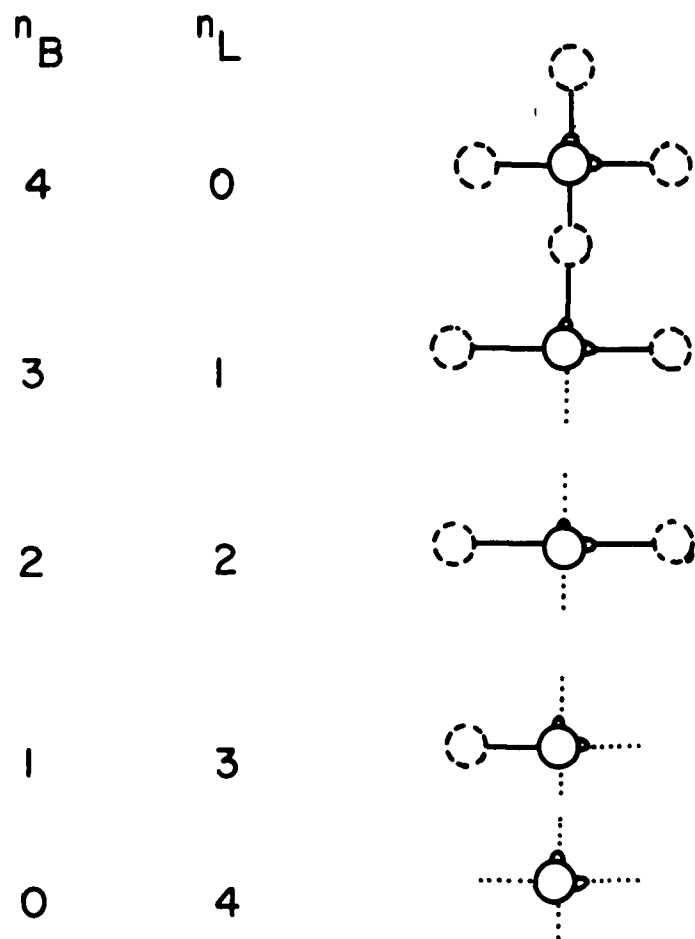
FIGURE 10. --Correspondence between vacancy defects and normal bonds of one water molecule and its neighbors.

The curve representing the number of vacancy defects as a function of temperature is shown in Figure 11. It is calculated from the data of Buchanan et al.[1] The curve for the number of double defects was graphically determined. The number of n_D defects in the temperature range from 370 to 300°C is assumed to be zero, and from those points a straight line is drawn, extrapolating back to 0°C. From 10 to about 30°C we assume the slope of the curve for vacancy defects and double defects to be equal because both of these defects are mainly caused by the reorientation of a four-bound molecule in that temperature region. If we also note that the curve for vacancies deviates from a straight line and that a point exists where this deviation is a maximum, we assume this maximum to coincide with the maximum in the number of double defects as a function of temperature. Since the line extrapolated from the number of vacancy defects in the high-temperature region represents the difference between the number of vacancy defects and double defects, it has to approach a value of zero at 0°C. Taking all these estimates of the behavior of the orientational defects together we were able to draw the curve for the number of double defects as a function of temperature, as shown in Figure 11.

The other parameters that have to be expressed in this model are the average dipole moments of these various types of molecules.

1. AVERAGE DIPOLE MOMENTS. The average dipole moment is the weighted average of the dipole moments associated with the presence of a defect in the structure:

$$\overline{(\mu^2)} = [\overline{(\mu_L^2)}\, n_L + \overline{(\mu_D^2)}\, n_D] \, / \, (n_L + n_D) \tag{20}$$

where $\overline{\mu_D^2}$ refers to the average dipole moment associated with a D-defect and $\overline{\mu_L^2}$ that concomitant with an L-defect.

We wish to calculate the average dipole moment of one water molecule surrounded by others. The calculation proceeds by vector
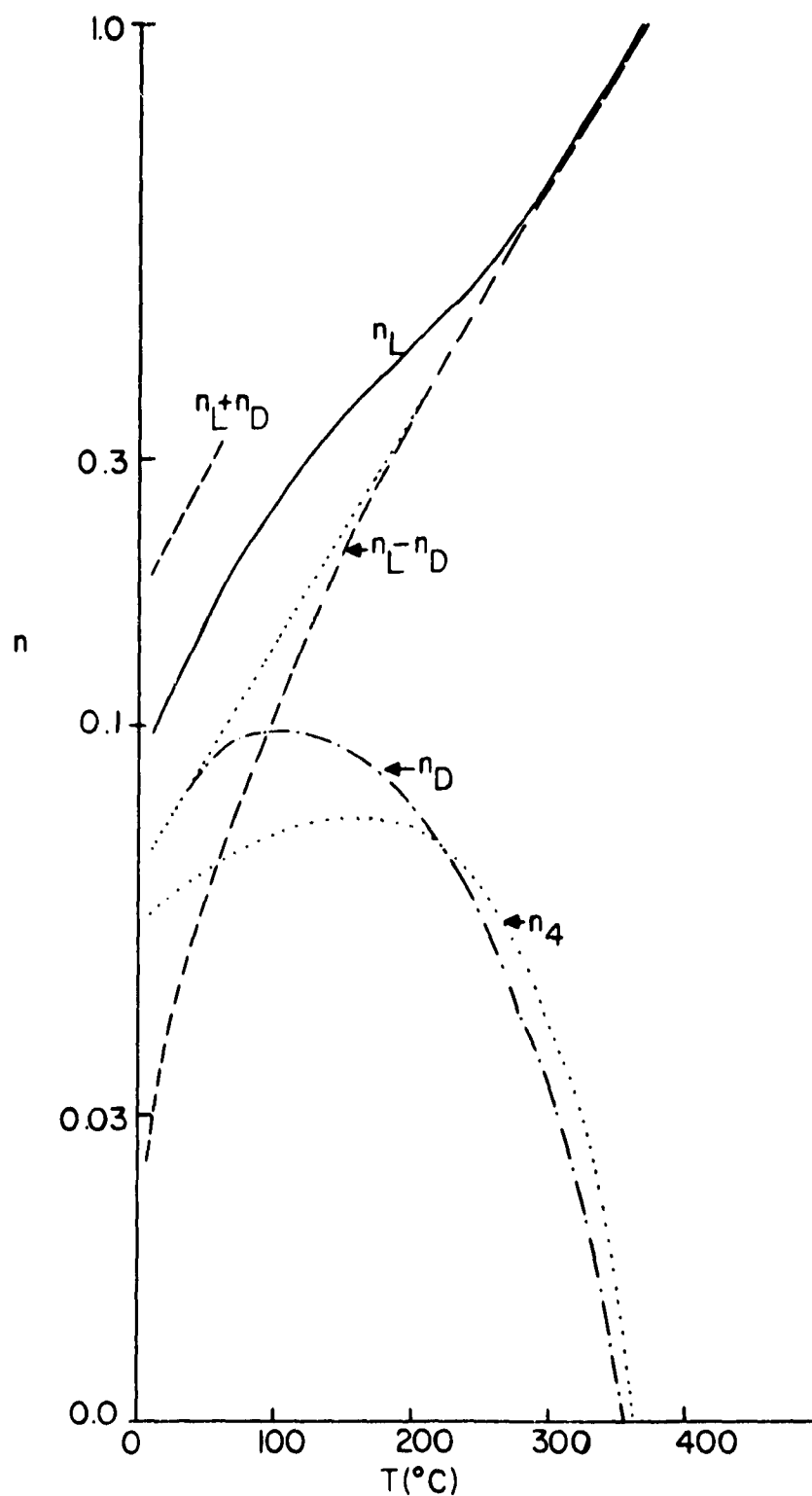
FIGURE 11. --Relative numbers of defects in water
structure as function of temperature.

addition of the moments of several layers of molecules, with care taken that the orientation of the molecules is a matter of the probabilities (g_i) given in Table 4, as function of temperature. Here ($\overline{\mu^2}$) is the product of the intrinsic dipole moment μ of a single water molecule and of $\overline{\mu} = g\mu$, the average dipole moment of a sphere of water immersed in a medium of the same dielectric constant, the central molecule being kept in the fixed orientation μ. The suffixes refer to 4-, 3-, 2-, 1-, and 0-bonded molecules in liquid water. For μ_4 we take Verwey's[33] value of 2.45D, which is not very different from the value calculated assuming dipole interaction[34] for which we have an equation of the type

$$\mu_4 = \mu_0 / [\ 1 - (k/d^3)\ ] \tag{21}$$

where k is a constant and d is the interoxygen distance. The value of μ_0, the dipole moment of the unbonded water molecule (whatever its environment) is taken as 1.88D. Values of μ_3, μ_2, and μ_1 are linearly interpolated between μ_4 and μ_0.

We calculate g_{4D} as follows: $\overline{\mu} = g\mu$ represents the average dipole moment of a macroscopic sphere, in which the central molecule remains in a fixed position μ. Protons can occupy various positions around a single water molecule held in a fixed orientation but the existence of a D- or L-defect limits the choice somewhat as shown in Table 4, where the probabilities of proton positions are depicted. If the angle between bonds is taken as 109°, the vector μ may be resolved into two vectors 0.862μ along the bonds. If we resolve in the direction of μ, we find that the contribution of the central molecule and near neighbors to $\overline{\mu}$ is in the case of a D-defect

$$\overline{\mu} = 0.862\ \mu\ [5 \cos 54^\circ 30' + \frac{5}{3} (\cos 71^\circ)\cos 54^\circ 30'] \tag{22}$$

If we include second and third layers, we have

$$\overline{\mu} = 0.862\ \mu\ \left(5a + \frac{5}{3}\ ab + \frac{7}{3}\ ab + \frac{17}{9}\ ab^2 + \frac{19}{9}\ ab^2 + \frac{53}{27}\ ab^3\right) \tag{23}$$

-41-

TABLE 4. Distribution of molecules around a central fixed molecule.

A. Normal 4-bonded molecule

$T(^\circ C)$	g_4	g_3	g_2	g_1	g_0
0	2.81	2.36	1.90	1.45	1.00
25	2.80	2.35	1.90	1.45	1.00
60	2.79	2.34	1.89	1.45	1.00
100	2.76	2.28	1.86	1.43	1.00
200	2.69	2.24	1.83	1.42	1.00
300	2.55	2.17	1.77	1.39	1.00
370	(2.34)	-	-	-	-
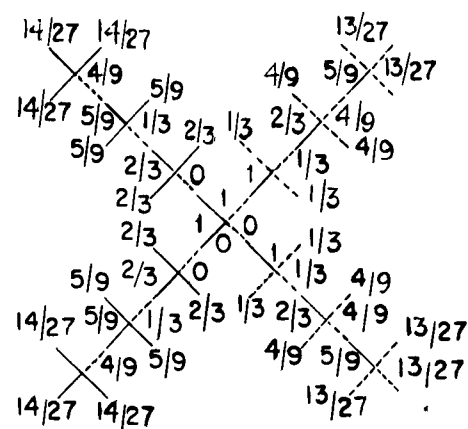
B. D-defect 4-bonded molecule

$T(^\circ C)$	g_{4D}	g_{3D}	g_{2D}	g_{1D}	g_{0D}
0	3.87	2.90	1.93	0.975	0
25	3.85	2.89	1.92	0.970	0
60	3.83	2.87	1.91	0.960	0
100	3.78	2.83	1.90	0.950	0
200	3.68	2.77	1.85	0.925	0
300	3.48	2.62	1.75	0.875	0
370	-	-	-	-	-
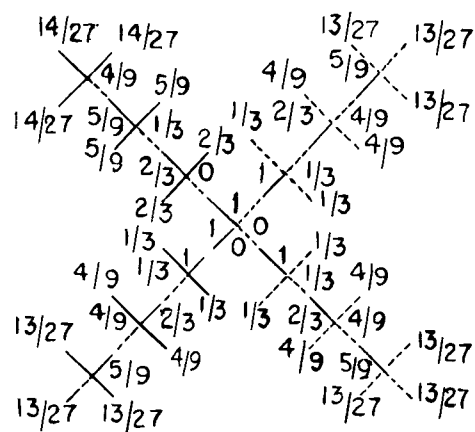
C. L-defect 4-bonded molecule

$T(^\circ C)$	g_{4L}	g_{3L}	g_{2L}	g_{1L}	g_{0L}
0	2.35	2.01	1.68	1.34	1.00
25	2.34	2.00	1.67	1.33	1.00
60	2.31	1.99	1.66	1.33	1.00
100	2.29	1.97	1.65	1.32	1.00
200	2.22	1.92	1.61	1.31	1.00
300	2.08	1.82	1.54	1.27	1.00
370	1.89	-	-	-	-
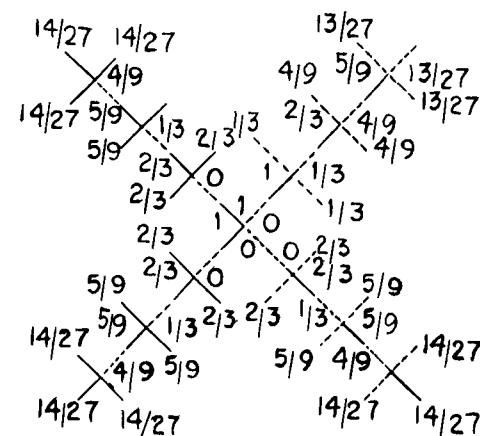
where $a = \cos 54^\circ 30'$ and $b = \cos 71^\circ$, giving

$$g_{4D} = \bar{\mu}/\mu = 3.94 \qquad (24)$$

The additional contribution from further bond layers and from closed rings is found to be negligible.

The values of the g_{4L} for the L-defect dipoles are computed in an exactly similar fashion but from a different proton distribution.

The values of both g_{4D} and g_{4L} vary with the temperature and the percentage of bonds broken. We first estimate the values of g_{4D} and g_{4L} as follows. At 370° C, where nearly all the bonds are broken we should include only one layer of water molecules, since the few molecules of a type that can be bound to others must be surrounded by molecules which form no other bonds. In this case we then have

$$g_{4D} = 0.862 \left(5a + \frac{5}{3} ab \right) = 3.21 \qquad (25)$$

and

$$g_{4D} = 0.862 \left(3a + \frac{7}{3} ab \right) = 1.89 \qquad (26)$$

We assume the percentage of broken bonds $(= n_L)$ to vary from 0 to 1, and g_{4D} to vary linearly with this percentage from 3.94 to 3.21.

We make the further assumption that there is no correlation between the orientations of nonbonded neighbors and the central molecule, so that $g_{0L} = 1$ and $g_{0D} = 0$.

The values of the g_{iLD} are tabulated on Figures 12 and 13 and in Table 4. These values, together with the dipole moments of the fixed molecules (Table 5) and the relative probabilities of the occurrence of those states, give the value of the average squares of the dipole moments according to the relations

$$\overline{(\mu_L^2)} = \frac{\sum \mu_i^2 \, g_{iL} \, n_{iL}}{\sum n_{iL}} \qquad \overline{(\mu_D^2)} = \frac{\sum \mu_i^2 \, g_{iD} \, n_{iD}}{\sum n_{iD}} \qquad (27)$$
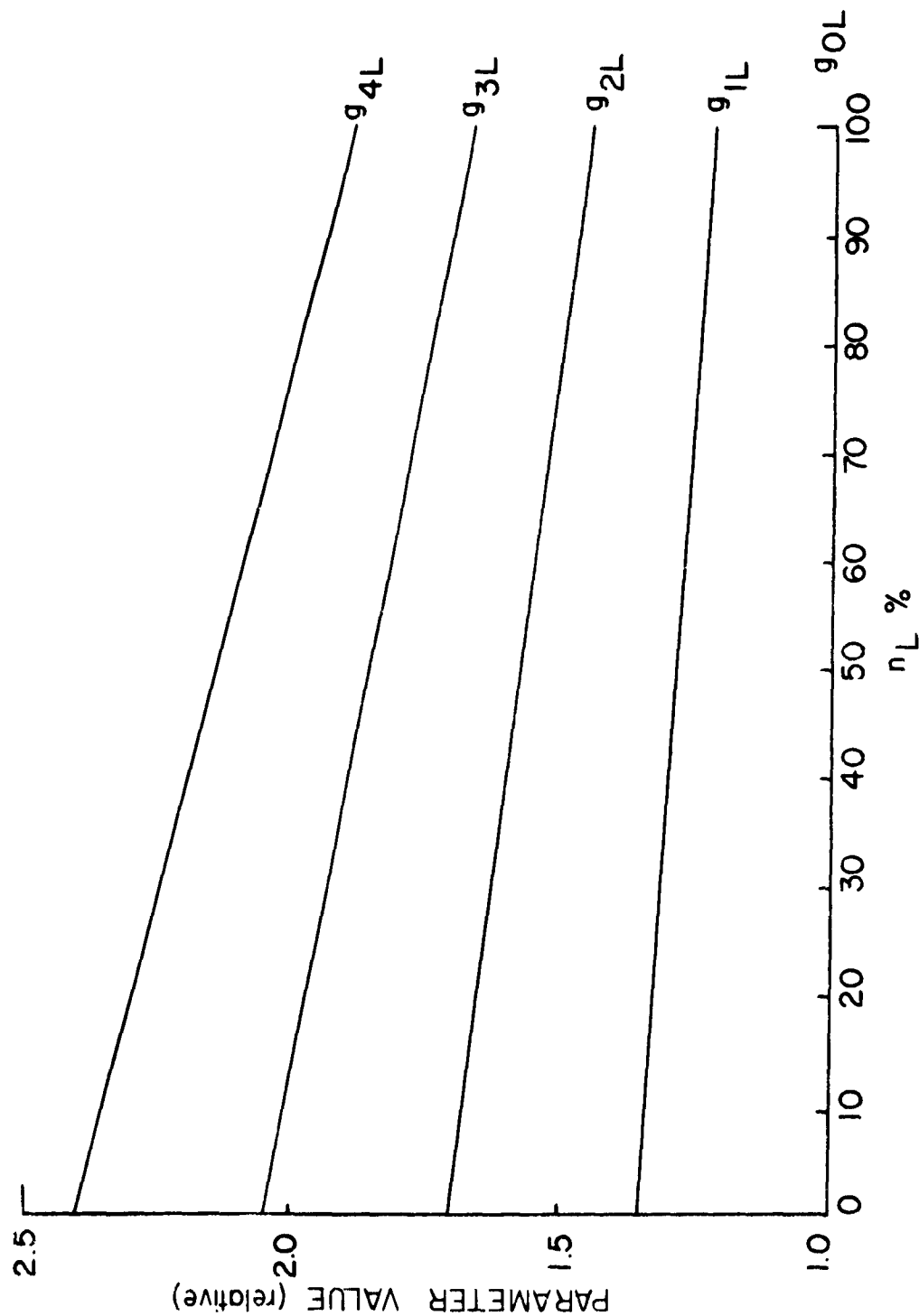
FIGURE 12. --Dipole-moment parameters associated with vacancy defects as function of the number of vacancy defects.

PARAMETER VALUE (relative)

n_L %

g_{4D}

g_{3D}

g_{2D}

g_{1D}

g_{0D}
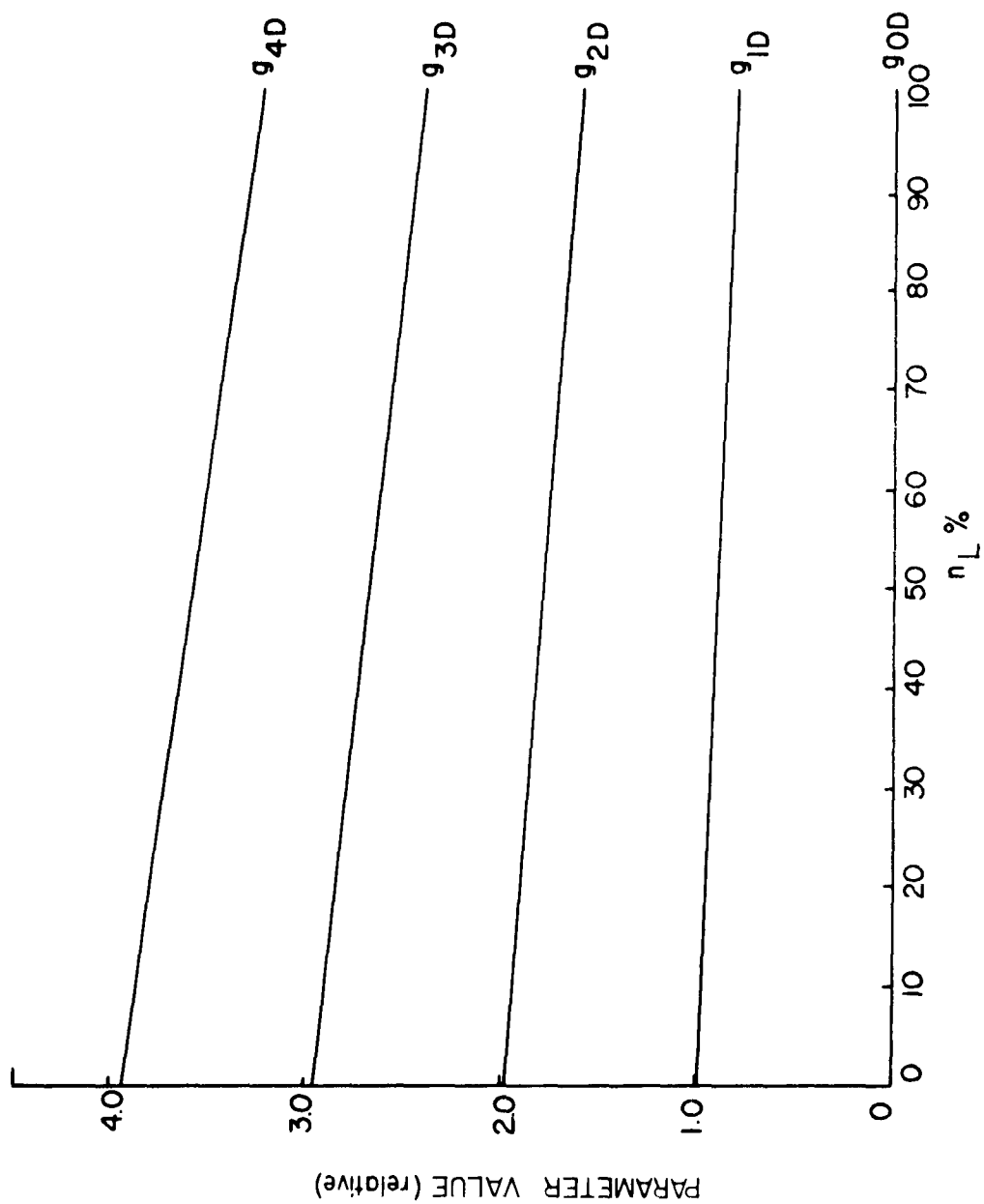
TABLE 5. Dipole moments of fixed water molecules bound to different numbers of neighbor molecules as function of temperature.

$T(^{\circ}C)$	μ_4	μ_3	μ_2	μ_1	μ_0
0	2.45	2.30	2.18	2.03	1.88
25	2.44	2.29	2.17	2.03	1.88
60	2.42	2.27	2.16	2.02	1.88
100	2.39	2.25	2.16	2.02	1.88
200	2.29	2.21	2.10	2.00	1.88
300	2.18	2.10	2.03	1.96	1.88
370	-	-	-	-	1.88

2. THE DIELECTRIC CONSTANT OF WATER, AS COMPUTED FROM THE ORIENTATIONAL DEFECT MODEL.

Fröhlich[35] has formulated a general theory of the dynamic behavior of a dielectric containing particles of charge e with two equilibrium positions separated by a distance δ and a potential barrier of height E between them. The distance of separation is actually a statistical average of the fraction of favorable jumps of the charges and of the shift components in the field direction of the individual jumps. In this theory, then, the product of charge and distance of separation of the charges is equivalent to a dipole moment and can actually be replaced by it if we use the average dipole moments in our calculations.

We first consider one charge that has two possible equilibrium positions. Without an external field this charge has a certain transition probability from one position to the other one that is equal to the probability w_0 of diffusion of that charge over the potential barrier:

$$w_0 = \nu \exp(-E/kT) \tag{28}$$

where ν is the frequency of oscillation of the particle. This argument is rather difficult to justify rigorously, but it may be taken as qualitatively reasonable. A careful discussion is given by Zener.[36]

Starting now from equilibrium in the absence of a field, the immediate effect of the application of a field in the $A \longrightarrow B$ direction is to lift the potential near A by the amount $e\delta F$ as illustrated in Figure 14. By introducing a normalization of the potential of the external field the two exponents can be written in a more symmetrical way as

$$E - [(e\delta F)/2] \quad \text{and} \quad E + [(e\delta F)/2] \tag{29}$$

With this normalization the probabilities for the transfer of a particle are

$$w_{12 \atop 21} = w_0 \left[1 \pm (e\delta F)/2kT \right] \quad kT < < E \tag{30}$$

if we introduce for $\nu \exp - (E/kT)$ the probability w_0, where ν is the rotational frequency of the molecule which depends somewhat on temperature.

Thus if at any instant in time there is a number of particles $N_1(t)$ at A and a number $N_2(t)$ at B, a number $N_1 w_{12}$ flows per unit time from A to B and a number $N_2 w_{21}$ from B to A. Therefore, the rates of change of N_1 and N_2, respectively, are given by

$$dN_1/dt = -N_1 w_{12} + N_2 w_{21} \tag{31}$$

$$dN_2/dt = -N_2 w_{21} - N_1 w_{12} = -dN_1/dt \tag{32}$$

It follows that the total number of particles N

$$N = N_1 + N_2 \tag{33}$$

is independent of time, as required, because

$$dN_1/dt + dN_2/dt = dN/dt = 0 \tag{34}$$
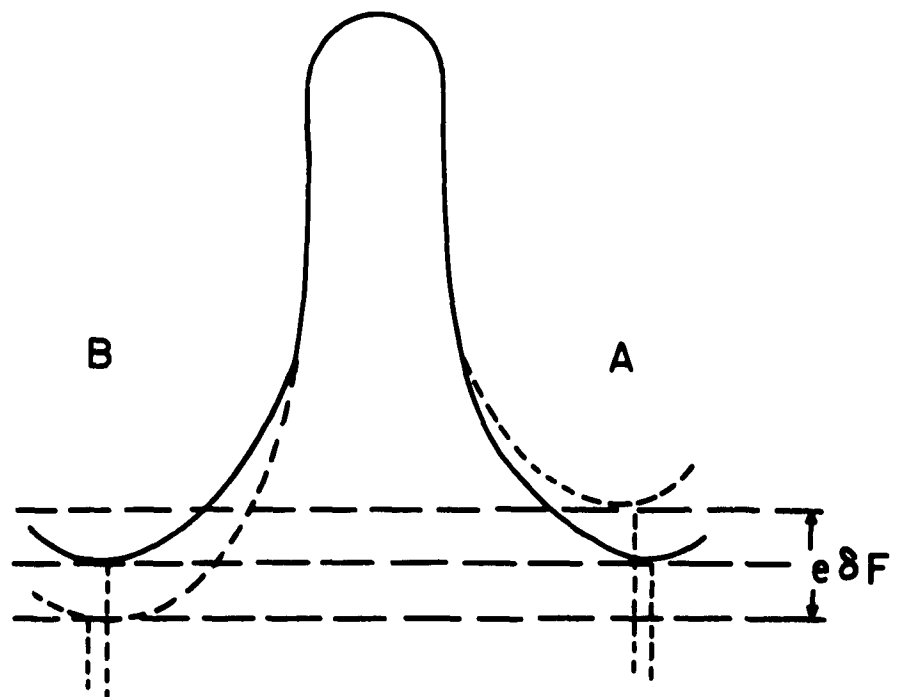
Dotted curve holds in external field F

FIGURE 14. --Potential energy of a charged particle
with two equilibrium positions.

Subtraction of (31) from (32) with the use of (33) yields

$$d(N_2 - N_1)/dt = -(w_{12} + w_{21})(N_2 - N_1) + (w_{12} - w_{21})(N_1 + N_2) \quad (35)$$

Substitution of (30) into (34) gives in place of equation (35)

$$\frac{1}{2w_0} \frac{d(N_2 - N_1)}{dt} = -(N_2 - N_1) + \frac{e\delta F(N_2 + N_1)}{2kT} \quad (36)$$

This equation can be solved for a periodic external field written in the form $F = F_0 e^{j\omega t}$:

$$(N_2 - N_1) = (N_2 + N_1) \frac{e\delta F_0}{2kT} \frac{e^{j\omega t}}{1 + (j\omega/w_0)} \quad (37)$$

since

$$(N_2 - N_1) e\delta = P_0 \quad (38)$$

$$\epsilon^*_{(\omega)} - \epsilon'_\infty = P_0 / \epsilon_0 F_0 \quad (39)$$

$$\epsilon^*_{(\omega)} - \epsilon'_\infty = \left[(N_2 + N_1) e^2 \delta^2 / 2\epsilon_0 kT \right] \{ 1 / [1 + (j\omega/2 w_0)] \} \quad (40)$$

If we compare this formula with the equation for a Debye dispersion and consider $\epsilon^* = \epsilon' - j\epsilon''$, we obtain

$$\Delta\epsilon' = \epsilon'_s - \epsilon'_\infty = (N_2 + N_1) e^2 \delta^2 / 2\epsilon_0 kT \quad (41)$$

where ϵ'_s is the static dielectric constant at $\omega = 0$ and τ_d is the relaxation time given by

$$\tau_d = 1/2w_0 \quad (42)$$

Since in this analysis we may use $e\bar{\delta}$ and $\bar{\mu}$ interchangeably Eq. (41) may also be written as

$$\Delta\epsilon' = \epsilon'_s - \epsilon'_\infty = (N_2 + N_1) \bar{\mu}^2 / 2\epsilon_0 kT \quad (43)$$

Following Debye's analysis[17] the various parts of the dielectric constant can then be computed by use of the formulae

$$\epsilon' = \epsilon_\infty + \frac{\epsilon_s - \epsilon_\infty}{1 + x^2} \quad (44)$$

$$\epsilon'' = (\epsilon_s - \epsilon_\infty) x / (1 + x^2) \qquad (45)$$

$$\tan \phi = (\epsilon_s - \epsilon_\infty) x / (\epsilon_s + \epsilon_\infty x^2) \qquad (46)$$

where

$$x = (\epsilon_s + 2) \omega \tau_d / (\epsilon_\infty + 2) \qquad (47)$$

To compute those values we have to know, in addition to $\Delta\epsilon'$, the value of x. Since

$$x = (\epsilon_s + 2) \omega \tau_d / (\epsilon_\infty + 2) \qquad (48)$$

this problem is reduced to finding the relaxation frequencies of the defects. In Eq. (42) we defined τ_d as equal to $1/2w_0$ where, according to (28), $w_0 = \nu \exp(-E/kT)$. As an electric field is applied to the dielectric the defects move and the probabilities of transition of D-defects w_D or L-defects w_L assume a value which is the product of the probability of having a defect, times the probability of transition of that defect:

$$w_D = w_0 n_{D'} \qquad\qquad w_L = w_0 n_L \qquad (49)$$

and since $\omega_D = 2w_{D'}$ the relaxation frequencies are

$$\omega_D = n_D (\nu_r / 2) \exp (-E_r^{(D)} / kT) \qquad (50)$$

$$\omega_L = n_L (\nu_r / 2) \exp (-E_r^{(L)} / kT) \qquad (51)$$

where ν_r = vibrational frequency of the molecule. The relaxation frequency ω_R of recombination of D- and L-defects is

$$\omega_R = n_D n_L (\nu_r / 2) \exp (-2E_r^{(D)} - 2E_r^{(L)}) / kT \qquad (52)$$

For ease in computing and tabulating we define

$$\epsilon' = \epsilon_\infty + B_L / (1 + x_L^2) \qquad \epsilon'' = B_L x_L / (1 + x_L^2) \qquad (53)$$

since in our experiment we only observe the dispersion due to vacancy defects. Here

$$x_L = [(\epsilon_s + 2)\, \omega / (\epsilon_\infty + 2)\, \omega_L] \qquad (54)$$

$$B_L = \frac{N(\overline{\mu^2})}{\epsilon_0 kT} = K\, \frac{(\overline{\mu^2})\, n_L}{n_L + n_D} \qquad (55)$$

where $K = N/\epsilon_0 kT$, $\epsilon_s = B + \epsilon_\infty$, and $\epsilon_\infty = 5.5$. The constant term in Eq (55) is computed to be $K = 3.03 \times 10^3$ in the absolute practical unit system. Here N is defined by

$$N = N_A \rho / M \qquad (56)$$

and μ is given in Debye units, ρ is the density of water, N is the number of molecules per cubic meter, and M is the molecular weight of water.

We have used this new model of the arrangement of water to compute the value of the dielectric constant as a function of temperature. The results of these calculations are tabulated in Table 6.

TABLE 6. Theoretical computations of the static dielectric constant of pure water.

T (°C)	$(\overline{\mu^2})n_L$	$n_L + n_D$	K	B	ϵ_s calc.	ϵ_s obs.	$\Delta\epsilon_s$
10	1.175	0.1620	10.75	78.0	83.5	84.1	0.6
15	1.225	0.1700	10.55	76.0	81.5	82.2	0.7
20	1.280	0.1775	10.40	74.9	80.4	80.4	0.0
25	1.330	0.1865	10.20	72.7	78.2	78.3	0.1
30	1.385	0.1940	10.05	71.8	77.3	76.7	0.6
35	1.440	0.2030	9.90	70.3	75.8	75.0	0.8
40	1.480	0.2120	9.75	68.1	73.6	73.4	0.2
45	1.545	0.2210	9.60	67.1	72.6	71.7	0.9
50	1.595	0.2310	9.50	65.6	71.1	70.1	1.0
55	1.650	0.2410	9.35	64.0	69.5	68.4	1.1
60	1.695	0.2520	9.25	62.1	67.6	67.0	0.6

The agreement is quite good in this temperature range. The errors arise partially from errors in the observed values (about 0.5%) and also from the uncertainty of the value of the dielectric constant at optical frequencies. In our calculations we assumed ϵ_∞ to be equal to 5.5 as was also assumed by Haggis et al.,[1] but this constant may well vary with temperature, as can be seen from the values for the high-frequency dielectric constant that was computed by Hasted and El Sabeh.[18] These values vary between 5.0 and 6.0 from 0 to 60° C. In our calculations, the average value of those constants was used.

The values of the average dipole moments of the molecules associated with vacancy defects are shown in Figure 15 and the numbers of the sum of both types of orientational defects as a function of temperature in Figure 16.

These calculations assume the theoretical values of n_L and n_D as given in Figure 8, and result in agreement between theory and experiment of better than 1.2%, compared with calculations by Lennard-Jones and Pople[31] (20%) and by Oster and Kirkwood[33] (10%).

C. DISCUSSION OF EXPERIMENTAL RESULTS

1. IONIC SOLUTIONS. As examples of ionic solutions we investigated aqueous solutions of sodium chloride and sodium iodide. The results of the dielectric measurements are given in Table 2.

From our theory of the dielectric constant of water we see that the effect of the introduction of an impurity (a solute molecule) changes the number of vacancy and double defects existing in the pure water, and that these numbers therefore have to be replaced by

$$n_{tot} = n_L \pm \Delta n \tag{57}$$

where n_{tot} is now the total number of vacancy defects and Δn signifies the increase or decrease in the original number of defects due to the rearrangement of the molecules around the impurity or solute molecule.
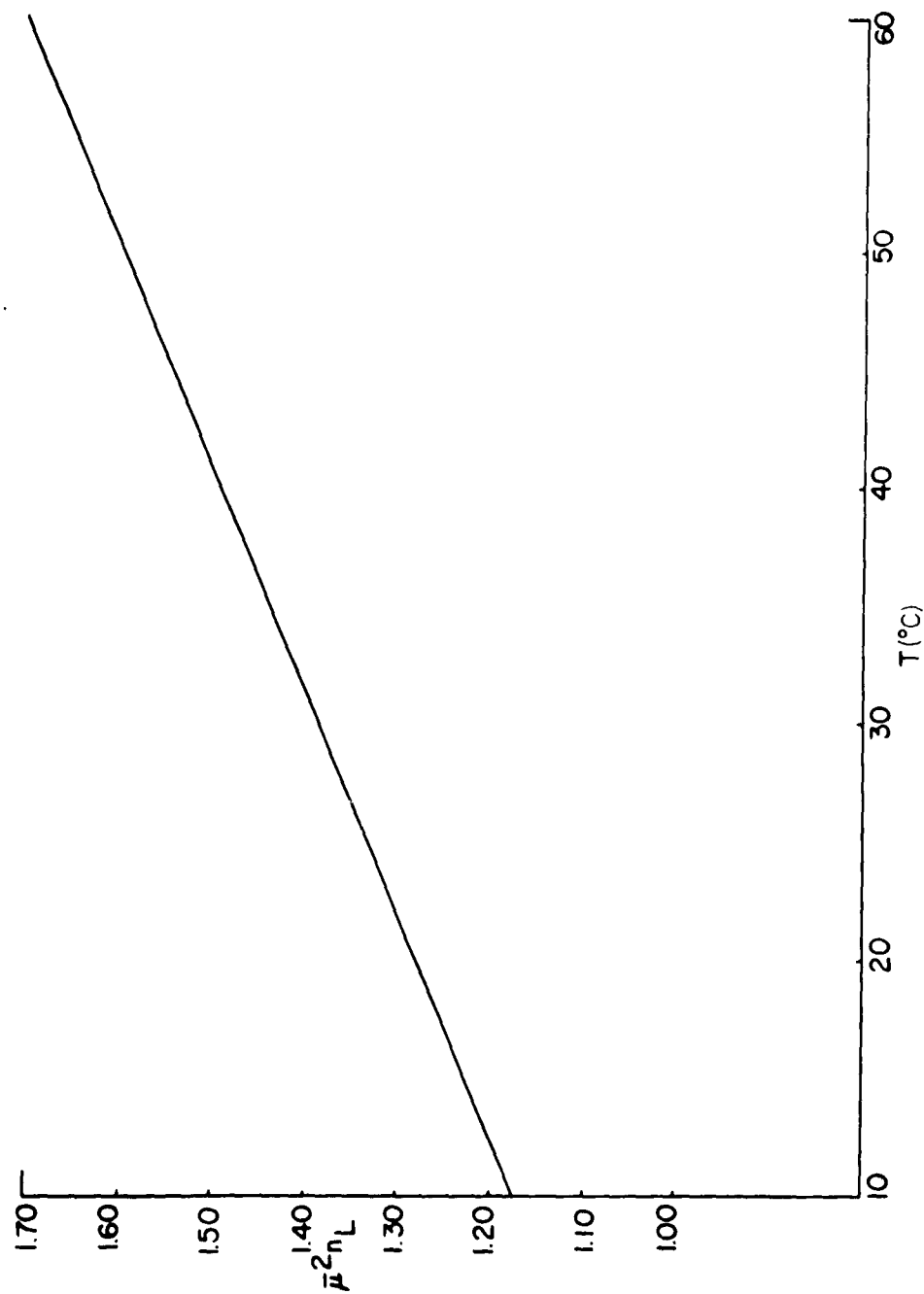
FIGURE 15. --Average dipole moment as function of temperature.
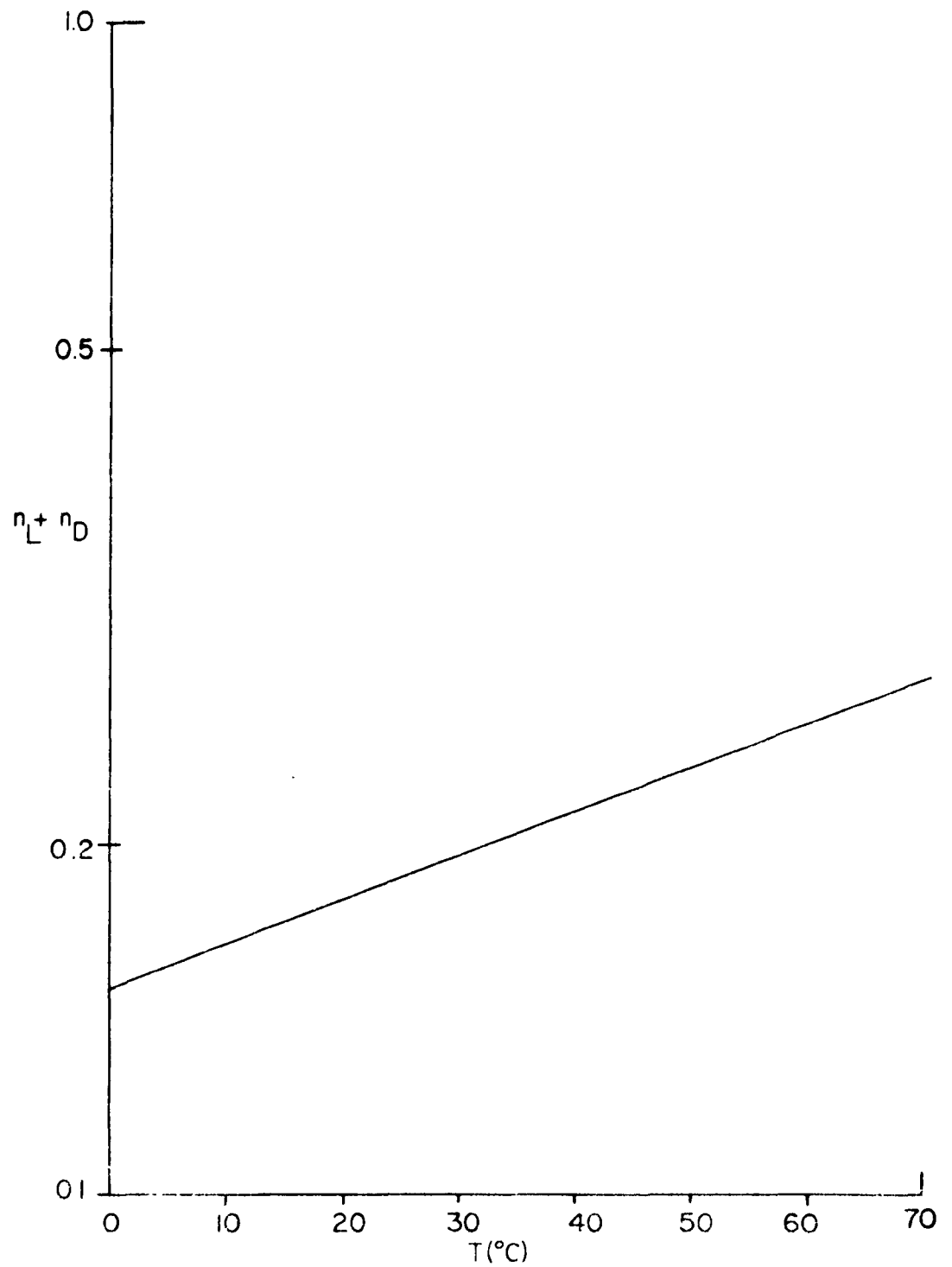
FIGURE 16. --Total number of defects as function of
temperature.

The Debye equations applicable in the region of the electro-magnetic spectrum which we chose for our study are those pertaining to the number of vacancy defects in the material:

$$\epsilon' = \epsilon_\infty + [B_L/(1 + x_L^2)], \quad \epsilon'' = B_L x_L/(1 + x_L^2) \tag{58}$$

Here we may solve for the parameter x:

$$x = \epsilon''/(\epsilon' - \epsilon_\infty) \tag{59}$$

For the parameter x we may also write (cf. Sec. IV-B-2),

$$x = \frac{B + \epsilon_\infty + 2}{\epsilon_\infty + 2} \cdot \frac{\omega}{\omega_L} = \frac{(B + \epsilon_\infty + 2)}{(\epsilon_\infty + 2)} \cdot \frac{K}{n_L} \tag{60}$$

where K is given by $K = 4\pi \exp E_r^L / kT$. We also note that a change in the value of B not only signifies a change in the value of n_L or n_D but also in the total number of water molecules N_B

$$B = K' N_B n_L/(n_L + n_D) \tag{61}$$

where N_B is the number of water molecules per unit volume. This number changes from the value in the pure substance to bne in which some water molecules are replaced by solute molecules.

If we want to correlate an increase or decrease in the number of vacancy defects owing to the presence of the solute molecule with a description of our experiment, we have to normalize our expression for x in order to refer to the same number of water molecules per unit volume:

$$\Delta n_L = n_{Lc} - n_{L0}; \; n_{Lc} = \frac{n_{L0} + n_{D0}}{n_{L0}} \left(\frac{B_c}{\epsilon_\infty + 2} + 1 \right) \frac{K}{x_c} \frac{B_0}{B_c} - n_{Dc} \tag{62}$$

Here the subscript c denotes values of the parameters at a certain concentration of solute molecules, and 0 in pure water.

In the case of the sodium chloride solution the change in vacancy defects at unimolar concentration (Figure 17) amounts to $\Delta n_L = 0.03$ which is equivalent to an increase of three vacancy
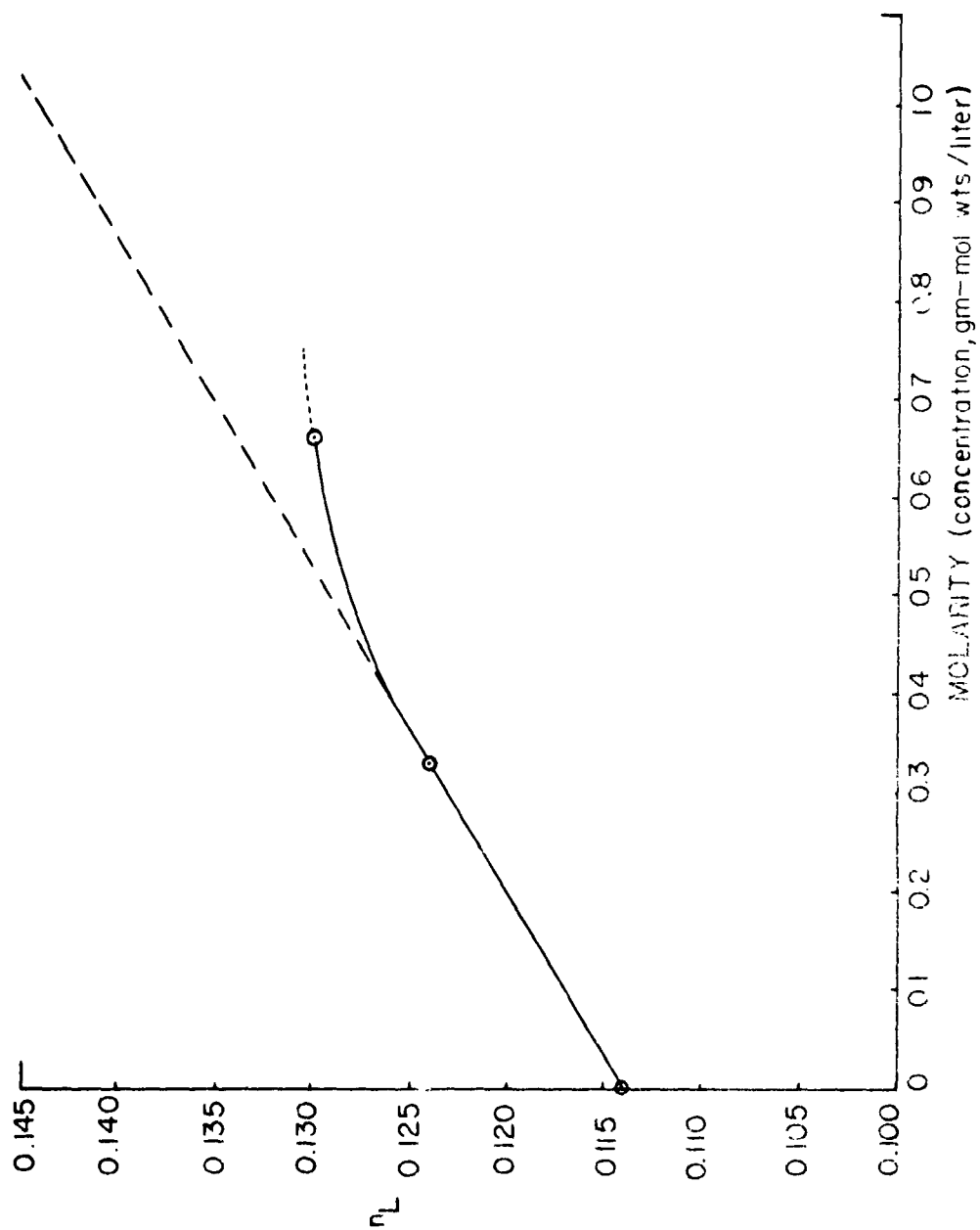
FIGURE 17. --Number of vacancy defects in sodium chloride solution as function of concentration.

MOLARITY (concentration, gm-mol wts/liter)

defects per 100 normal water bonds. At that concentration there are 50 water molecules per ion pair and about 100 bonds per 50 water molecules, so that three new vacancy defects are created per ion pair (Figure 18). We assume that the variation of defects with concentration of the substance in water varies linearly at least at low concentrations. Figure 17 shows these values graphically.

The constant of proportionality is computed to be

$$K = \frac{n_{LW} \epsilon_W'}{\epsilon_W' - \epsilon_{\infty W}} = \frac{0.114 \times 29.4}{63.3 - 5.5} = 0.060 \tag{63}$$

where the subscript w denotes values for pure water.

The value of the number of vacancy defects is then obtained by

$$n_{LM} = K(\epsilon_M' - \epsilon_\infty)/\epsilon_M'' \tag{64}$$

where the subscript M denotes the quantity observed at molarity M.

For unimolar concentration change, the change in the number of vacancy defects is 3% or three vacancy defects per 100 normal bonds. Since there are 50 H_2O molecules per ion pair and 100 bonds per 50 H_2O molecules at a concentration of 1 mole/liter, we see that an increase of three vacancy defects results per single ion pair.

2. SOLUTIONS OF MATERIALS FORMING HYDROGEN BONDS. The changes in the dielectric constant resulting from the addition of propionic acid to water are tabulated in Table 2. For the determination of n_L and n_D the same procedure as described above for the ionic solutions was followed with the exception that here it was not necessary to correct the data obtained at the lower frequency for the contribution of the relaxation due to ionized states.

As more hydrogen bonds are formed owing to the addition of propionic acid a decrease in the number of vacancy defects is observed corresponding to the fact that a water molecule adjacent to the COOH group can form four hydrogen bonds. Before the introduction

-57-

H₂O MOLECULE
AND POSITIVE ION
(a)

H₂O MOLECULE
AND NEGATIVE ION
(b)

(A)

(B)

(C)
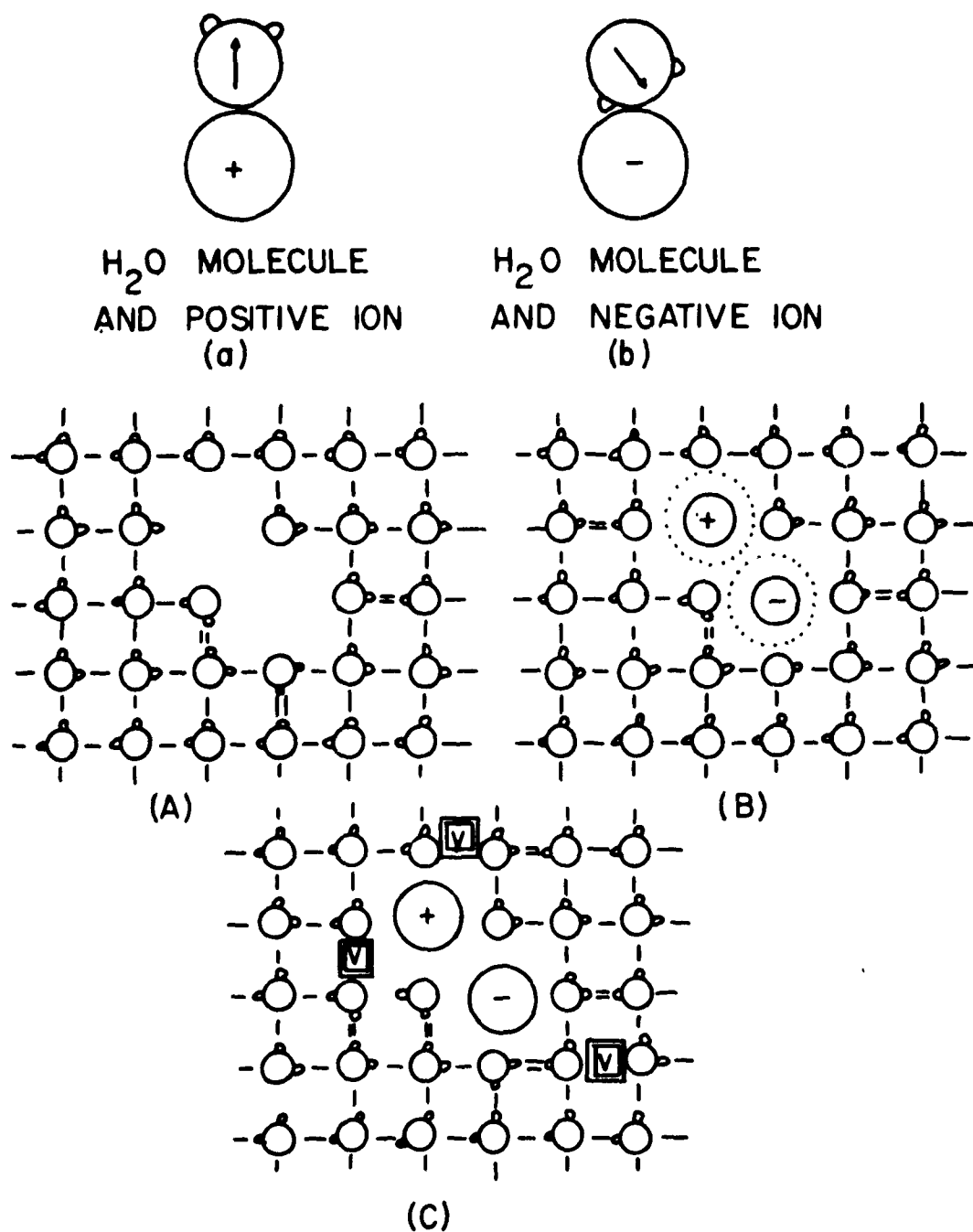
FIGURE 18. --Rearrangement of dipole moments of water
molecules owing to introduction of an ion pair.
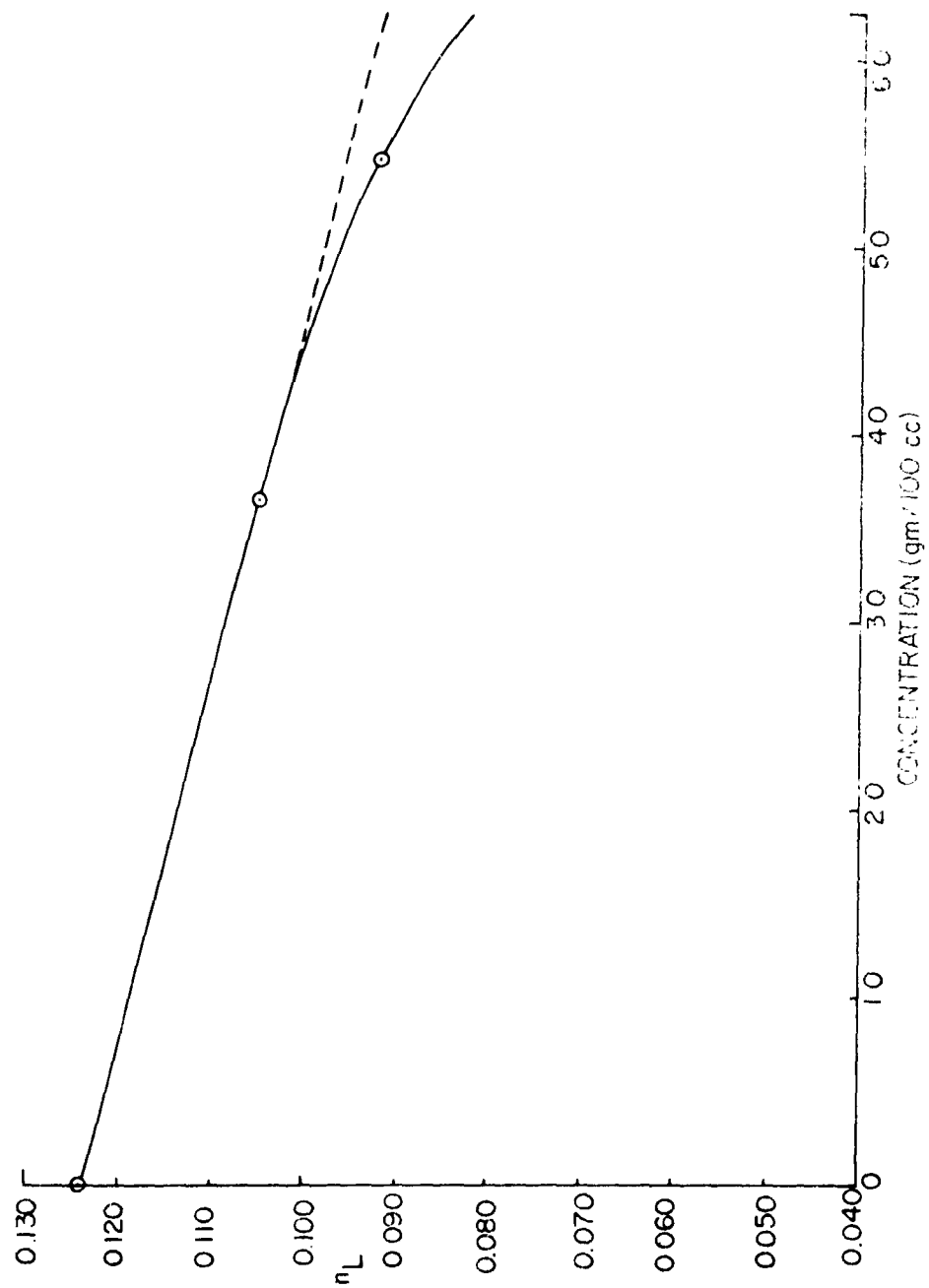
FIGURE 19.--Number of vacancy defects in solution of pepsin as function of concentration.
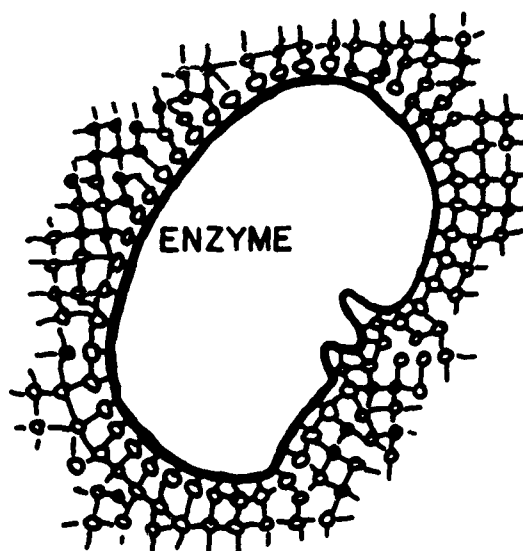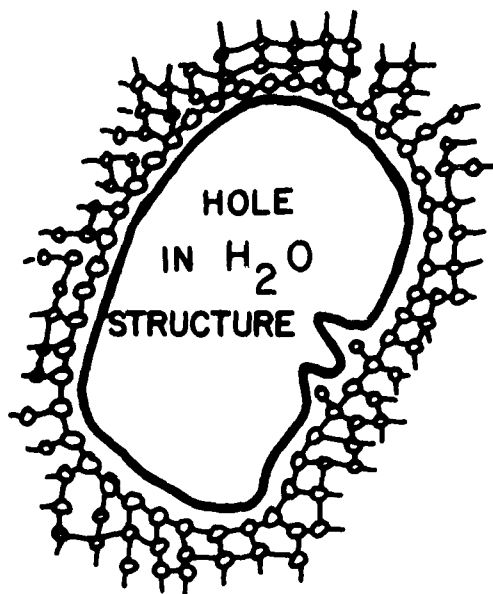
FIGURE 20. --Difference in the relative number of vacancy
defects on introduction of pepsin into the
water structure.

of that group an unbonded space existed temporarily that made it possible for the COOH group to be introduced into the structure. After the group had become a part of the structure, some vacancy defects could vanish, because some molecules could form bonds with the molecules of the COOH group.

3. ENZYME SOLUTION. By the same method as described above the number of vacancy defects was determined in a solution of 3.64% pepsin in pH = 4 buffer solution at $37^{\circ}C$ (Figure 19). The resultant changes are also shown in Table 2 and in Figure 20. One pepsin molecule corresponds to a decrease of approximately 2000 vacancy defects. This result is not unexpected if we note, as shown on Table 7, that about 1000 water molecules are bound to every pepsin molecule, as computed from the coordination numbers of the amino acid residues of the protein.[37, 38] For the enzyme solution the constant of proportionality is determined similarly as for the salt solutions. Since the pure water is at $37^{\circ}C$ rather than at $25^{\circ}C$ the constant of proportionality assumes a different value:

$$K = \frac{n_{LW}\, \epsilon_W{}''}{\epsilon_W{}' - \epsilon_\infty} = \frac{0.124 \times 24.2}{59.7} = 0.050 \tag{65}$$

and the decrease in the number of vacancy defects with the addition of 10^{-3} M pepsin is found to be 2% or two vacancy defects per 100 normal bonds. Since at 10^{-3} M concentration there are 50×10^3 water molecules per pepsin molecule and 100 bonds per 50 water molecules we find that one pepsin molecule is responsible for a decrease of approximately 2000 in the number of vacancy defects.

TABLE 7. Amino acid composition of the enzyme pepsin.

Amino acid	Number of residues/mole	Assoc. H_2O molec./residue	Total number assoc. H_2O
Aspartic acid	44	6	264
Glutamic acid	27	6	162
Glycine	38	0	0
Alanine	18	0	0
Valine	21	0	0
Isoleucine	27	0	0
Leucine	28	0	0
Serine	44	3	132
Threonine	28	3	84
Half-cystine	6	3?	18?
Methionine	5	3?	15?
Proline	15	3?	45?
Hydroxyproline	0.1		
Phenylalanine	14	3?	42?
Tyrosine	18	3	54
Tryptophan	6	3?	18?
Histidine	1	2	2
Lysine	1	3	3
Arginine	2	3	6
Amide NH	36	3	108
Phosphate	1	5?	5?
Total	343		815 + 143?

Total number of bound water molecules $\cong$ 1000

Sum of weights of amino acid residues = 36,422

D. DISCUSSION OF THE MECHANISM OF ENZYMATIC CATALYSIS

1. INTRODUCTION. Because of the numerous similarities between solids and proteins as catalysts one may expect the possibility of some useful extension of the results of one field into the

other. Enzymes, however, cannot be considered a special branch of catalysis by solids since proteins have quite unique aspects of their own, such as higher specificity in substrate fitting, variety in functional groups, and involvement of structural change.

Four useful properties of possible catalytic importance may be considered:[39]

(a) crystal-like electronic states and energy migration devices;

(b) cooperative action by orientation of functional groups;

(c) dynamic participation of the protein structure; and

(d) special electrical properties arising from the interaction of ionized groups with each other and with substrates.

Since we found in our experiments data pertaining mostly to the fourth class, we shall consider only that one more closely.

2. CHARGE FLUCTUATIONS. Not much is definitely known about the interactions of the ionized groups of proteins, although an abundance of titration curves for proteins and pH data is available in general. The electric interaction energies between these charges may be quite appreciable,[40,41] since the effective dielectric constant between them is doubtless much lower than the value in bulk water[42] and since the charges are on the average not more than 10 Å apart on many enzymes. The energies are at least large enough to insure a maximum concentration of the charges on the surface of the protein, where the electrostatic potential energy is least. It is also very likely that there are partially coupled fluctuations of charge change across the surface of the protein resulting from the interaction of neighboring ionic groups. Regions of high charge density of a single sign are quite unstable. Thus the production of swelling of proteins at extremes in pH has often been attributed to high values of net charge.[43]

Even though there is a constant conversion of charge isomers, certain ionizable groups of both signs are charged most of the time,

and the protein therefore exhibits a net permanent dipole moment. When such a molecule is subjected to an electric field, the molecule tends to orient itself in such a way that its dipole opposes the field. When the field is removed, the dipole returns to a random orientation. If the superimposed field is varied in frequency a rotational relaxation time of the molecule can be found. Such experiments not only give the characteristic relaxation time of the molecule but also the net dipole moment. This phenomenon has been effectively exploited by Oncley and Wyman in protein studies. [44]

The above description is due to Debye[17] and holds only for a rigid molecule with a fixed dipole. Jacobsen[45] has questioned this classical picture of a rigid sphere of fixed dipole moment rotating in the solution and no longer finds it satisfactory. He found that such a concept was particularly inconsistent with his dielectric studies on folded polyacidbase macromolecules. When these molecules in solution were fully oriented in an annulus across which there was a high shear gradient, the dielectric properties were the same whether measured across the long or short axis of the molecules. As a substitute for the rotational picture of Debye he suggested that proteins have a large effect in organizing the structure of water and that it is this structure as modified by the protein that is seen in the dielectric experiments.

In a different kind of explanation, Kirkwood and Shumaker[46, 47] have introduced concepts that may change the interpretation of all dielectric phenomena in proteins. They assert that charge fluctuations occur as proteins pass through a series of charge isomeric states and that they have a constant dipolar field associated with them. The fluctuations are thought of as the migration of protons among an excess of available basic groups. Although the time-average dipole moment of these fluctuations is zero, there is a nonvanishing quadratic term in the moment that may be large and even larger than the permanent dipole of the fixed charge. They originally proposed this dipolar field as a source of protein-protein interaction,

and recent experiments with light-scattering techniques have indirectly shown that this may be the correct explanation.[48] Their study indicates that the dipole interaction of albumin molecules accompanies the fluctuation of 3.58 charge units per molecule.

3. **DIELECTRIC DISPERSION OF HEMOGLOBIN.** Kirkwood and Shumaker's hypothesis and the supporting data suggest that the dynamic interaction of ionized groups of proteins may play an important role in protein reactions. Dielectric studies on hemoglobin suggest that unusual effects of ionized groups may be associated with the normal function of at least that protein. In the latter study the dielectric relaxation time and the dipole moment of hemoglobin were investigated at various degrees of saturation with oxygen and carbon monoxide. A parallel series of large maxima and minima were found with an increase of the amount of bound oxygen or carbon monoxide.[2, 49] The effects could not be attributed to the bound molecules because of their relative magnitude and were completely controlled by the state of oxygenation or monoxide addition of the molecule. By studying the effect as a function of protein concentration, aggregation or dissociation of the protein into subunits was eliminated as a source for the change in the dielectric parameters.

It therefore appears that the only remaining possible explanation is that the oxygenation produces changes in the distribution of the charge on the protein. The data of the change in the electrical parameters are quite similar to the experimental data of our study of enzymatic catalysis, although at a very different frequency. In both cases the most probable conclusion is that changes in the charge distribution of the protein molecule occur.

4. **KIRKWOOD'S HYPOTHESIS OF ENZYME CATALYSIS.** Kirkwood[50] has extended the theory of charge fluctuations he developed with Shumaker[46, 47] to provide an explanation for some types of enzymatic catalysis. Fluctuation forces arising from fluctuations in protonic charge and charge configuration are considered to be

of importance in an analysis of the interaction of the protein moiety of an enzyme molecule and a substrate molecule bound to the active site. He established that if there is an increase in the dipole moment of the active site-plus-substrate complex in its activation to the transition state, interaction with neighboring basic groups of the protein by the fluctuation mechanism can produce a substantial decrease in the free energy of activation. Laidler[51] has pointed out that the relationship between the pH and the rate parameters predicted by the theory is not found experimentally. This criticism would appear to be a strong one, but it is probably unwise to ignore the possibilities of proton-charge-charge interactions as a factor in enzymatic catalysis either in ways we do not yet fully understand or in simpler field effects of the type considered by Kirkwood and Westheimer.[52]

E. A NEW MODEL OF ENZYMATIC CATALYSIS

In the following pages we shall attempt to show that the decisive factor for the catalytic action of a protein is two-fold. First, and of prime importance, is the ice-like character of the water molecules surrounding the protein; second, the special configuration of the protein makes it unique and enables it to act as a catalyst in conjunction with the ice-like surface onto which it is adsorbed.

This way of looking at an enzyme system may seem backward since so far the blame for the catalytic activity has never been put on the surrounding water, but always on the polypeptide chain. As new properties of ice were discovered quite recently, however, which led to the hypothesis that ice with certain impurities is a protonic semiconductor, we used this analogy with electronic semiconductors to investigate the question of catalytic activity of a surface of ice. We shall show that the parallel with electronic semiconductors, which have been known to be good catalysts, can be extended to provide some good theoretical reasons to suspect that a protonic semiconductor like ice has similar catalytic potentialities.

We arrive from a completely different direction of attack at a view similar to Kirkwood's[50] about the mobility of the protons or defect protons on the surface but again follow a different route to explain the actual catalytic action. We shall use the terminology employed in solid-state integrated electronic circuits since we have to deal with such parameters as junctions of p- and n-type regions and as three-dimensional configurations exhibiting impedances to current flow.

1. ELECTRONIC CONDUCTION IN SEMICONDUCTORS. In some solids electrons can be raised to the conduction band not only by the absorption of light but also by the thermal vibrations of the lattice, if the temperature is not too low.

Electronic conductivity in a nonmetallic solid (semiconductor) is thus due to electrons that are released by thermal lattice vibrations (similar to thermal collisions) and raised to a conduction band that is unoccupied at zero absolute temperature. This process is possible in a pure crystal only if the energy difference between the normally empty and normally filled energy bands is not too large compared with the thermal energy. Such a crystal with a small gap between the two bands (e. g. , germanium with a gap of 0. 75 v) is called an intrinsic semiconductor.

A crystal that is not an intrinsic semiconductor may be made into a semiconductor by introducing into it foreign atoms or a stochiometric excess of one of the component atoms which has a sufficiently small ionization energy in the crystal. It is then called an extrinsic semiconductor. In the energy-band model (Figure 21a) the energy states D of the valence electrons of these interstitial atoms are situated so closely below the normally unoccupied conduction band B that electrons can get from D into the band B as a result of thermal ionization of the metal atoms. This type of crystal is called an excess or n-type semiconductor, because negative charges are released from the D (or donor) levels.

CONDUCTION BAND — B

D

VALENCE BAND — A

(a) EXCESS OR n-TYPE

CONDUCTION BAND — B

C

VALENCE BAND — A
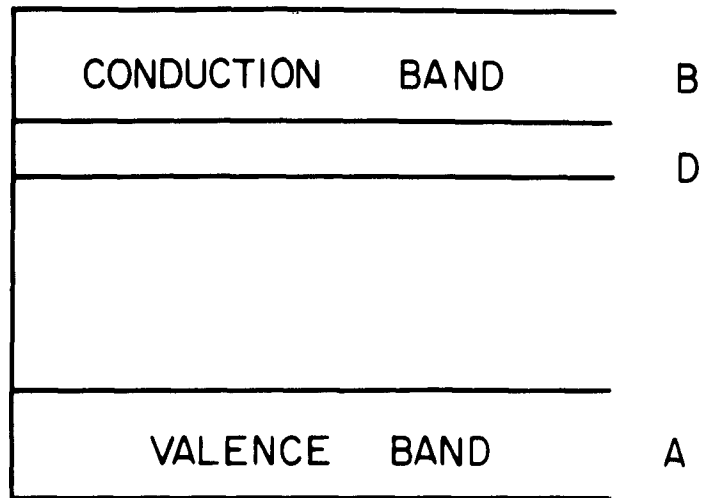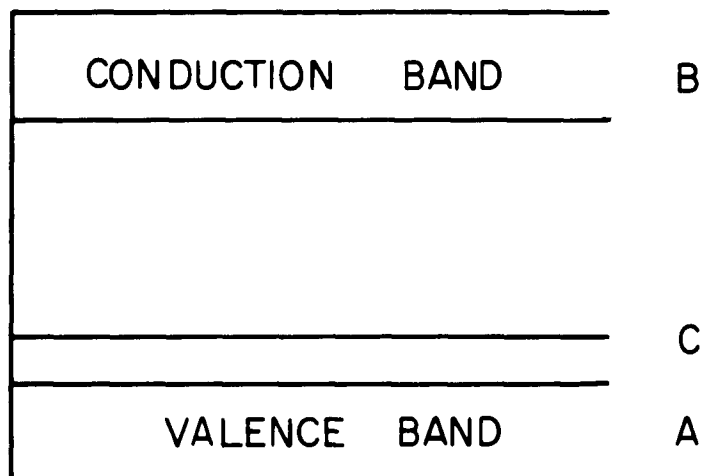
(b) DEFECT OR p-TYPE

FIGURE 21. --Energy levels of electronic semiconductors.

The third possible type of semiconductor is called the p-type or defect semiconductor because it has a defect of metallic atoms in the lattice or an excess of electronegative constituents. The energy states of these electronegative atoms lie closely above the band A of the crystal which is completely occupied by electrons. Only a small amount of energy is necessary to capture an electron, i.e., to bring it from the crystal energy band A to the normally unoccupied levels C of the electronegative atoms, where it is held fast (Figure 21b). The "holes" which are thus produced in the previously full band of the crystal have an effective positive charge and are mobile. These atoms are also called acceptor atoms.

Depending on the treatment of the crystal by external "doping" agents, the same crystal can be made an excess or defect semiconductor, a typical indication of the "structure dependency" of the properties of a semiconductor.

Since the energy required for the transition $D \rightarrow B$ (n-type) or $A \rightarrow C$ (p-type) in the conductivity of semiconductors is supplied by thermal collisions, the conductivity can be represented by a formula of the general form

$$\sigma = A \exp (-W/kT) \tag{66}$$

where σ is the conductivity and W is the activation energy of the process (the energy difference from D to B or A to C) and is, in general (just as is the constant A), a function of the temperature. W depends on the loosening of the lattice, which is determined by temperature.

2. PROTONIC CONDUCTION IN ICE. By analogy with a useful method in semiconductor technique, so-called "sandwich" electrodes have been employed to determine the dc conductivity of ice.[21] The surface of a pure ice crystal was covered by a thin layer of ice containing HF in high concentration. Platinum or gold electrodes were then frozen to the contaminated layers. Such "sandwich" crystals always showed ohmic contact and a time-independent conductivity at all temperatures. The

potential distribution was measured with two potential probes and found to be linear. Thus they were assured of measuring true conductivity. With an applied voltage of 100 v the conductivity between 250° and 125° K is represented by

$$\sigma(T) = C \exp(-E_{\sigma}/kT) \qquad (67)$$

with $E_{\sigma} = 0.325 \pm 0.005$ ev; C varies for different crystals from 3.6 to 5.0 ohm^{-1} cm^{-1}. The diffusion of fluorine atoms into the bulk of the crystals was found to be negligible.

Although the intrinsic absorption of ice lies at 1670 $\overset{\circ}{A}$ (which corresponds to a forbidden gap of 7.42 ev, so that intrinsic semiconduction is ruled out). extrinsic conduction (as defined above) seems possible.

Quantitative electrolysis experiments at $-10^{\circ}C$ have been performed with pure ice crystals with "sandwich" electrodes.[21] Measurement of the volume of hydrogen found at the cathode of the crystal reveals within experimental errors (1-2%) that the conduction is entirely ionic by a proton transfer mechanism. Further evidence for ionic conduction is obtained from the current-voltage characteristics. With voltages below about 1 v, which is the dissociation potential of water, practically no current is observed.

Dc conductivity in pure ice crystals therefore requires proton transfer along hydrogen bonds, since the ionic character of the conduction has been ascertained. The conductivity therefore depends on the activation energy E_I for ion-pair formation and on E_{tr}^{+} and E_{tr}^{-} for translational motion. If a crystal had on the average no polarization before a dc field is applied, an H_3O^{+} state can move by proton transfer on a chain of molecules through the crystal. The molecules on the chain are left in an orientation that corresponds to a polarization opposite to the field. The existence of a time-independent current requires that after a certain time the same chain must be again able to conduct another ionic state, which is possible only if the molecules have changed their polarization from opposite the field to a polarization parallel to the field. These molecular turns, which are necessary to reactivate the chains for conduction,

are possible only with the aid of orientational defects (doubly occupied or vacant bonds). Hence the concentration of these defects and the activation energies for rotation $E_r^{(L)}$ and $E_r^{(D)}$ must be also considered.

The dc conductivity of HF contaminated ice crystals measured by the "sandwich" method is explained in the following way:

In the electrode layer the H_3O^+ concentration is much higher than in the bulk of the crystal and the diffusion of the ions would soon be counteracted by a diffusion potential since a negative space charge and the immobile F^- ions remain at the surface layer. However, the surface also contains a high number of L-defects which have a tendency to diffuse into the bulk. The molecules which permitted this diffusion by molecular rotations are left behind in a state of polarization pointing toward the surface. Thus the combined diffusion of H_3O^+ ions and vacant bonds does not give rise to a resultant diffusion potential. One must therefore assume that the bulk of the "sandwich" crystals is homogeneously crowded by defects which were generated by the HF content of the electrode layers.

The conductivity is therefore given by

$$\sigma_F = \text{const } N_F^{\frac{1}{2}} \; e^{-(\frac{1}{2}E_F + E_r^{(L)} + E_{tr}^+)/kT} \tag{68}$$

where N_F is the number of fluorine atoms per unit volume, and where the activation energy E_σ is the sum of the activation energies for the three different processes necessary for conduction, namely dissociation $(\frac{1}{2}E_F)$, rotation $(E_r^{(L)})$, and translation (E_{tr}^+). This type of conduction--an excess proton conduction--is a fast controlling process that is usually only known in electronic systems, where it is termed excess semiconduction, and where the charge is carried by electrons. The analog to hole conduction can also be produced in ice crystals by contaminating them with a base (LiOH, NH_3).

Here, however, only a relatively small amount of doping agents (compared with HF) can be built into the ice lattice.[53]

We are now able to draw an analogy for semiconduction by protons in ice crystals doped with HF. Here excess positive charges are released from the D levels whenever the activation energy (difference between D and B) is supplied by the system; B signifies the level of mobile protons, and A that of immobile protons, as shown in Figure 22a. The forbidden gap A → B is the gap in Figure 22a corresponding to intrinsic conduction and is of magnitude 7.42 ev; whereas the energy difference from D to B is 0.325 ev.

Carrying the analogy further, in the LiOH contaminated crystal there exists an excess of positive constituents (Li^+). The energy states of these positive atoms lie at the level C closely above the band A of the crystal, which is completely occupied by protons. Only a small amount of energy $(\frac{1}{2} E_{Li} + E_r^{(D)} E_{tr}^+)$ is necessary to capture a proton. The proton "holes" which are thus created in the previously full band of the crystal have an effective negative charge and are mobile, as shown in Figure 22b.

The ice crystal may also become semiconductive by a stochiometric increase of one of its constituent atoms. This process occurs owing to the dissociation of water molecules in the ice crystal and the donor and acceptor levels, respectively, are then $\frac{1}{2} E_I + E_r^{(L)} + E_{tr}^+$ and $\frac{1}{2} E_I + E_r^{(D)} + E_{tr}^-$. These states become more abundant as the temperature is increased or as the ice crystal is brought into the vicinity of liquid water where a larger number of dissociated states exist.

3. CATALYSIS ON THE SURFACE OF ELECTRONIC SEMICONDUCTORS. Chemists and physicists both are interested in surface properties of semiconductors. Heterogeneous catalysis on semiconductors represents an important branch of catalytic science and it is well known that the concentration of carriers, electrons, and holes is a

MOBILE   PROTON   BAND   B
_____

_____ D

_____

BOUND   PROTON   BAND   A
_____
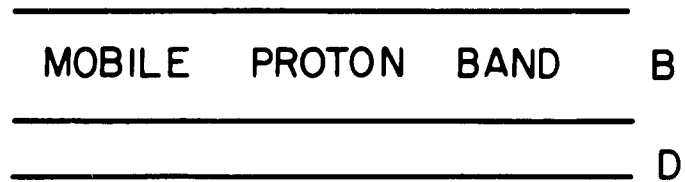
(a) EXCESS OR PROTON
CONDUCTION

_____

MOBILE   PROTON   BAND   B
_____

_____ C
_____

BOUND   PROTON   BAND   A
_____
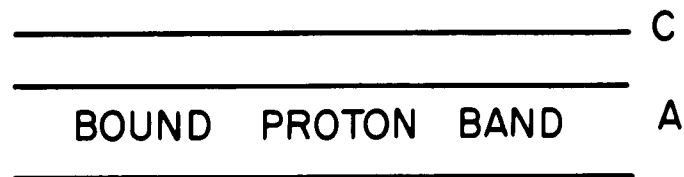
(b) DEFECT OR "HOLE"
CONDUCTION

FIGURE 22. --Energy levels of protonic semiconductors.

decisive factor in catalysis. With the advent of Eigen and deMaeyer's hypothesis of protonic semiconduction in ice crystals and its surmised importance in biological reactions, it may be valuable to draw a parallel between these two types of semiconductors. One may use this resemblance to build an analogy of catalysis aided by protonic charge carriers as opposed to the one that has been for a long time the subject of studies, namely the catalytic properties of electronic semiconductors.

Let us first review briefly how catalytic properties of electronic semiconductors can be linked to their electrical and physical characteristics and then study some resemblances with protonic semiconductors.

The band theory of solids on which the current concept of semiconductor properties is based presents a very complex and formidable model for consideration of the effects occasioned by an adsorbed species on the surface of a semiconductor, so that most authors have followed the assumptions of Hauffe,[54] Aigrain,[55] and others[56, 57, 58, 59] by adopting some simplifications. Attention has been drawn to these aspects by Gray[60] and Morin,[61] the latter invoking certain aspects of crystal field theory to emphasize the complexities encountered with the transition metal oxides where pseudo-metallic properties can be associated with certain oxides.

Despite the theoretical difficulties of the band theory concept, Wolkenstein[62, 63] has presented a hypothesis which links the catalytic activity of a semiconductor with its ability to adsorb substances and its electronic structure. We review this hypothesis briefly.

Usually the adsorbed particles are looked upon as a gas that covers the surface of the adsorbing substance, in this case the semiconductor. This view is only correct as long as there is only a very weak interaction between the two substances, which may be termed physical adsorption. In the case of a chemical adsorption the particles can no longer be thought of as a two-dimensional gas, since a new whole is produced by the interaction of the adsorbed

particles and the crystal lattice of the semiconductor. A chemical adsorption, which usually is a part of a catalytic process, forms a new quantum-mechanical system.

The chemically adsorbed particles can be treated as doping additions which are located in the crystal surfaces, or as lattice imperfections which distort the periodic structure of the crystal surface.

Wolkenstein[64] showed in theoretical treatments of this problem that the chemically adsorbed particle acts as the acceptor atom of the free electron of the lattice or as the donor atom (depending on the nature of the particle). The bond of this particle to the surface is thereby changed and the electron or hole becomes a part of the bond.

According to this treatment two different forms of chemisorption may be distinguished:

(1) "Weak" chemisorption, where the chemisorbed particle stays electrically neutral and the bonding occurs without the participation of electrons or holes (physical adsorption); and

(2) "strong" chemisorption, in which the chemisorbed particle holds the free electron or hole of the crystal lattice and where this electron or hole takes part in the formation of the bond: in this case we may distinguish two further types,

(a) strong acceptor formation (n-bonding), where the free electron partakes in the bond, and

(b) strong donor formation (p-bonding), where the hole takes part in the bond mechanism.

An analysis of these types of chemisorption leads to the following conclusions, as given by Wolkenstein:[62,63]

(1) There exist different types of chemisorption, which have different bond characters with the crystal lattice.

(2) The reactivity (i. e., the ability to combine chemically with other chemisorbed particles) is different for different forms of chemisorption.

(3) Different types of chemisorbed particles are interchangeable. In other words, the adsorbed particle can change its bond type to the surface by localization or delocalization of a free electron or hole.

(4) The relative number of the various types of chemisorbed particles on the surface, their ability to react with other substances, and therefore the catalytic activity of the surface are determined by the position of the Fermi level (or chemical potential). The velocity of the heterogeneous reaction is expressed by the relative population of the bond types on the surface. Thus the Fermi level is present in the exponent of the equation for the rate of the reaction.

As an example we may take the oxydation of CO as shown in Figure 23. We assume that chemisorbed oxygen atoms in an ionic radical condition act as adsorption centers for the CO molecule. Then after the adsorption of CO an intermediate product is formed, the surface radical CO_2^-, which after the liberation of an electron becomes a CO_2 molecule.

If the CO adsorption is rate determining, the new reaction rate is

$$k'' = k_1 \exp \left[-(E_1 + E_F)/kT \right] \tag{69}$$

where k_1 is the reaction rate of the homogeneous reaction and E_1 its activation energy; E_F is the energy of the Fermi level.

If the desorption of the CO_2 molecule is rate determining, then the new reaction constant is

$$k' = k_2 \exp \left[-(E_2 - E_F)/kT \right] \tag{70}$$

where k_2 is the reaction rate of the homogeneous reaction and E_2 its activation energy.

It is seen therefore that the Fermi level determines the catalytic activity of the semiconductor surface. The dependence of the reaction velocity on the position of the Fermi level on the
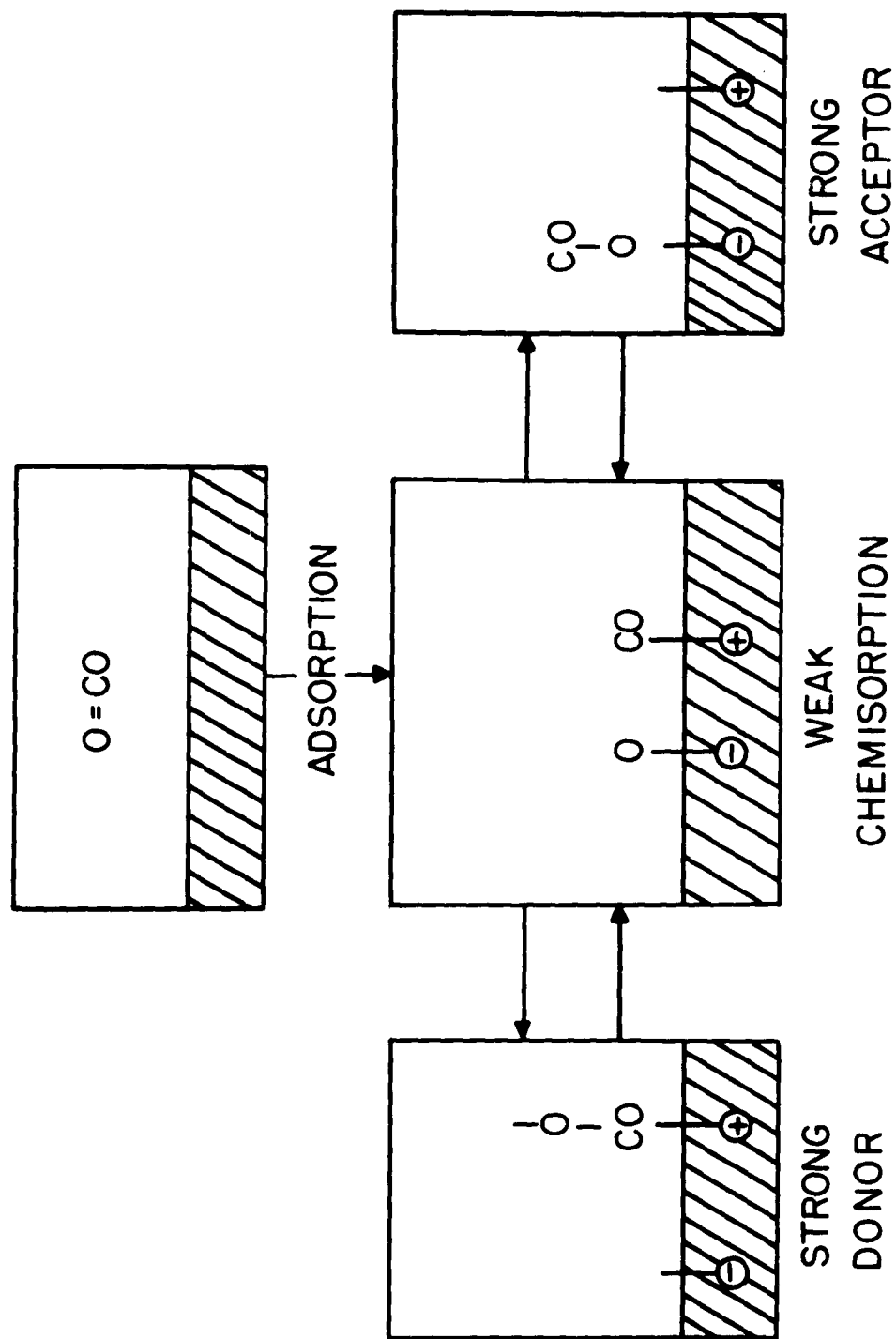
FIGURE 23.--Schematic diagram for the oxydation of carbon monoxide on a semiconductor surface.

surface of the catalyst for the oxidation of hydrogen was experi-
mentally determined by Boreskow and Popowsky[65] and agree very
well with the theoretical values of Wolkenstein's analysis.[64]

4. CATALYSIS ON THE SURFACE OF A PROTONIC
SEMICONDUCTOR. Just as the nature of the bond of a particle
chemisorbed to an electronic semiconductor can change from an
excess to a defect-type bond, so it is possible that the molecule
chemisorbed to the surface of an ice crystal changes the character
of its bond. Here we consider as an example a carboxyl group and
an amino group as shown in Figure 24. As the carboxyl group
approaches the surface one molecule rotates, creating a vacancy
defect in the structure (equivalent of a hole) and forming a
homopolar bond with the surface of the crystal (Figure 24b). If
the surface has a different character, the approaching residue may
enter into an ionic bond and create a double bond which may travel
through the crystal lattice (Figure 24d). An alternate way of
looking at this phenomenon is to note that whenever a vacancy
defect approaches the surface, it may be localized in a bond, and
a double defect may become localized in the ionic type of bond
formation. If there is an equal number of vacancy and double
defects in the lattice at a certain temperature then there is an
equal chance of either type of bond being formed, and the two
types are mutually interchangeable.

In the case of an amino group a similar phenomenon is
noted, as depicted in Figure 25, but here the formation of the
homopolar bond is associated with the formation of a double defect,
and the ionic bond is concomitant with a vacancy defect in the lattice
structure of the crystal.

Either type of residue of an amino acid can therefore act as
either proton donor or proton acceptor. By analogy with the energy
level scheme of an electronic semiconductor we may show an energy
level diagram of the protonic type of semiconductor in Figure 26.
After equilibrium is established in the lattice one finds a certain
number of particles in a weak state of adsorption (by van der Waals
forces) or in a homopolar bond or in an ionic type of bond. These

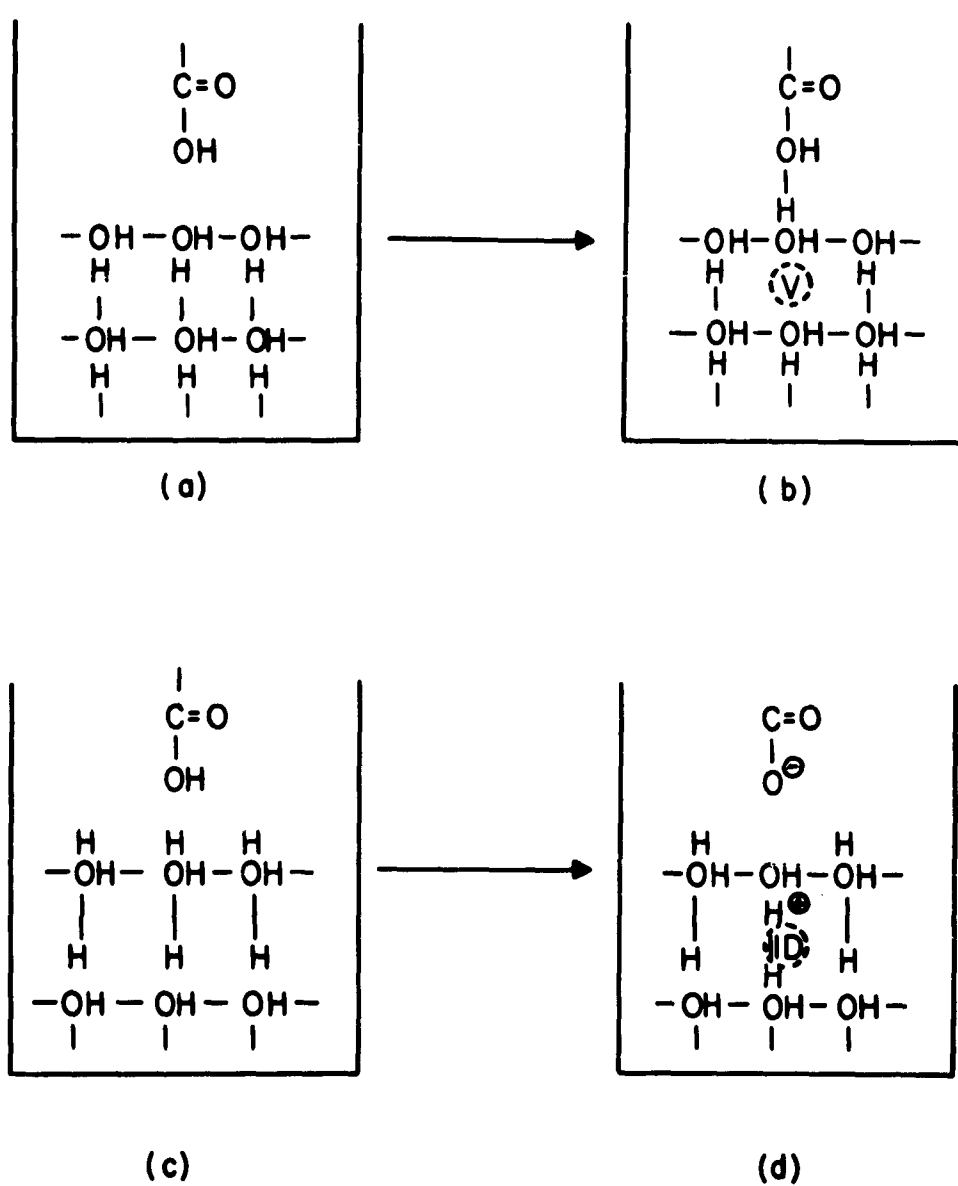FIGURE 24.--Schematic diagram for a carboxyl group bound to a water surface.
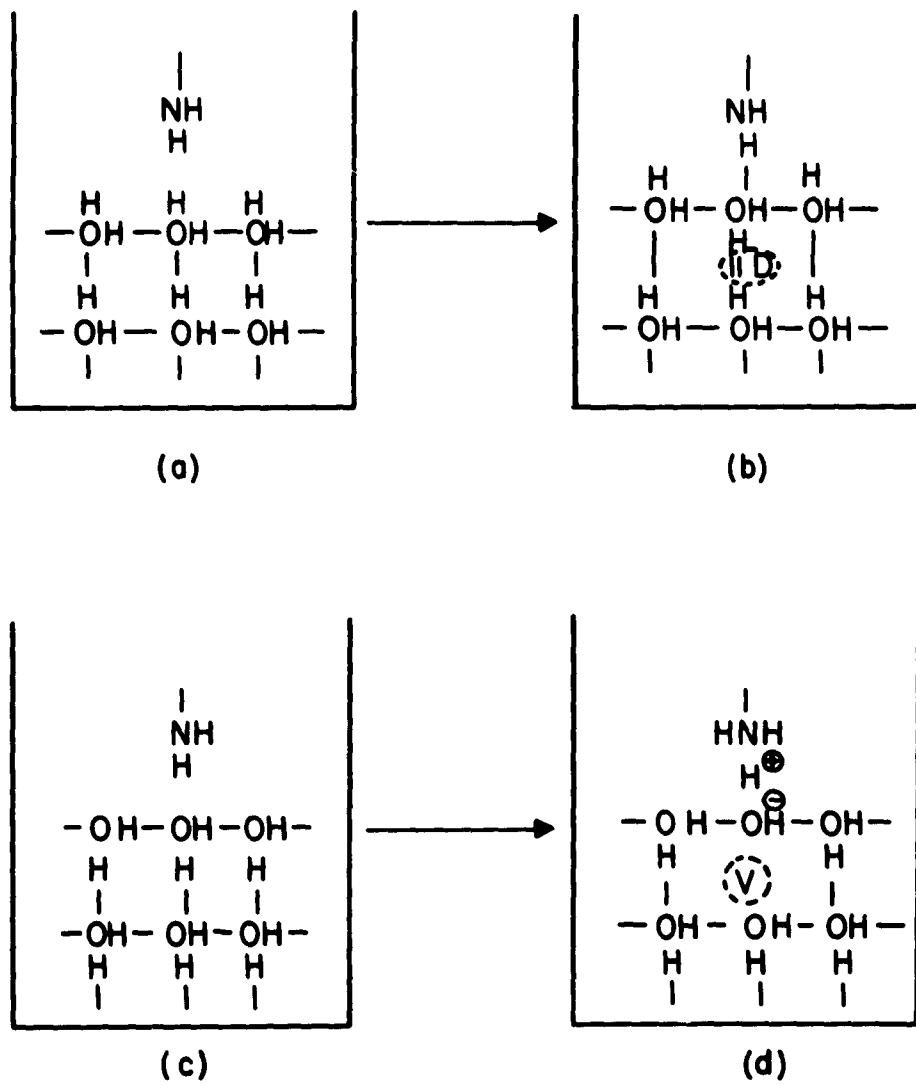
FIGURE 25. --Schematic diagram for an amino group
bound to a water surface.

CONDUCTION   PROTONS

A   ACCEPTOR
           LEVEL

_ _ _ _ _ _ _ "FERMI" LEVEL

D ——————— DONOR
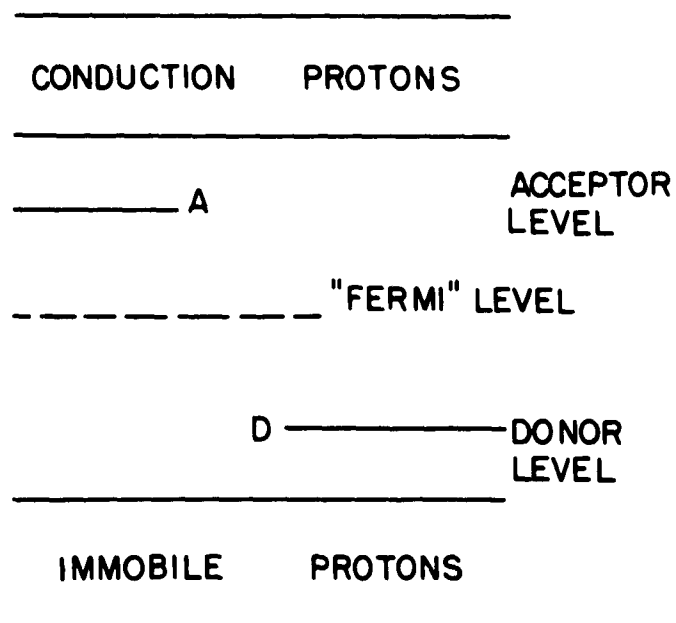   LEVEL

IMMOBILE   PROTONS

FIGURE 26.--Energy-level diagram of a protonic semi-
        conductor in reference to catalytic
        properties.

-81-

relative numbers of occupancy of the various bond states may be
computed, and also their relative lifetimes in these states. In the
further analysis one has to define an energy level similar to the
Fermi level of electronic semiconductors, which determines the
reactivity of the adsorbed molecular groups, and therefore the
catalytic activity of the crystal surface. Since the velocity of the
catalyzed reaction is given by the relative numbers of occupancy of
the various bond states, the equivalent of the Fermi-level will have
to be entered in the rate equation of the catalyzed reaction in a
manner similar to that of electronic semiconductor catalysis.

V. APPLICATION OF THE MODEL OF ENZYME ACTION

Proteins immersed in the water phase have an ordering
influence on the water molecules and create an ice-like sheath
around them, as has been shown by Schwan[66] and by Takashima.[67]
We may regard the protein in water in a different way. The groups
of the aminoacids which form the peptide chain of the protein may
be regarded as the molecular units on the surface of an ice-like
crystal, where now the previous analysis may be applied.

Since in the case of a whole protein we shall have a multitude
of acceptor and donor levels and junctions thereof, the process may
be more easily visualized if, first, we only consider the so-called
"active" site of the protein molecule or enzyme; and second, if we
resort to a description of the happenings in the language used in
designing and constructing integrated solid-state circuits. Since in
our experiments we were able to gain information about changes in
the number of vacancy or double defects on the surface of the enzyme
during catalysis we shall analyze these currents and show how even
in such an approximate description the energy requirements can be
seen to coincide well with the observed values.

A. MEASUREMENTS OF POPULATIONS OF MOLECULES AND THE BEHAVIOR OF A SINGLE MOLECULE

A source of some difficulty, which can be alleviated by the
use of a computer, is the fact that we have a certain distribution of

the times at which the assumed processes happen on the various molecules that are in solution. We have derived an analytical method that can give (from the observed data) the functions appropriate for the reactions of single molecules, provided the distribution function for the onset of the reactions is known. This distribution may safely be assumed to be a continuous one and therefore presents no major obstacle. Meanwhile in our analysis we assume that there is no distribution of the reaction times of the enzyme molecules, i.e., that mixing is complete and instantaneous. If one considers the relative times required for mixing $(10^{-1}$ to 1 sec) and the time of a reaction (approximately 10 min) one is reassured that no large mistake is made by this assumption.

The mathematical procedure for determining the behavior of a single molecule from an observation on a population of such molecules is given as follows. If $f_i(t)$ is the time course of a single reaction, where τ_i indicates the onset of the reaction, then $F(t)$ is the observed behavior of the sum of the individual reactions, where

$$F(t) = \sum_{i=1}^{N} f_i(t) \tag{71}$$

and N is the total number of molecules. Functions $f_i(t)$ and $F(t)$ are shown schematically in Figures 27(a) and (b).

We assume a normal distribution of the τ_i about some mean τ_0 so that

$$\frac{dn}{d\tau} = \frac{N}{\sqrt{\pi}} \exp \left[\frac{-(\tau - \tau_0)^2}{2\sigma} \right] \tag{72}$$

as depicted in Figure 27(c), i.e., we assumed a continuous distribution.

We also assume that $f_i(t)$ is the same for all molecules except for a translation in time
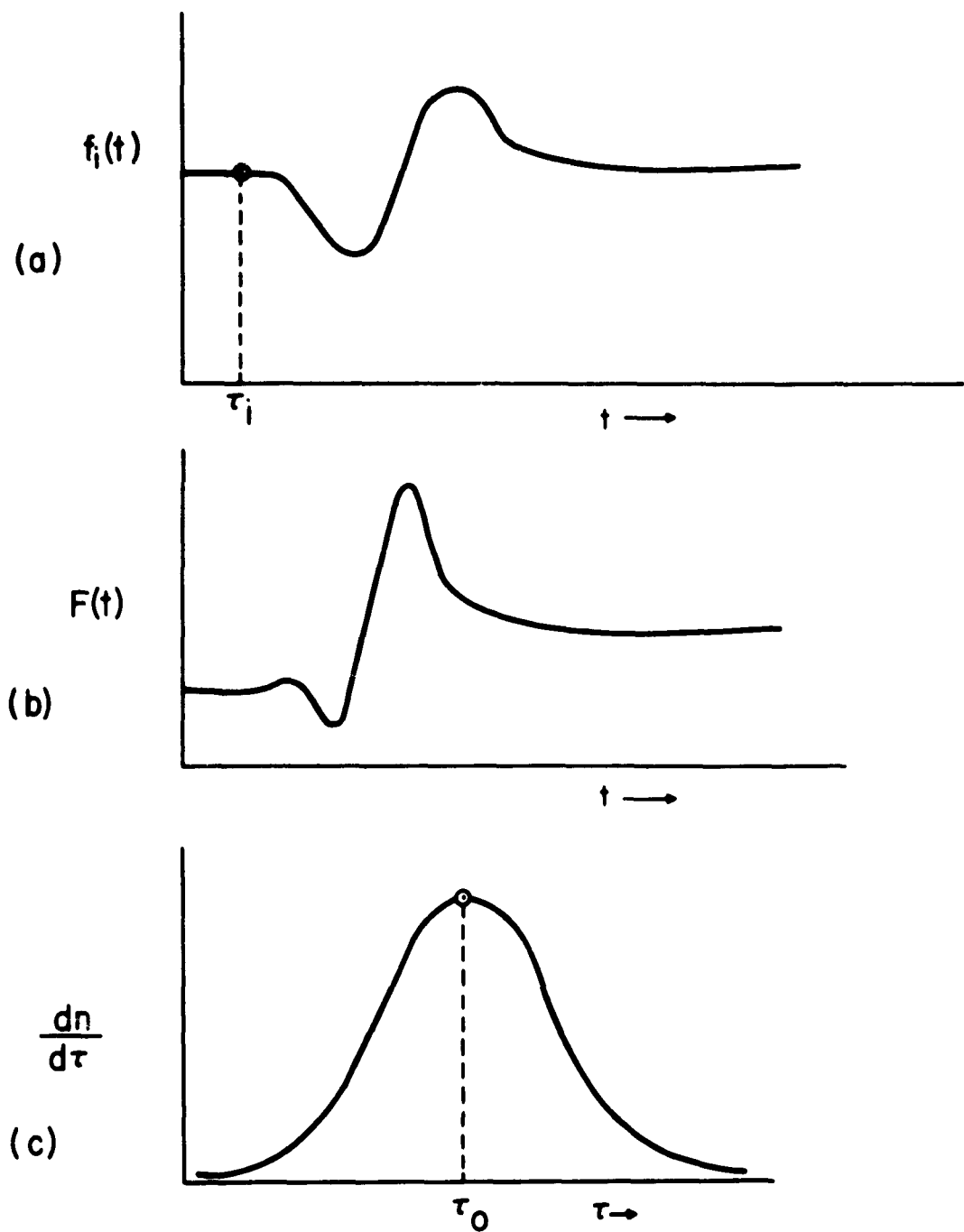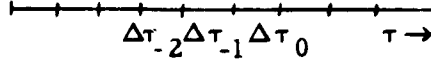
$$f_i(t) = g(t \mp \tau_i) \tag{73}$$

FIGURE 27. --Time-dependent behavior of single molecules and populations.

then

$$F(t) = \sum_{i=1}^{N} g(t-\tau_i) \tag{74}$$

Consider a partition of the τ_i

$$\overline{|\!\!-\!\!+\!\!-\!\!+\!\!-\!\!+\!\!-\!\!+\!\!-\!\!+\!\!-\!\!+\!\!-\!\!+\!\!-\!\!+\!\!-\!\!|}$$
$$\qquad \Delta\tau_{-2}\Delta\tau_{-1}\Delta\tau_0 \qquad \tau \rightarrow$$

associated with the $\Delta\tau_i$. There are a number of molecules $n(\Delta\tau_i)$ such that

$$\sum_{i=-\infty}^{\infty} n(\Delta\tau_i) = N \tag{75}$$

With each of these molecules there is associated the function

$$g(t-\tau) \quad , \quad \tau \in \Delta\tau_i \tag{76}$$

If the interval $\Delta\tau$ is small, this will be substantially the same function as that which may be characterized by some value of $\tau \in \Delta\tau_i$, such as the midpoint of the interval $\Delta\tau_i$. Call such a value τ_i.

Then

$$F(t) = \sum_{i=-\infty}^{\infty} n(\Delta\tau_i)\, g(t-\tau_i) \tag{77}$$

and for a continuous distribution of the states

$$\Delta\tau_i \rightarrow d\tau \tag{78}$$

$$n(\Delta\tau_i) \rightarrow \frac{N}{\sqrt{\pi}} \exp\left[\frac{-(\tau_0-\tau)^2}{2\sigma}\right] d\tau \tag{79}$$

Also, the sum becomes an integral

$$F(t) = \int_{-\infty}^{\infty} g(t-\tau)\, \frac{N}{\sqrt{\pi}}\, \exp\left[\frac{-(\tau_0-\tau)^2}{2\sigma}\right] d\tau \tag{80}$$

and may be rewritten as

$$F(t) = \frac{N}{\sqrt{\pi}} \int_{-\infty}^{\infty} g(t-\tau)\, \exp\left[\frac{-(\tau_0-\tau)^2}{2\sigma}\right] dt \tag{81}$$

This is a convolution of the functions

$$g(-\tau) \quad \text{and} \quad \frac{N}{\sqrt{\pi}} \exp\left[\frac{-(\tau_0 - \tau)^2}{2\sigma}\right] \tag{82}$$

There is a theorem: let $\mathcal{F}$ represent Fourier transforms, then

$$\mathcal{F}(f * g) = \mathcal{F}(f) \cdot \mathcal{F}(g) \tag{83}$$

where $f * g$ represents the convolution of f and g; so that

$$\mathcal{F}(F) = \mathcal{F}\left[g(-\tau)\right] \cdot \mathcal{F}\left\{\frac{N}{\sqrt{\pi}} \exp\left[\frac{-(\tau_0 - \tau)^2}{2\sigma}\right]\right\} \tag{84}$$

and therefore

$$g(-\tau) = \mathcal{F}^{-1}\left\{\frac{\mathcal{F}(F)}{\frac{N}{\sqrt{\pi}} \exp\left[\frac{-(\tau_0 - \tau)^2}{2\sigma}\right]}\right\} \tag{85}$$

This means that $g(-\tau)$, the time course of a single reaction, can be computed, if the Fourier transform $\mathcal{F}[F(t)]$ can be found, and if a continuous distribution around a mean can be assumed for $g(-\tau)$.

B. INTERPRETATION OF THE DIELECTRIC DATA OF THE ENZYME-SUBSTRATE SYSTEM

In the previous sections the mechanisms of the enzyme action that are based on the special electrical characteristics of the protein in a water medium are reviewed. We see that much more definite information is needed to arrive even at a working hypothesis of a mechanism based on electrical properties of proteins.

We shall now suggest a mechanism of enzymatic action in more detail. This hypothesis is based on the data of the catalytic site, on its three-dimensional configuration, and mainly on the new evidence of protonic conduction on the surface of active enzyme molecules.

As Eigen and de Maeyer[32] have shown in their study of the structure of electrolytic solutions, the protonic mobility in the H-bond lattice of ice exceeds the drift mobility of the proton in water

by one to two orders of magnitude. The "excess" and "defect" proton-conducting H-bond systems show certain parallels to electronic semiconductors.

Other investigators, notably Schwan[66] and Takashima,[67] have concluded from their studies of the relaxation times of proteins in aqueous solutions that the arrangement of the water molecules on the surface of the macromolecule should be very similar to that of ice.

These two characteristics of proteins in water, their ice-like hydration shell, and the high mobility of protons in such an H-bond system show the need for a closer examination of mechanisms that may rest on this peculiar property of proteins.

We may therefore list the properties that a polypeptide chain in a water medium will exhibit.

(1) There will be some resistance to the proton transfer mechanism along the surface of the chain owing to either chemical or potential gradients.

(2) If there is a higher concentration of basic amino-acid residues on one end of the chain than at the other, an excess of vacancy defects results at the basic end. By the same token if there is an excess of acid groups on one end, an excess of double defects exists in the ice lattice in that region. Where these two regions join one will naturally have a junction that closely resembles the junction in a pn rectifier. As the dimensions of the molecule are rather small and the concentration of the defects relatively high, the junction would more nearly resemble a tunnel diode junction than that of a macroscopic diode. The proton mobility in H-bonds differs from electron mobility in metals only by one to two orders of magnitude, approximately corresponding to the square root of their mass ratio. This result strongly suggests a quantum-mechanical mechanism (tunnel effect) for the proton transfer within the H-bond.[32]

(3) Two widely (at the ends of the chain) separated ionic groups create a potential difference between them and a current of

protons may flow along the H-bond system joining the ends of the protein. Since the defects are produced by expenditure of thermal energy new ones will be substituted for those that were deleted in the process of conduction. This type of mechanism is usually termed a battery in electronic circuits.

(4) The protein chain may assume three-dimensional configurations that are different from that of a straight line. The flow of protons then experiences effects owing to this different structure which are like the effects of an inductance or a capacitance.

We see from this list of electrical characteristics that we have all the necessary elements for the construction of a tunnel-diode oscillator. In order to make a prediction about the behavior of the relative number of defects while the enzyme passes through its active state, we have to assume that those circuit elements are linked together in a meaningful way.

From the chemical evidence of the catalytic action of pepsin a schematic model (Figure 28) can be constructed. In such a model one can find the places where the above-mentioned circuit elements should be, as shown in Figure 29.

On the basis of this model we are able to predict what changes of a purely qualitative nature will occur as the enzyme becomes active (Figure 30). While the enzyme is catalytically inactive it exerts an influence on resonant structures in its vicinity by virtue of a London-Eisenschitz-Wang force[68] that arises from the interaction of the dipole radiators a and b. Since these oscillators are coupled their resonant frequency differs from their individual self-resonant frequencies. A highly specific influence can therefore be exerted on a protein or on a dipeptide (in our particular case). In this first step a specific group of bound amino acids is attracted to the active site of the enzyme.

In the second step of our reaction scheme the substrate has been attracted and lodged itself into the template structure on the surface of the protein. During this process of attachment the resonant
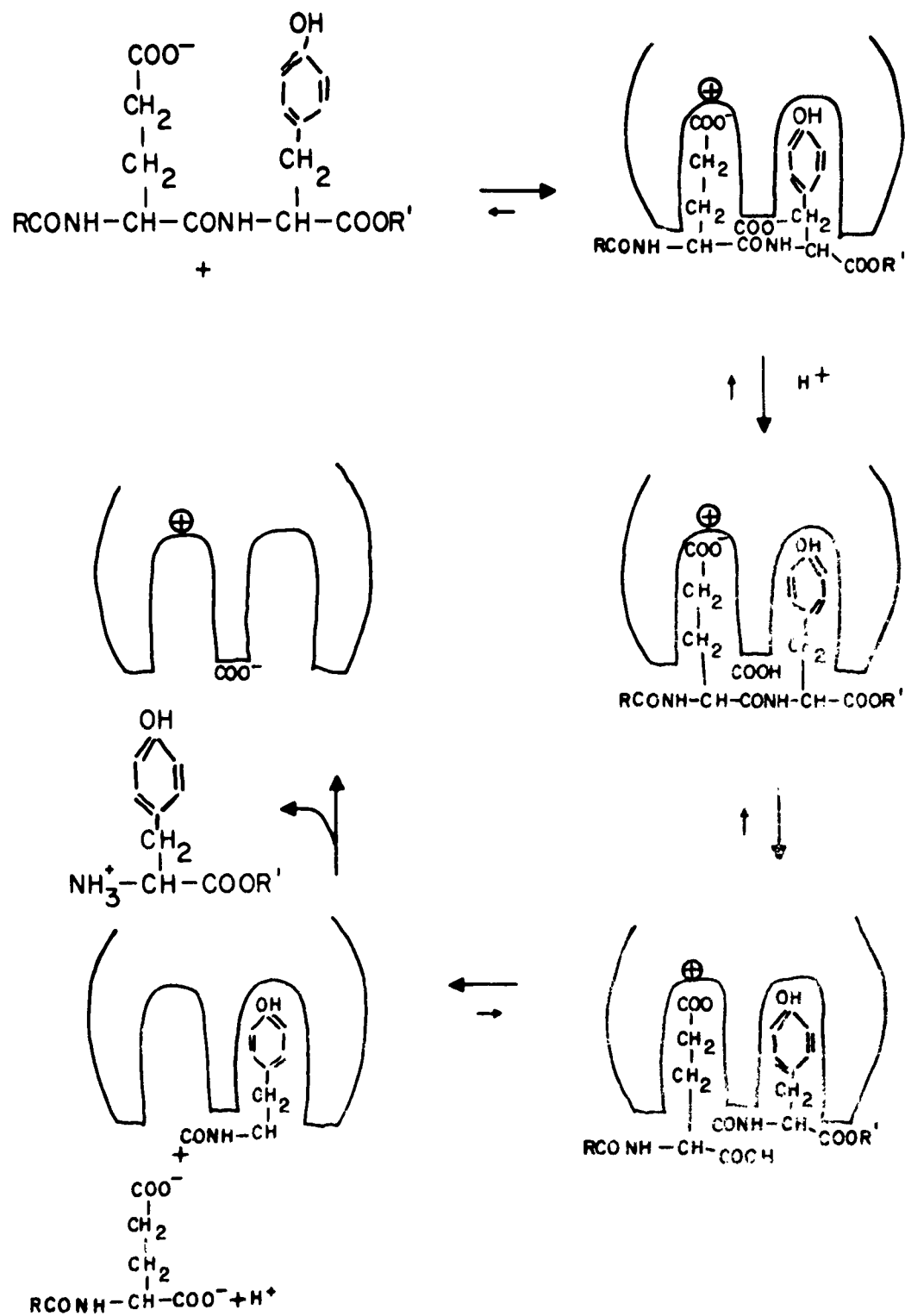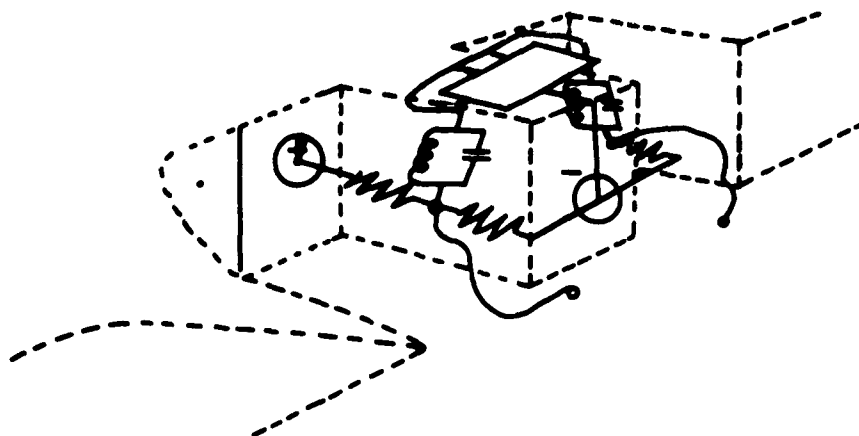
FIGURE 28. --Scheme of chemical reaction of pepsin and
substrate molecule.

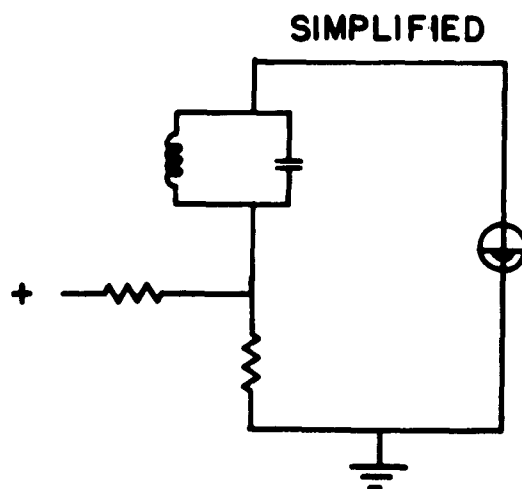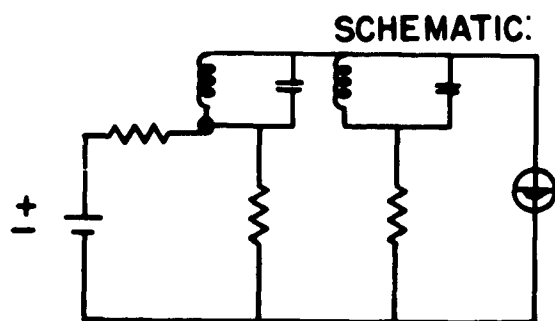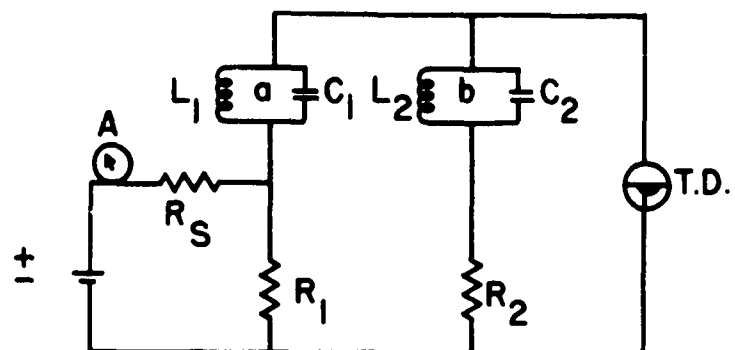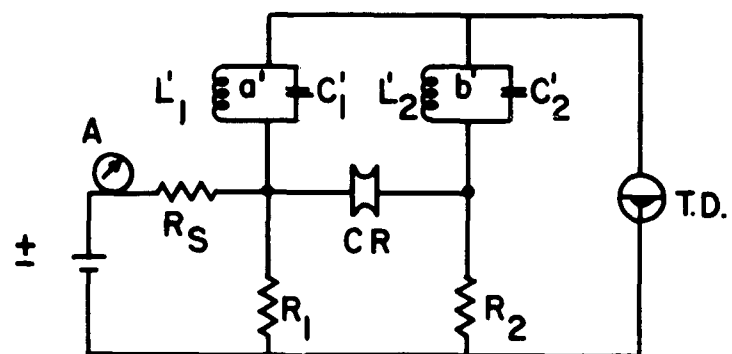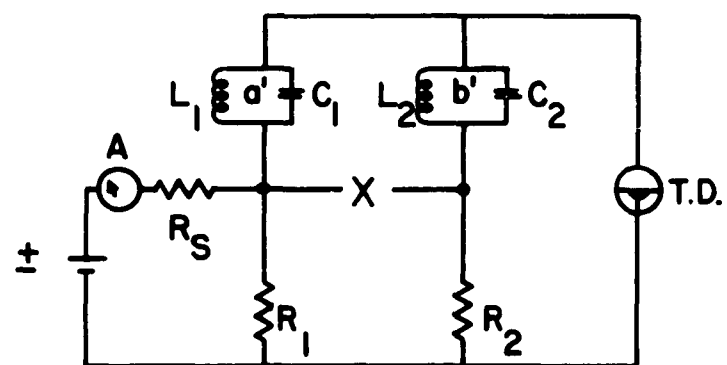CIRCUIT ON ACTIVE SITE

SCHEMATIC:

SIMPLIFIED

FIGURE 29. --Electronic analog of active site of enzyme.

(a) Attraction of substrate

(b) Attachment and activation

(c) Breakage of bond and detachment

FIGURE 30. --Operation of schematic circuit.

structures a and b are temporarily detuned and they provide a wider spectrum of frequencies out of which the crystal (the peptide bond) determines the actual resonant frequency. The crystal acts like a short circuit at its own resonant frequency and therefore halves the values of the resistances R_1 and R_2 and makes it possible for the oscillator to radiate at the new frequency. At this point in the operation more power is needed owing to the reduction of the resistances, and the current through R_s has to increase. The total power output of the oscillator is concentrated in the crystal and increases the amplitude of its oscillation until the crystal itself breaks. At that moment the current through R returns to its original low value, the products of the reaction are repelled from the site on the protein, and a new substrate molecule is attracted. This process can then be repeated exactly as described above.

To test this hypothesis of enzyme action we tried to observe the increase in the current during the active phase of the catalytic process. From our model of water and the resulting computations of the dielectric constant we saw that we actually could measure changes in the relative number of defects on the surface of the protein molecule while it went through the activated state. We computed the number of vacancy defects on the enzyme molecule from our dielectric measurements by the formula

$$n_L(t) = [R \cdot B(t)/a' \, x(t)] + [R/x(t)] \tag{86}$$

and

$$n_D(t) = n(t) \left[\frac{b}{B(t)} - 1 \right] \tag{87}$$

The numerical values of the constants R and b are determined from the initial conditions at time zero where the values of B and x were measured and the value of the number of defects was determined as shown in Figure 19. By the same method as the one that was used for the evaluation of the number of vacancy defects the number of double defects was computed. The number of vacancy defects is tabulated as a function of time in Table 8, and the values of the double defects in Table 9.

TABLE 8. Computation of the number of vacancy defects on the enzyme surface during interaction with its substrate molecule as function of time after mixing.

t(min)	B/x	RB/a'x	x	R/x	n_L
0	138.0	0.0942	0.476	0.0107	0.1049
3.6	143.2	0.0977	0.450	0.0114	0.1091
4.6	145.8	0.0995	0.439	0.0117	0.1122
6.0	140.5	0.0960	0.460	0.0111	0.1071
7.1	140.0	0.0956	0.463	0.0110	0.1066
10.0	138.2	0.0945	0.467	0.0110	0.1055
15.0	140.0	0.0956	0.463	0.0110	0.1066
20.0	140.2	0.0957	0.462	0.0111	0.1068
25.0	140.5	0.0960	0.458	0.0112	0.1072
30.0	135.7	0.0927	0.467	0.0110	0.1037
35.0	140.0	0.0956	0.468	0.0109	0.1065
40.0	135.8	0.0928	0.479	0.0107	0.1035
45.0	137.5	0.0940	0.476	0.0107	0.1048
60.0	140.8	0.0963	0.469	0.0109	0.1072

TABLE 9. Computation of the number of vacancy and double defects during the first 10 min of the enzymatic reaction.

t(min)	n_L	B	b/B	(b/B)-1	n_D
0	0.1049	65.6	1.755	0.755	0.0792
3.6	0.1091	64.5	1.785	0.785	0.0856
4.6	0.1122	64.0	1.800	0.800	0.0897
6.0	0.1071	64.7	1.780	0.780	0.0835
7.1	0.1066	64.8	1.775	0.775	0.0825
10.0	0.1055	64.6	1.780	0.780	0.0823

The variation of the number of vacancy defects with time
is shown in Figure 31. From this representation and from Figure
7 we conclude that the peak in the vacancy defects occurs when the
enzyme is in its activated state. The rest of the curve we leave
uninterpreted at the moment and concern ourselves only with the
changes that occur in the time range of 0 to 10 min. We expand
this time section of Figure 31 in Figure 32 and then take the
derivative of this curve to give the value of the current that is pro-
duced by this rate of change of the number of vacancy defects. The
same operation is performed on the curve representing the number
of double defects in the time interval from 0 to 10 min in
Figure 33. The time derivative is then tabulated in Table 10. From
these derivatives the actual current flow per molecule per second
can easily be computed and is shown in Figure 34 for the current due
to vacancy defects only, and in Figure 35 for the total current
that flows on the surface of the molecule.

TABLE 10. Currents on the surface of the enzyme molecule
during the first 10 min of the reaction.

t(min)	dn/dt	i_L	dn/dt	i_D
0	+4	+130	+6	+195
1	+6	+195	+11	+355
2	+8	+260	+18	+600
3	+18	+600	+27	+880
4	+51	+1650	+66	+2140
5	-59	-1900	-58	-1880
6	-12	- ?0	-20	-650
7	-5	-180	-4	-130
8	-4	-130	0	0
9	-3	-97	0	0
10	-2	-65	0	0

Units: dn/dt in vacancy defects x 10^{-2}/100 molec. -min
dn/dt in double defects x 10^{-2}/100 molec. -min
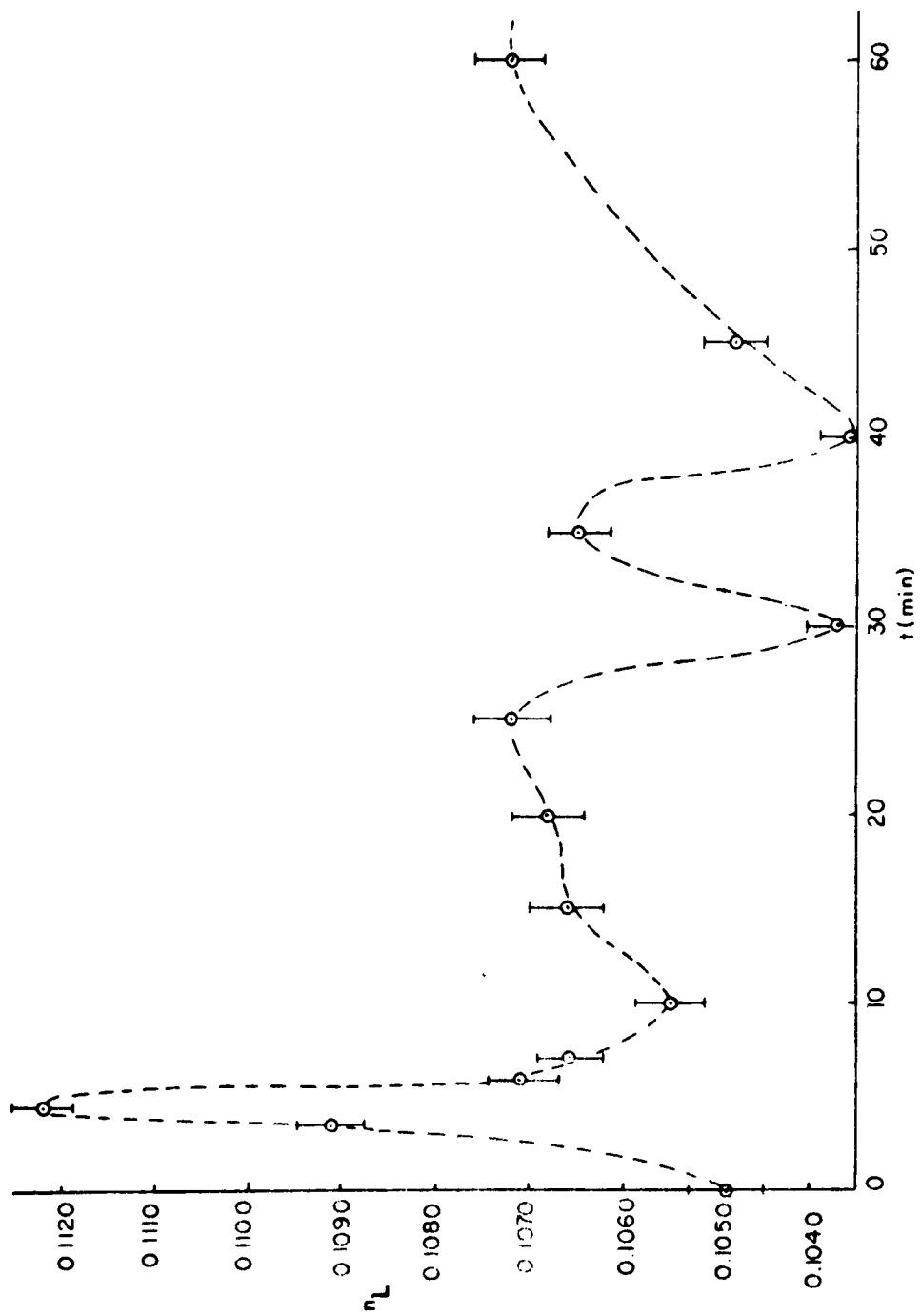i_L in "holes"/pepsin molecule-sec
i_D in protons/pepsin molecule-sec

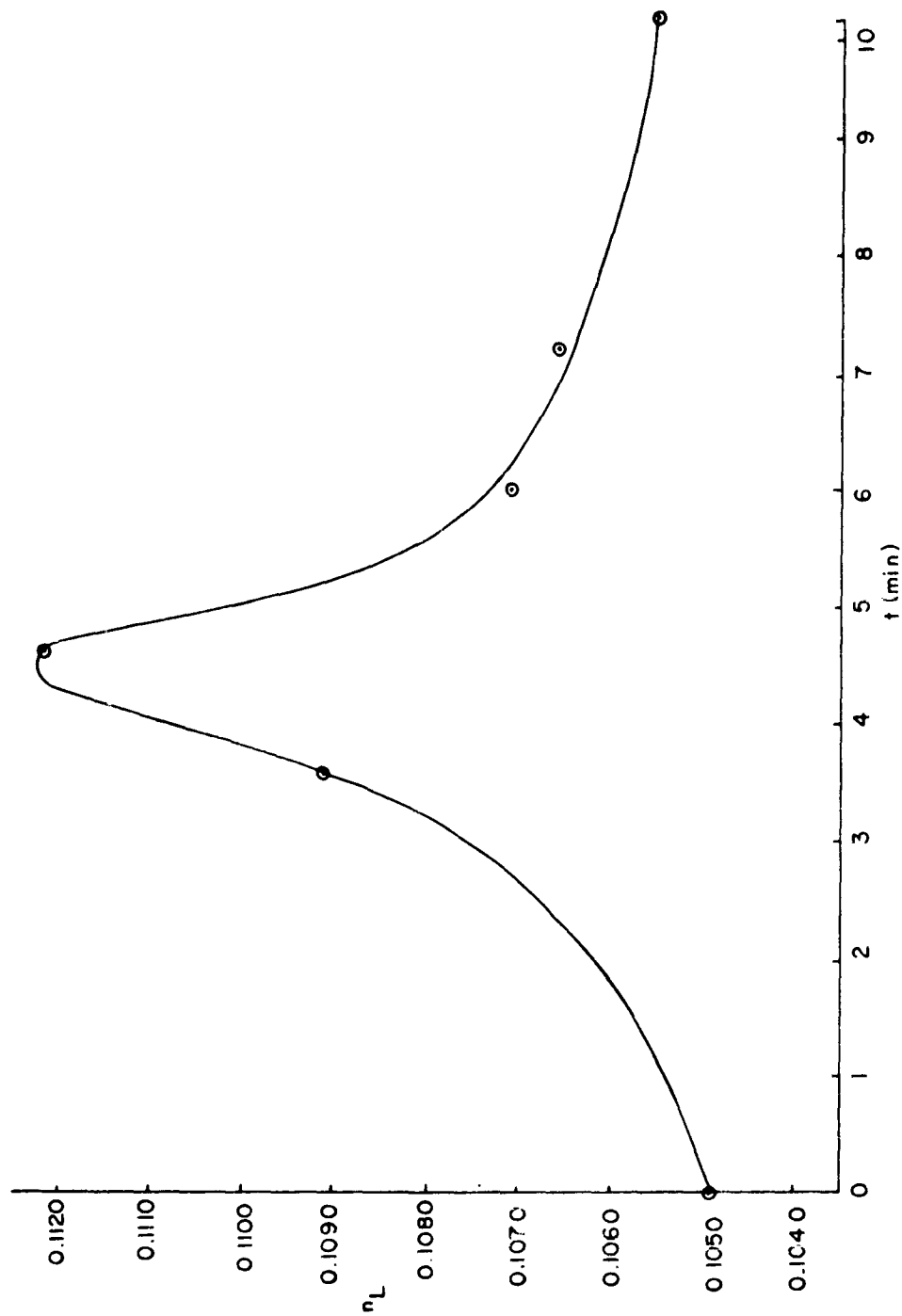FIGURE 31. --Number of vacancy defects on surface of enzyme as function of time during reaction.

FIGURE 32. --Number of vacancy defects as function of time during active period of the reaction of pepsin.
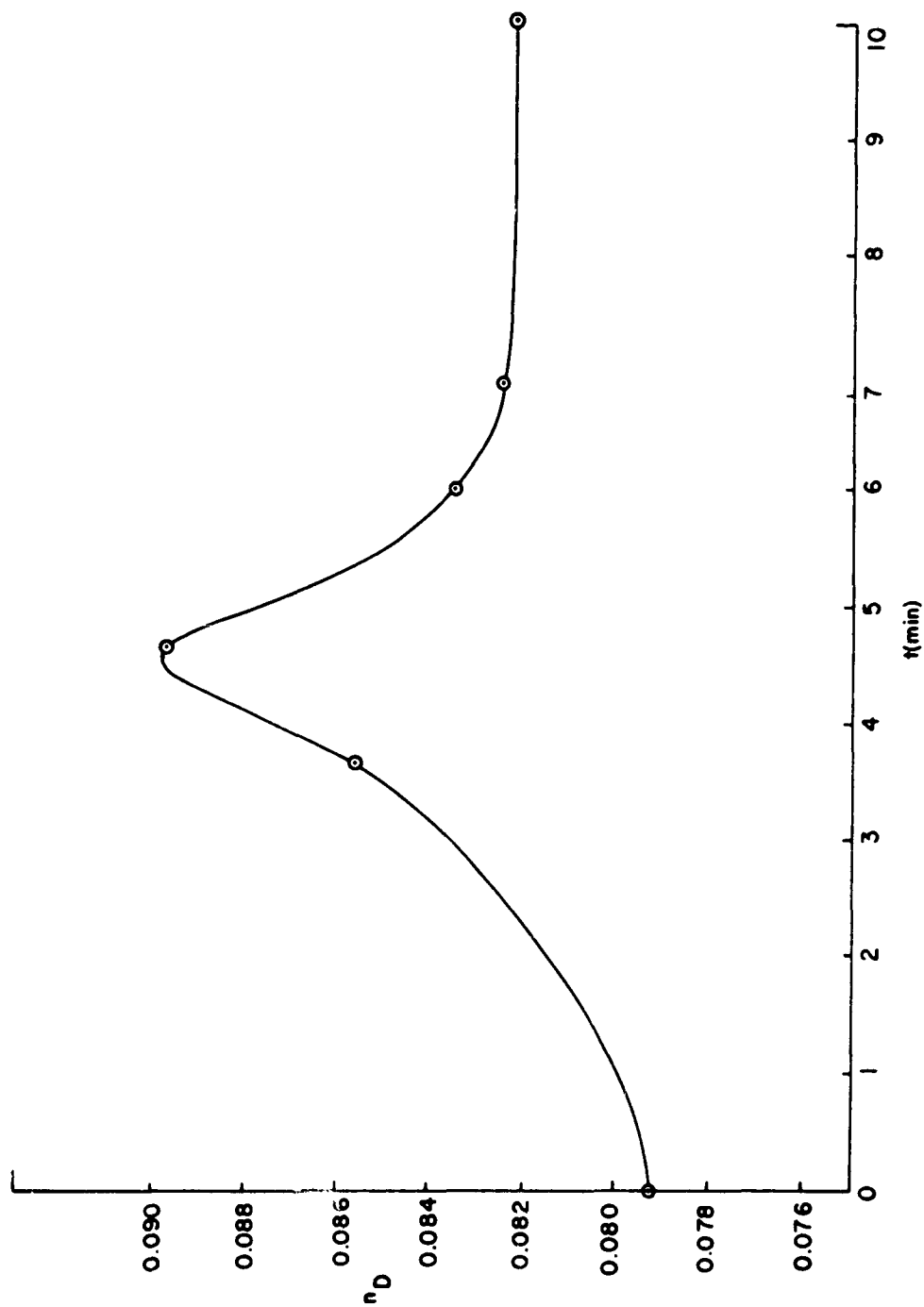
FIGURE 33. --Number of double bond defects as function of time during the active period of the reaction of pepsin.

As one can see from Figure 35 (and from Figure 36, its schematic representation) our prediction of the behavior of the current in the assumed electronic model of the enzyme coincides quite well with the actual physical data that we were able to compute from our dielectric measurements on the basis of the improved model of the water molecule. The initial increase in current is due to the power-output change of the attracting oscillator as the substrate molecule approaches the enzyme, the steep increase is due to the changeover of the oscillator to the crystal (peptide bond)-controlled operation with a transient following as the crystal (bond) is broken, and finally we have the recovery current back to the original value.

C. ENERGY CONSIDERATIONS OF THE ENZYMATIC REACTION

Our analysis of the protonic conductivity characteristics of doped ice has not proceeded far enough to give a quantitative estimate of the energy level equivalent to the Fermi level of electronic semi-conductors. In a rigorous analysis this energy would appear in the activation energy of the catalytic process and modify the velocity of the reaction correspondingly.

In the meantime we consider the energy output of the tunnel-diode oscillator at the active site of the enzyme molecule. The power output is given by

$$P_{out} \cong \left(\frac{V_v - V_p}{2\sqrt{2}} \right)^2 \frac{C}{L} R_L \qquad (88)$$

where V_v is the valley voltage of the diode, V_p the peak voltage, L the circuit inductance, C the circuit capacitance, and R_L the load resistance (in our case the resistance of the crystal or dipeptide). The magnitudes of C and L are comparable and cancel out. The voltage amplitude is assumed to be 10 mv from considerations of operations in solid-state circuits and R_L is computed from data on the conductivity of proteins.[66]
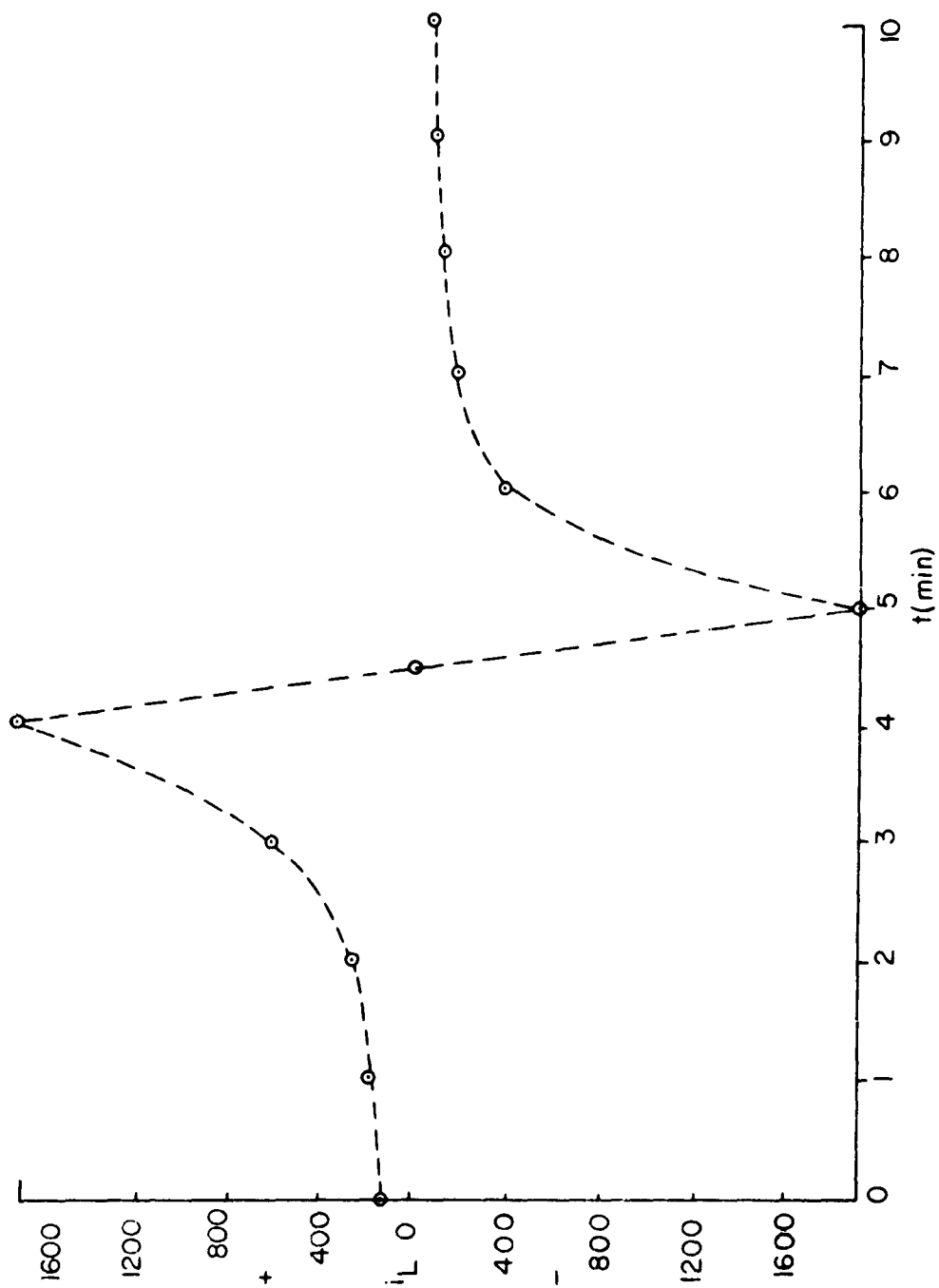
$$R_L = l / \sigma A \qquad (89)$$

-98-

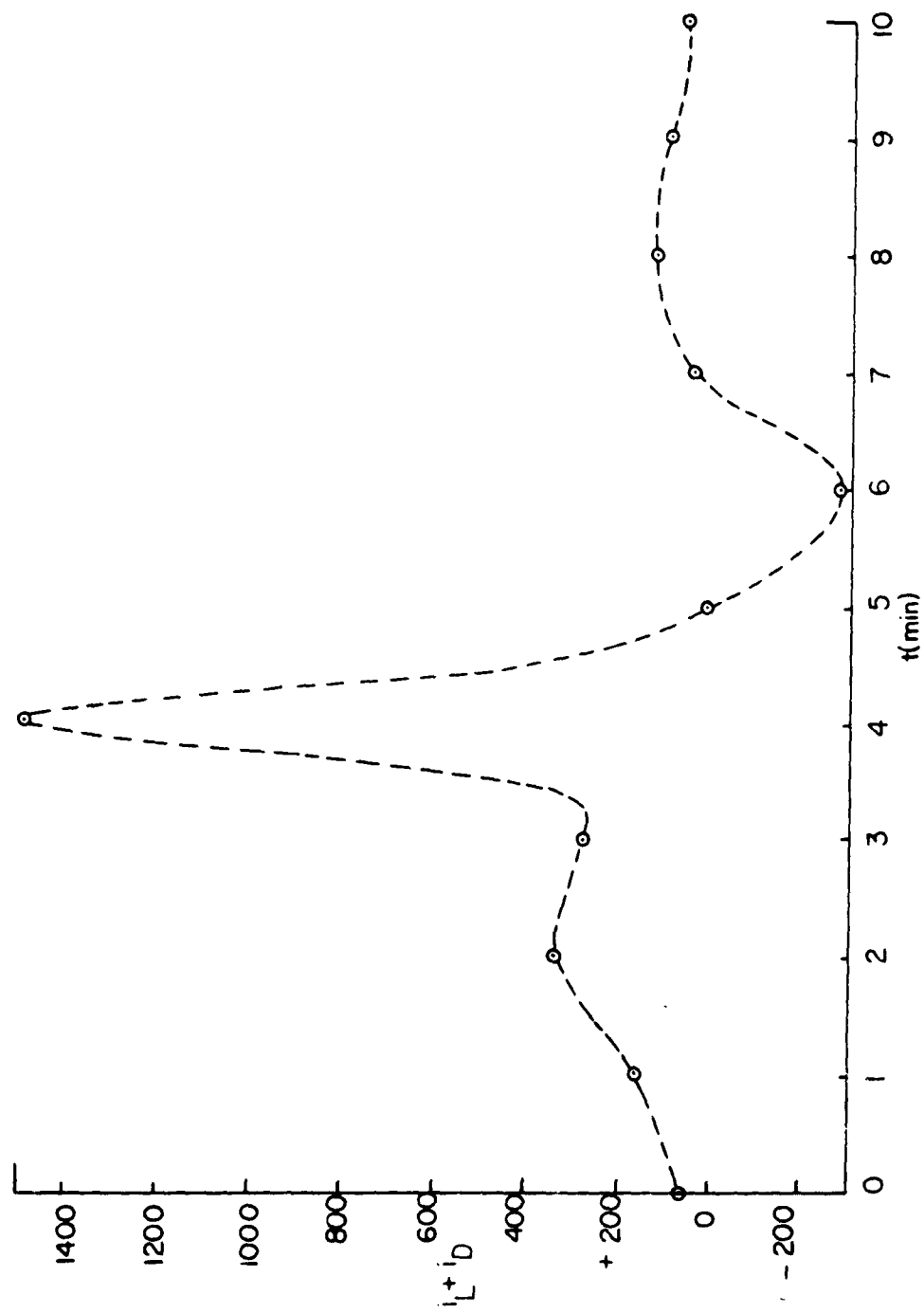FIGURE 34.--Defect current on the surface of the enzyme molecule.

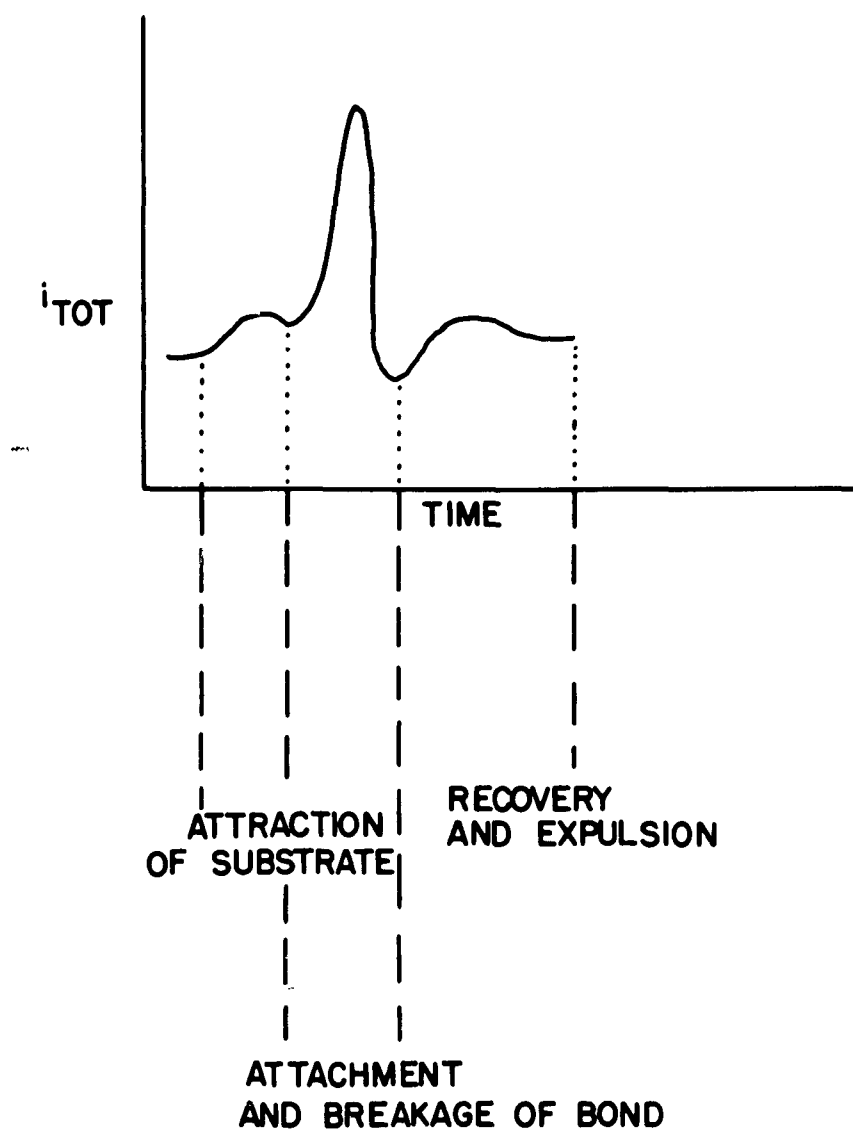FIGURE 35. -- Total current on the surface of the enzyme molecule.

FIGURE 36. --Schematic diagram of the total current on the
surface of the enzyme molecule during the
active period of the reaction.

where l is the length of the conductor, A its cross-sectional area, and σ its conductivity.

Let σ = 1 mmho/cm, l = 10 Å, and A = 1 Å^2. Then R = 10^3 x 10 x 10^{-8} x 10^{16} = 10^{12} ohms.

The value of P therefore is

$$P \cong 10^{-4} \times 10^{12} \text{ watts} = 10^8 \text{ joules/sec} \qquad (90)$$

This value of P is approximately equivalent to 30 kcal delivered in 0.1 msec, an energy sufficient for breakage of the peptide bond.

VI. CONCLUSIONS

These experimental data are only an indirect proof of our hypothesis of enzymatic action; they only show that our assumptions have been consistent with a certain type of process that occurs in the interaction of pepsin and one of its synthetic substrates. In other enzyme systems a different behavior may be found. If our explanation is found to apply in other cases as well, then there will be many other systems of molecular interdependence that may profit from an application of the knowledge we have gathered in electronics to problems that exist in biophysics. The similarity in the shape of the current on the surface of the enzyme and the action potential of nerve fibers, for example, may not be at all accidental.

The oscillatory behavior of the active site of the enzyme molecule only provides enough energy to ensure a lower energy of activation than would be predicted on a chemical basis alone. This additional energy, which is provided by the oscillations at the active site, actually speeds up the reaction and one is in a position to understand now why so many schemes of enzymatic catalysis were accurate in their chemical aspects but nevertheless failed sometimes by several orders of magnitude to give the correct reaction velocities.

In addition to the above suggestion of an added energy source for the lowering of the activation energy of the reaction it seems possible now for the first time to investigate with some theoretical

basis the effects of electromagnetic radiation on enzyme systems. If radiation of a given wavelength is present during the reaction, then the distribution of the charges on the surface is influenced to some extent and the normal course of events is impeded. Both the frequency and the power of the incident radiation are important in influencing the operation of our electronic analog of the active site. It is understandable, therefore, that so many controversial observations of the effects of electromagnetic radiation on enzyme systems and other biological systems were reported in the literature. It does not seem to be feasible on the basis of our theory to classify such effects in terms of thermal and nonthermal effects; a wholly new way of interpreting previous data will have to be found.

The electrical description of events taking place on the surface of the enzyme in no way subtracts from the validity of the chemical picture of catalysis, but it adds detail to the physico-chemical aspects of the enzymatic action. One is now in a position to speculate about the generality of the concepts that evolved from an examination of changes in the electrical parameters on the surface of the protein molecule.

Our type of analysis of molecular transformations connected with the general activity of systems of such transformations--the phenomenon called life--may be termed "distributed molecular circuit analysis." It is generally applicable to single macromolecules that exhibit an ability of influencing changes of other molecules and also, after a better understanding of the inidividual processes has been gained, to systems of active macromolecules. In this approach one is able to draw on the accumulated knowledge of solid- and liquid-state physics as well as network and communication theory and so has the opportunity to grasp in a precise way the complex relations that must exist in even the smallest subunits of a living cell.

REFERENCES

1. G. H. Haggis, J. B. Hasted, and T. J. Buchanan, "Dielectric properties of water in solutions," J. Chem. Phys. 20: 1452-1465, 1952.

2. S. Takashima and R. Lumry, "Dielectric properties of hemoglobin: II. Anomalous dispersion during oxygenation," J. Am. Chem. Soc. 80: 4238-4244, 1958.

3. Q. H. Gibson and F. J. W. Roughton, "The kinetics of haemoglobin and haem compounds as models for enzyme action," Disc. Faraday Soc. 20: 195-204, 1955.

4. G. King and J. A. Medley, "II. The influence of temperature and adsorbed salts on the d. c. conductivity of polar polymer adsorbate systems," J. Colloid Sci. 4: 9-19, 1949.

5. M. H. Cardew and D. D. Eley, "The semiconductivity of organic substances: Part 3. Haemoglobin and some aminoacids," Disc. Faraday Soc. 27: 115-128, 1959.

6. R. M. Fuoss, "Ionic association: III. The equilibrium between ion pairs and free ions," J. Am. Chem. Soc. 80: 5059-5061, 1958.

7. N. Riehl, "Zum Zusammenhang zwischen elektrischer Leitfähigkeit und Energiewanderung in Proteinen," Kolloid Z. 151: 66-74, 1957.

8. C. P. S. Taylor, "The Electrical Conductivity of Dry Cytochrome c, a Failure of the Electronic Conduction Hypothesis of Charge Transfer Through Protein," Ph. D. thesis, Univ. of Pennsylvania, 1960.

9. B. Rosenberg, "Electrical conductivity of proteins," Nature 193: 364-365, 1962.

10. H. Eyring, S. Glasstone, and K. J. Laidler, "Application of the theory of absolute reaction rates to overvoltage," J. Chem. Phys. 7: 1053-1065, 1939.

11. B. Rosenberg, "Electrical conductivity of proteins: II. Semiconduction in crystalline bovine hemoglobin, " J. Chem. Phys 36: 816-823, 1962.

12. G. Birnbaum and J. Franeau, "Measurement of the dielectric constant and loss of solids and liquids by a cavity pertur- bation method, " J. Appl. Phys. 20: 817-818, 1949.

13. J. C. Slater, "Microwave electronics," Rev. Mod. Phys. 18: 441-512, 1946.

14. B. Bleaney, J. H. N. Loubeer, and R. P. Penrose, "Cavity resonators for measurements with centimetre electromagnetic waves, " Proc. Phys. Soc. (London) 59: 185-199, 1947.

15. L. E. Baker, "New synthetic substrates for pepsin, " J. Biol. Chem. 193: 809-819, 1951.

16. S. Moore and W. H. Stein, "Photometric ninhydrin method for use in the chromatography of aminoacids," J. Biol. Chem. 176: 376-388, 1948.

17. P. Debye, "Polar Molecules," Chemical Catalog Company, Inc., New York, N. Y., 1929.

18. J. B. Hasted and S. H. M. El Sabeh, "The dielectric properties of water in solutions," Trans. Faraday Soc. 49: 1003- 1011, 1953.

19. C. H. Collie, J B. Hasted, and D. M. Ritson, "The dielectric properties of water and heavy water, " Proc. Phys. Soc. (London) 60: 145-160, 1948.

20. F. Buckley and A. A. Maryott, "Tables of Dielectric Dispersion Data for Pure Liquids and Dilute Solutions, " U. S. Nat. Bur. of Standards, Circular 589: 1-95, 1958.

21. H. Gränicher, C. Jaccard, P. Scherrer, and A Steinemann, "Dielectric relaxation and the electrical conductivity of ice crystals," Disc. Faraday Soc. 23: 50-62, 1957.

22. P. C. Cross, J. Burnham, and P. A. Leighton, "The Raman spectrum and the structure of water," J. Am. Chem. Soc. 59: 1134-1147, 1937.

23. J. D. Bernal and R. H. Fowler, "A theory of water and ionic solution, with particular reference to hydrogen and hydroxyl ions, " J. Chem. Phys. 1: 515-548, 1933.

24. L. Pauling, "The Nature of the Chemical Bond," Cornell University Press, Ithaca, N. Y. , 1960.

25. S. W. Peterson and H. A. Levy, "A single-crystal neutron diffraction study of heavy ice," Acta Cryst. 10: 70-76, 1957.

26. N. Bloembergen, E. M. Purcell, and R. V. Pound, "Relaxation effects in nuclear magnetic resonance absorption," Phys. Rev. 73: 679-712, 1948.

27. G. E Pake and H. S. Gutowsky, "Nuclear relaxation in ice at -180°C, " Phys. Rev. 74: 979-980, 1948.

28. N. Bjerrum, "Structure and properties of ice," Dan. Mat. Fys. Medd. 27: 1-56, 1951.

29. S. Katzoff, "X-ray studies of the molecular arrangement in liquids, " J. Chem. Phys. 2: 841-851, 1934.

30. B. E. Warren, "X-ray determination of the structure of liquids and glass," J. Appl. Phys. 8: 645-654, 1937.

31. J. E. Lennard-Jones and J. A. Pople, "Molecular association in liquids: I. Molecular association due to lone-pair electrons; II. A theory of the structure of water," Proc. Roy. Soc. (London) 205(A): 155-176, 1951.

32. M. Eigen and L. De Maeyer, L. , "Self-dissociation and protonic charge transport in water and ice," Proc. Roy. Soc. (London) 247(A): 505-533, 1958.

33. E. J. W. Verwey, "The charge distribution in the water molecule and the calculation of the intermolecular forces," Rec. Trav. Chim. 60: 887-896, 1941.

34. G. Oster and J. G. Kirkwood, "The influence of hindered molecular rotation on the dielectric constants of water, alcohols, and other polar liquids," J. Chem. Phys. 11: 175-178, 1943.

35. H. Fröhlich, "Theory of Dielectrics," Clarendon Press, Oxford, 1958.

36. C. Zener, "Theory of diffusion" in "Imperfections in Nearly Perfect Crystals" (W. Shockley, ed.), John Wiley and Sons, New York, N. Y., 1952.

37. F. A. Bovey and S. S. Yanari, "Pepsin," in "The Enzymes," vol. IV P. D. Boyer, H. Lardy, and K. Myrbäck, eds.), Academic Press, New York, N. Y., 1960.

38. O. L. Sponsler, J. D. Bath, and J. W. Ellis, "Water bound to gelatin as shown by molecular structure studies," J. Phys. Chem. 44: 996-1006, 1940.

39. H. Eyring, R. Lumry, and J. D. Spikes, "Kinetic and thermodynamic aspects of enzyme-catalyzed reactions," in "The Mechanism of Enzyme Action" (W. D. McElroy and H. B. Glass, eds.), Johns Hopkins Press, Baltimore, Md., 1954.

40. T. L. Hill, "Titration curves and ion binding on proteins, nucleic acids, and other macromolecules with a random distribution of binding sites of several types," J. Am. Chem. Soc. 78: 5527-5529, 1956.

41. C. Tanford, "The electrostatic free energy of globular protein ions in aqueous salt solution," J. Phys. Chem. 59: 788-793, 1955.

42. J. A. Schellman, "The application of the Bjerrum ion association theory to the binding of anions by proteins," J. Phys. Chem. 57: 472-475, 1953.

43. C. Tanford, J. G. Buzzel, D. G. Rands, and S. A. Swanson, "The reversible expansion of bovine serum albumin in acid solutions," J. Am. Chem. Soc. 77: 6421-6428, 1955.

44. E. J. Cohn and J. T. Edsall, "Amino Acids, Peptides, and Proteins," Reinhold Publishing Corp. , New York, N. Y. , 1943.

45. B. Jacobsen, "On the interpretation of dielectric constants of aqueous macromolecular solutions: Hydration of macromolecules," J. Am. Chem. Soc. 77: 2919-2926, 1955.

46. J. G. Kirkwood and J. B. Shumaker, "The influence of dipole moment fluctuations on the dielectric increment of proteins in solution," Proc. U. S. Natl. Acad. Sci. 38: 855-862, 1952.

47. J. G. Kirkwood and J. B. Shumaker, "Forces between protein molecules in solution arising from fluctuations in proton charge and configuration," Proc. U. S. Natl. Acad. Sci. 38: 863-871, 1952.

48. S. N. Timasheff, H. M. Dintzis, J. G. Kirkwood, and B. D. Coleman, "Light scattering investigation of charge fluctuations in isoionic serum albumin solutions," J. Am. Chem. Soc. 79: 782-791, 1957.

49. S. Takashima, "Dielectric properties of hemoglobin. I. Studies at 1 megacycle," J. Am. Chem. Soc. 78: 541-546, 1956.

50. J. G. Kirkwood, "The influence of fluctuations in protein charge and charge configuration on the rates of enzymatic reactions," Disc. Faraday Soc. 20: 78-82, 1955.

51. K. J. Laidler, in "General discussion," Disc. Faraday Soc. 20: 254, 1955.

52. J. G. Kirkwood, and F. H. Westheimer, "The electrostatic influence of substituents on the dissociation constants of organic acids: I and II," J. Chem. Phys. 6: 506-517, 1938.

53. M. Eigen and L. De Maeyer, "Hydrogen bond structure, proton hydration, and proton transfer in aqueous solution," in "Structure of Electrolytic Solutions" (W. F. Hamer, ed.), John Wiley and Sons, New York, N. Y., 1959.

54. K. Hauffe and H. J. Engell, "Zum Mechanismus der Chemisorption vom Standpunkt der Fehlordnungstheorie," Z. Elektrochem. 56: 366-372, 1952.

55. P. Aigrain and C. Dugas, "Adsorption sur les semi-conducteurs," Z. Elektrochem. 56: 363-366, 1952.

56. P. B. Weisz, "Electronic barrier layer phenomena in chemisorption and catalysis," J. Chem. Phys. 20: 1483-1484, 1952.

57. P. B. Weisz, "Effects of electronic charge transfer between adsorbate and solid on chemisorption and catalysis," J. Chem. Phys. 21: 1531-1538, 1953.

58. J. E. Germain, "Modèle cinétique de l'adsorption activée sur les catalyseurs semi-conducteurs," Compt. Rend. 238: 236-238, 1954.

59. Germain, J. E., "Relation entre la forme de l'isotherme, la cinétique et la variation de la chaleur d'adsorption activée sur les catalyseurs semi-conducteurs," Compt. Rend. 238: 345-347, 1954.

60. T. J. Gray, "The Defect Solid State," Interscience Publishers, New York, N. Y., 1957.

61. F. J. Morin, "Oxides of the $3d$ transition metals," Bell Syst. Tech. J. 37: 1047-1084 (1958).

62. T. Wolkenstein, "Elektronentheorie der Katalyse an Halbleitern (1. Teil)," Chem. Techn. 11: 8-12, 1959.

63. T. Wolkenstein, "Elektronentheorie der Katalyse an Halbleitern (2. Teil)," Chem. Techn. 11: 103-107, 1959.

64. T. Wolkenstein, "O dvuch typach homeopoliarnoi sviazi pri chimecheskoi adsorbcii," J. Phys. Chem. (Sov.) 28: 422-432, 1954.

65. G. K. Bereskow, and W. W. Popovsky, "Problems in the Kinetics of Catalysis," in press.

66. H. P. Schwan, "Electrical properties of tissue and cell suspensions," Adv. Biol. Med. Phys. (Academic Press, New York, N. Y.) 5: 147-209, 1957.

67. S. Takashima, "Dielectric properties of hemoglobin: VI. Measurements with solid materials," J. Am. Chem. Soc. 80: 4474-4480, 1958.

68. J. M. Yos, W. L. Bade, and H. Jehle, "Specificity of the London-Eisenschitz-Wang force," Proc. U. S. Natl. Acad. Sci. 43: 341-346, 1957.